

Author's Response

Trends and Emissions of Six Perfluorocarbons in the Northern and Southern Hemisphere

Journal of Atmospheric Chemistry and Physics

21 February 2020

Please find in this document our responses to the referee comments, followed by marked changes in the manuscript and Supplementary Material document.

Kind regards,

Elise Droste

Response to Referee Comments

Trends and Emissions of Six Perfluorocarbons in the Northern and Southern Hemisphere

Journal of Atmospheric Chemistry and Physics

February 2020

In this document, we address the comments of anonymous referees #1, #2, and #3 to our paper on *Trends and Emissions of Six Perfluorocarbons in the Northern and Southern Hemisphere*. Referees' comments are highlighted in blue and are numbered according to referee number, page of the comment, and comment number, the latter of which we attributed ourselves wherever original comments were unnumbered. For example, the 23rd comment made by Referee #2, which can be found on page C3, will be referred to as 2.3.23 (ref.page.comment). General comments have been addressed within our responses to the specific comments of the referees.

References made to page and line numbers in our responses refer to the page and line numbers in the original documents of the paper and Supplement, *not* the revised documents, unless stated otherwise.

On behalf of myself and all co-authors of this work, I would like to thank the referees for their constructive comments and detailed input to this paper.

Elise Droste

Karina E. Adcock¹, Matthew J. Ashfold², Charles Chou³, Zoë Fleming^{4,*}, Paul J. Frasers⁵, Lauren J. Gooch¹, Andrew J. Hind¹, Ray L. Langenfelds⁵, Emma Leedham Elvidge¹, Norfazrin Mohd Hanif^{1,6}, Simon O'Doherty⁷, David E. Oram^{1,8}, Chang-Feng Ou-Yang⁹, Marios Panagi⁴, Claire E. Reeves¹, William T. Sturges¹, and Johannes C. Laube^{1,10}

¹Centre for Ocean and Atmospheric Sciences, School of Environmental Sciences, University of East Anglia, Norwich, NR4 7TJ, UK

²School of Environmental and Geographical Sciences, University of Nottingham Malaysia, 43500 Semenyih, Malaysia

³Research Center for Environmental Changes, Academia Sinica, Taipei 11529, Taiwan

⁴National Centre for Atmospheric Science (NCAS), Department of Chemistry, University of Leicester, UK

⁵Commonwealth Scientific and Industrial Research Organisation, Oceans and Atmosphere, Climate Science Centre, Aspendale, Australia

⁶School of Environmental and Natural Resource Sciences, Faculty of Science and Technology, Universiti Kebangsaan Malaysia, 43600 Bangi, Selangor, Malaysia

⁷Department of Chemistry, University of Bristol, Bristol, UK

⁸National Centre for Atmospheric Science, School of Environmental Sciences, University of East Anglia, Norwich, NR4 7TJ, UK

⁹Department of Atmospheric Sciences, National Central University, Taoyuan, Taiwan

¹⁰Institute of Energy and Climate Research – Stratosphere (IEK-7), Forschungszentrum Jülich GmbH, Jülich, Germany

*now at Center for Climate and Resilience Research (CR2), University of Chile, Santiago, Chile

General Notes:

- Table 4 has been changed to table 3; table 3 is now table 4.
- Referees have been included into the Acknowledgements section

Response to Referee #1

General Comments:

NA

Specific Comments:

1.2.1 Abstract, p. 1, l. 5: Perhaps add 'analytically', to clarify what 'separation' is discussed here (analytically separated from their isomers : : :)

Done.

1.2.2 p. 2, l. 4: is 'metric' necessary (isn't ACP using SI units anyway?).

After considering this comment, we decided to keep "metric" for extra clarity on the unit of measurement.

1.2.3 p. 2, l. 6 'despite what?', what does 'this' reference to?

Original sentence: "Despite this, the sources of all PFCs covered in this work remain poorly constrained and reported emissions in global databases do not account for the abundances found in the atmosphere."

"this" referred to the continuing emissions of the PFCs. However, we have decided to update the sentence and remove "despite this", since it is unnecessary and the remainder of the sentence brings across the message we would like to make: "Sources of all PFCs covered in this work remain poorly constrained and reported emissions in global databases do not account for the abundances found in the atmosphere."

1.2.4 p. 2, l. 5: Does the two-thirds refer to the emissions of the last 8 years or to the emissions since 1978?

Original sentence: "... 23% of which has been emitted in the last eight years. Almost **two-thirds** of the CO₂ equivalent emissions are attributable to c-C₄F₈, which ... "

The two-thirds refer to the emissions of the last 8 years. This has been clarified in the text in the following manner:

Revised sentence: "Almost two-thirds of the CO₂ equivalent emissions in the last eight years are attributable to c-C₄F₈, which currently also has the highest emission rates that continue to grow"

1.2.5 p. 3, l. 18: is decofluorobutane. Spelling here different to abstract

We thank the referee for spotting these details.

Decofluorobutane has been changed to decafluorobutane

1.2.6 p. 3, l. 19: hexodecafluoroheptane. Spelling here different to abstract.

Done. Hexodecafluoroheptane has been changed to hexadecafluoroheptane

1.2.7 p. 3, l. 21: same issue for perfluoro-2-methylpentane. Suggest to recheck spelling of all chemicals and use consistently throughout.

Done. Perfluoro(2-methylpentane) has been changed to perfluoro-2-methylpentane

1.2.8 p. 3, l. 24. ‘: : : of these: : ’ would strictly refer to c-C4F8 and n-C5F12, but I presume that the author means all compounds handled in this manuscript.

Correct. “of these” replaced with “all six compounds studied in this manuscript”

1.2.9 p. 3, l. 24. In Table 1, there is a compound with a GWP outside the range indicated here (i-C6F14).

Original range on p. 3 line 24: “range between 7820 (n-C7F16) and 9540 (n-C4F10)”

This has been updated to “range between 7370 (i-C6F14) and 9540 (n-C4F10)”

1.2.10 p. 4 objective 2: There is something fundamentally unclear here. 1) Why were new calibration scales needed? I understand that with new methods, isomers could now be separated. 2) However, were the old calibration scales not made with pure reagents, e.g pure n-C4F10, no i-C4F10? If so, then why weren’t the old calibration reference standards used for the present work, and the air sample data corrected for the fact that now the two isomers are separated? 3) It appears that the old calibration reference standards would still be good, but the measurement of the air samples would need to be redone or the old ones corrected. 4) Was the same raw material used to produce the new scales. 5) How many cali-bration reference standards were produced — just one?

- 1) The reason that new calibration scales were needed is that, when the PFCs had been calibrated, the isomers had not been separated isomers yet. We were not able to keep the calibration standards used to construct the previous calibration scale and so these could not be re-used.
- 2) We were not able to confirm that the pure compounds from previous calibrations indeed consisted of one isomer only. We used a technical mixture for n-C7F16 in the previous calibration due to lack of availability of a more pure compound, which only contained about 85% n-isomer.
- 3) Calibration references cannot be kept in our lab. The only thing we keep are the secondary standards (working standards), which contain clean Northern Hemispheric air and therefore a mixture of PFC isomers.
- 4) The same material was used of nC6F14, nC4F10. It was confirmed for these reagents that they did not contain any detectable amount of any other isomer. The pure reagents for nC7F16 and iC6F14 were newly purchased at purities specified in the manuscript.
- 5) For each of the calibrated PFCs, three calibrations were done. For each of these calibrations, the pure compound was diluted to mixing ratios anywhere between 4 and 10 ppt. This information has now been included in an additional table in the supplement, following suggestions in comment 1.5.32.

The following paragraph has been added at the beginning of Section 2.3:

“The mixing ratios in the samples are determined based on a secondary calibration standard, which we refer to as the working standard. Our working standard consists of clean Northern Hemispheric air, which therefore contains all relevant PFCs. For many gases, the mixing ratios in the working standard have been calibrated by NOAA. As certified values do

not exist for the relevant PFCs, we calibrate them at UEA using an independent calibration scale (see more details in the Supplement).”

We also added the following statement on line 1 on page 7:

“We used the same compounds as in Laube et al. (2012) for n-C4F10 and n-C6F14, for which we now confirm their isomeric purity. For i-C6F14 and n-C7F16 we used newly purchased pure compounds, which were also confirmed to be isomerically pure. In addition, for n-C7F16 this represents a significant improvement to Laube et al. (2012), as the latter used a technical mixture with an 85% n-isomer content.”

1.3.11 p. 5, l. 14 – 16. It seems that this was already explained in the Intro objective 1.

Correct. Lines 14-16 on p5 have been removed (“Air samples collected for the Cape Grim Air Archive and UEA represent well-mixed, clean, Southern Hemispheric air, as the sampled air masses originate from the long trajectories over the Southern Ocean. Hence, the trace gas abundances in these samples can be considered as mid-latitude Southern Hemispheric background levels.”).

1.3.12 p. 6, l. 7: Were compounds used in this study also affected? If not, perhaps be more specific by saying ..‘number of compounds not used in this study’.

We are not stating that CO₂ affected the signal of any compound. We are explaining that the placement of an Ascarite trap removes the CO₂ and that its removal means that none of the measurements are distorted. We have clarified the sentence by re-phrasing it like so:

Original sentence: “For compounds analysed on the CP-PLOT column, an Ascarite (NaOH-coated silica) trap is included before the magnesium perchlorate trap to remove CO₂, which can distort or reduce the signal of a number of compounds.”

Revised sentence: “... an Ascarite (NaOH-coated silica) is included before the magnesium perchlorate trap to remove CO₂, which can **otherwise** distort or reduce the signal of a number of compounds, including those discussed in this study.”

1.3.13 p. 7, second para. Comment here is similar to p. 4, objective 2.: 1) ‘..from the observe isomer’ observed where – in the old primary calibration standards? 2) If there was i-C4F10 in the old standards, why wasn’t it precisely quantified by measuring it vs the new cal standards, then allowing to separate the <2.8% difference into the two factors ‘leak-tightness’ and ‘i-C4F10’ influence. 3) Line 9. Lack of observed iso-mers where?

- 1) We have observed the i-C4F10 isomer in the working standard and atmospheric samples. We have now clarified this by modifying this sentence:

Original sentence: “...any bias from the observed i-C4F10 isomer, and to ...”

Rephrased sentence: “...any bias from the observed i-C4F10 isomer (**a small side peak of which was observed in both the working standard and atmospheric samples**), and to ...”

- 2) The i-C4F10 isomer can currently not be quantified yet with the current method, because, apart from having a very small signal, its main quantifying ion is not well separated from one of the quantifying ions for n-C4F10. Even if we were able to separate it completely, it would also have to be calibrated using a pure i-C4F10 reagent, which we were unable to acquire. Hence, we are unable to quantify what fraction of the 2.8% is due to leak-tightness and to the influence of i-C4F10. This statement has been included in the Supplementary Material document under a new section, named “Additional Calibration Details”, and we refer the reader to the Supplement for more details in line 8 on page 7.
- 3) P. 7, line 9: Original sentence: “Due to the leak-tightness of the system and a lack of observed isomers, a revision of the calibration scales for c-C4F8 and n-C5F12 was deemed unnecessary.”

Revised sentence: “Due to the leak-tightness of the system and a lack of observed isomers **of c-C4F8 and n-C5F12 in the working standard and atmospheric samples**, a revision of the calibration scales was deemed unnecessary **for these two compounds.**”

1.3.14 P. 7 l. 12: ‘The confidence in the complete separation of all isomers for C6F14 and C7F16 : : ’ This sen-tence is in conflict with earlier mentioning of inabilities of separating all isomers of e.g. C7F16.

We are able to separate the two significant isomers of C6F14 (n and i) and C7F16 (n and i), but the latter also has a third peak that is not well separated from the peak for the i-C7F16 isomer. In this line, we are referring to the complete separation of the i- and n- isomer of C6F14 and similarly for C7F16. In other words, we have confidence that the peak for i-C6F14, n-C6F14, and n-C7F16 indeed only represent the signal for i-C6F14, n-C6F14, and n-C7F16, respectively.

To clarify, we have rephrased the sentence on lines 26-27 on page 6:

Original sentence: “Additionally, these two smallest peaks are not well separated from each other and the number of possible isomers with very similar mass spectra is too high to allow for a high-confidence identification.”

Revised sentence: “Additionally, these two smallest peaks are not well separated from each other **(but are well separated from the main isomer peak)** and the number of possible isomers with very similar mass spectra is too high to allow for a high-confidence identification.”

1.3.15 p. 7, l. 19: ‘: : did not differ significantly: : ’ seems incorrect, According to Fig. S2 they differ very strongly and significantly and are rather concerning.

We disagree with the referee on this point. Given the error bars on the ion ratios for the Cape Grim samples and the uncertainty of the ion ratios of the calibrations, the difference is

not significant. The sentence prior to the one this comment refers to also states that we can attribute the confidence “within the uncertainties”. We have changed the sentence on line 19-20 on page 7 as follows:

Original sentence: “For i-C6F14, n-C6F14, and n-C7F16, the ion ratio in the Cape Grim samples did not differ significantly from the ion ratio in the calibrations (Fig. S2).”

Revised sentence: “For i-C6F14, n-C6F14, and n-C7F16, the ion ratio in the Cape Grim samples did not differ significantly from the ion ratio in the calibrations **within 1 sigma measurement uncertainty** (Fig. S1).”

1.3.16 p. 7, l. 27. The abbreviation does not seem to match the first letters of the full name.

We thank the referee for noticing this mistake. We have now corrected both the abbreviation and the name itself.

Original: “... CMD (Global Measurement Division) ...”

Revised: “... GMD (Global Monitoring Division)...”

1.3.17 p. 7, l. 30: 1) Could you provide a guess why there is a difference between the bootstrapped

CFC-11 and that measured on the NOAA scale. 2) There is a lot of plural mentioning, but isn't it only one comparison, that of the (single) working tank vs the primary calibration tanks?

- 1) The overall volume uncertainty of the sample loops that were filled with pure compounds during both dilution steps is 5%, as has been outlined in Laube et al., 2010. This is the likeliest and highest source of uncertainty in the entire calibration procedure. As has been shown in multiple previous papers (Laube et al., 2010; 2012; 2014; 2016; Oram et al., 2012; Kloss et al., 2014), the overall calibration uncertainty is very likely about 7%. Our measurements fall well within that envelope. This information has now been included in a new section in the Supplement, named “Additional Calibration Details”.
- 2) For each compound in this work, dilutions of the pure compound were created three times (on different days) and these were analysed (along with CFC-11) on the day that they were created. Each compound has thus been calibrated at three times in order to obtain calibrations uncertainties. This has been clarified in the text by adding the following sentence on line 34 on page 6:

“This calibration procedure was repeated three times for each compound and for a range of dilutions (Table S1).”

We have also included more detailed information on the mixing ratios the diluted compounds in an additional table in the Supplement (see comment 1.5.32), to which we now refer in the text.

1.3.18 p. 7, l. 31. How can an accuracy be negative (-5.5%).

This is a good point. It is strictly speaking indeed not the accuracy, but instead an offset of our calibrations compared to calibrations done by NOAA. We use this offset as a measure of

the accuracy of our calibrations, as the NOAA CFC-11 scale is one of the most internationally recognised calibrations. The negative value therefore indicates that the lab calibrated mixing ratio determined for the reference compound is lower than the mixing ratio certified by NOAA. To make this clearer, we have amended lines 25-30 on page 7:

Original text: “To determine the accuracy of the calibrations, trichlorofluoromethane (CFC-11) was diluted along with the pure PFCs as a reference compound, as our working tank has been calibrated by the globally recognised CMD (Global Measurement Division) of the NOAA-ESRL (National Oceanic and Atmospheric Administration - Earth System Research Laboratory) for CFC-11. For all UEA calibrations, the average difference with values determined by NOAA show that the UEA calibrated concentrations for CFC-11 are consistently slightly lower by on average 4.2%± 0.3%.”

Revised text: “**To obtain a measure of accuracy** of the calibrations (**as in Laube et al. 2010; 2012**), trichlorofluoromethane (CFC-11) was diluted along with the pure PFCs as a reference compound, as our working tank has been calibrated by the globally recognised CMD (Global Measurement Division) of the NOAA-ESRL (National Oceanic and Atmospheric Administration - Earth System Research Laboratory) for CFC-11. For all UEA calibrations, the average **offset** with values determined by NOAA show that the UEA calibrated concentrations for CFC-11 are consistently slightly lower by on average 4.2%± 0.3%.”

Original text in caption of Table 4: “Mixing ratios determined in the working standard, precisions of the calibrations, and accuracies of CFC-11 calibrations compared to NOAA scales.”

Revised text: “Mixing ratios determined in the working standard, analytical precisions of the calibrations, **and measures of** accuracies of CFC-11 calibrations **expressed as relative differences to NOAA scales ((UEA-NOAA)/UEA).**”

“Accuracy for CFC-11 [%]” in header of Table 4 has been changed to “**CFC-11 Difference to NOAA [%]**”

1.3.19 p. 7, l. 31: It is incorrect to say that the improvement by the new calibration scale is significant. The improvement is max 2.8% as stated earlier. What improved a lot are the measurement results of the field samples, because i-C4F10 is now excluded from the n-C4F10 measurements. Again, this is mainly a correction of older air measurements, not an improvement of a scale.

We agree that the improvement is max. 2.8% for C4F10. However, we are not stating that there is a significant improvement of the C4F10 calibration scale. In the text referred to by the referee, we are specifically referring to the calibration scales of C6F14 and C7F16. We are also not stating that the improvement for these two PFCs is significant. Instead, we state that it is substantial, as indicated by the degree of overestimation of the mixing ratios for the n-isomer of C6F14 and C7F16. With regards to the improvement of the calibration scale, please also see our response to comment 1.2.10.

1.3.20 p. 7, l. 34: 1) How did you get to the 20% and 11%. Perhaps explain in more detail in the supplement. 2) Labeling a calibration scale 'new' calls for problems down the road. It would be much clearer to give it a name.

- 1) The 20% and 11% is determined based on the relative difference in the concentration determined for the n-isomer of C6F14 and C7F16, respectively, in the working standard between the two (old and new) calibration scales. The old calibration scale was derived before the isomers were separated (i.e. when the signal in the working standard was calibrated against pure n-isomer when it actually consisted of multiple isomers) and the new calibration scale was derived when isomers in the working standard were analytically separated. Instead of including this in the supplement, we decided to clarify this in the text (page 7, line 34) by inserting the following: "These levels of improvement in the UEA2018 calibration scale are determined based on the relative difference in concentration determined for the respective n-isomers in the working standard between using the UEA2010 and the UEA2018 calibration scales."
- 2) We agree with the referee that this is a good idea. We have done so by modifying p. 6 line 31, in which we now give the old calibration and new calibration scale the following labels: UEA2010 and UEA 2018, respectively. Please also see the given labels used in the response to the previous comment.

Original sentence: "The previously reported calibration scales (Laube et al., 2012) were revised to accommodate the separated isomers."

Revised sentence: "The previously reported calibration scales (Laube et al., 2012) (**now referred to as UEA2010**) were revised to accommodate the separated isomers. **The new calibration scale is referred to as UEA2018**"

1.4.21 p. 8, l. 4: 'horizontal'. Shouldn't this be 'vertical'?

To avoid confusion, we have removed "horizontal" and replaced it with "atmospheric".

Original sentence: "The model domain consists of 24 equal-area, zonally averaged latitudinal bands, which each have twelve horizontal layers between the surface and the maximum altitude represented in the model."

Revised sentence: "The model domain consists of 24 equal-area, zonally averaged latitudinal bands, which each have twelve **atmospheric** layers between the surface and the maximum altitude represented in the model."

1.4.22 p. 8, l. 7: Why would a 'not fully represented' atmospheric layer justify leaving it out, there is a good part of the stratosphere in the model.

PFCs are only destroyed by photolytic processes in the mesosphere, which is not represented in the model. Since there are no sources in the upper part of the model domain, there is no gain in including the stratosphere for the purposes of determining global emissions. It has been recently pointed out by Ray et al., Nature Geoscience, 2020, that the stratosphere can indeed have an impact on tropospheric long-term mixing

ratio trends. However, this is only the case for species that have their main sink region in the stratosphere and can also be measured with very good precisions of <0.3%. Neither is the case for any of the PFC species measured in this work.

While responding to this comment, we noticed that we had mistakenly stated that photolytic loss of PFCs also occurred in the stratosphere. We have now corrected this sentence. See below.

Original sentence: “Photolytic loss would only be relevant at stratospheric and mesospheric altitudes (Morris et al., 1995), which are not fully represented in the model domain.”

Revised sentence: “Photolytic loss would only be relevant at mesospheric altitudes (Morris et al., 1995), which are not represented in the model domain.”

1.4.23 p. 10, l. 10: 1) Provide some more intercomparison for the c-C4F8 mixing ratio of this study and that of Muhle et al., 2019, either here or in the supplement. 2) Add the Muhle et al. CGAA mixing ratio to the present results. Are the deviations a constant ratio or are there potential nonlinearity issues. 3) Can you derive a calibration scale factor between the UEA and the SIO scales, perhaps based on the CGAA re-sults, or other ways of intercomparisons (Tacolneston?). A well-derived conversion factor is extremely useful e.g. for users of the many data sets presented here and in Muhle et al.

- 1) A comparison has already been done in the Muhle et al., 2019 paper, up until 2010 in the time series. Since the focus of our paper is on updating the time series, we have now included the following text on page 10 line 20-26, quantifying the differences between the results in Muhle et al. and in our work:

Original paragraph: “The c-C4F8 mixing ratio in the Southern Hemisphere increased from 0.31 ppt in 1978 to 1.52 ppt by the end of 2017 (Fig. q3). This is slightly less than the mixing ratios of 1.6 ppt reported in the recent work of Mühle et al. (2019) with the difference most likely being due to the two independent absolute calibration scales. As reported previously by Oram et al. (2012), the mixing ratios seemed to stabilise in the 1990s, but picked up again in the 2000s. The extended time series since 2008 indicate a continuing increasing trend similar to the one pre-1990, totalling in a 27 % enhancement in the last eight years (2010-2018). In fact, atmospheric c-C4F8 abundances show accelerating growth in recent years, potential reasons for which are explored in Section 3.2.1.”

Revised paragraph: “The c-C4F8 mixing ratio in the Southern Hemisphere increased from 0.31 ppt in 1978 to 1.52 ppt by the end of 2017 (Fig. q3). As reported previously by Oram et al. (2012), the mixing ratios seemed to stabilise in the 1990s, but picked up again in the 2000s. The extended time series since 2008 indicate a continuing increasing trend similar to the one pre-1990, totalling in a 27 % enhancement in the last eight years (2010-2018). In fact, atmospheric c-C4F8 abundances show accelerating growth in recent years, potential reasons for which are explored in Section 3.2.1. **Muhle et al. (2019) reported a slightly higher mixing ratio of 1.61 ppt at the end of 2017 in the high latitude Southern Hemisphere. Since Muhle et al. (2019) already compared their Southern Hemisphere time series**

to ours until 2008 (published in Oram et al., 2012), we here focus our comparison on the extended part of the record, i.e. from 2008 until 2017. The average difference of annual mixing ratios for this part of the time series is 0.09 +- 0.01 ppt (1-sigma). This difference, which is equivalent to an average of 7%, is to some degree likely due to the two different independent absolute calibration scales. However, since the difference is clearly not constant over time (see Fig. 3A), which has also been discussed in Muhle et al. (2019), no simple conversion factor can be derived for the two data sets.”

Similarly, we have included more information on the comparison of the emission estimates for c-C4F8 between the two papers on page 14 line 15-17.

Original text: “Annual emission are now approaching rates of 2.0 Gg yr⁻¹, which are, within uncertainties, comparable to rates determined for the mid-1980s. This compares quite well with the estimated global emissions of 2.2 Gg yr⁻¹ in 2017 by the recent work of Mühle et al. (2019).”

Revised text: “Annual emission are now approaching rates of 2.0 Gg yr⁻¹, which are, within uncertainties, comparable to rates determined for the mid-1980s. This compares quite well with the estimated global emissions of 2.2 Gg yr⁻¹ in 2017 by the recent work of Mühle et al. (2019). The average difference between Muhle et al.’s (2019) and our emission estimates for 2008-2017 is 0.17 +_0.09 Gg yr⁻¹ (1-sigma). However, the two data sets agree within the uncertainty ranges.”

- 2) Done.
- 3) Please see our response to point 1.

1.4.24 p. 12, l. 12. ‘smaller elevations’ Relative or absolute, or both?

Original sentence: “Third of all, smaller Northern Hemispheric sources of n-C4F10 and n-C5F12 compared to c-C4F8 are reflected by the smaller elevations of their mixing ratios measured in Taiwan, despite their enhancement compared to Cape Grim measurements”

Rephrased to “Third of all, smaller Northern Hemispheric sources of n-C4F10 and n-C5F12 compared to c-C4F8 are reflected by the smaller elevations of their mixing ratios measured in Taiwan relative to those of c-C4F8, despite their enhancement compared to Cape Grim measurements”.

1.4.25 p. 12, l. 22 and 25. The mentioning of the chemical formula in the parentheses is not necessary as already introduced earlier on p. 4.

The chemical formulas in lines 22 and 25 on page 12 have been removed.

1.4.26 p. 13, l. 14. ‘Mixing ratios in Taiwan : : :’ for which years?

We are here referring to the mixing ratios measured in Taiwan between 2015-2016. The text has been updated: “Mixing ratios in Taiwan in 2015 and 2016 ...”

1.4.27 p. 16, l. 34: Can you rule out that EDGAR has taken some emission results from Laube et al., 2012 to feed into their calculations and output? There are rumors that

EDGAR is not always strictly taking in-ventory emission estimates. It might be worth to ask. Similar question for EDGAR and Ivy results (n-C7F16).

The EDGAR emissions and the differences between the EDGAR emissions and top-down emission estimates have not notably changed since the publication of the data in Laube et al., 2012, and Ivy et al., 2012. We therefore have no reason to believe such rumours.

1.4.28 p. 17, l. 17. Please rephrase second part of that sentence, it is difficult to understand. Also the comment in parentheses (our calibration changed by 11%) appears odd, it does not seem to be the calibration that changed much, but the measured air samples changed a lot due to the fact that separation is now possible.

Original sentence: "However, to assume that the measured C7F16 in previous work only consists of n-C7F16 would overestimate n-C7F16 mixing ratios by an unknown amount (our calibration changed by 11 %, see Section 2.3), because even though previous work diluted high purity compounds in calibration work, the amount of likely unseparated isomers present in their working standard tanks and samples remains unknown."

Revised sentence: "However, to assume that the measured signal for C7F16 in previous work only consists of the n-C7F16 isomer would overestimate n-C7F16 mixing ratios by an unknown amount (see Section 2.3), because the signal for C7F16 in the working standard tanks and in the air samples is not exclusive to the n-isomer, as isomers were not separated in the earlier studies."

We have removed the mentioning of the 11%, because it has been explained in Section 2.3 and is clarified according to comment 1.3.20. The second part of this comment (1.4.28) has also already been addressed in our response to comment 1.2.10.

1.4.29 p. 18, l. 1: eliminate one of the 'with'

Done.

1.5.30 p. 18, l. 28. 1) How can cumulative emissions represent a percentage increase?

Please

rephrase. 2) Publish the measurement results in the supplement, preferably, in tables/files that are easy to download and use for future users. 3) Clearly state, which calibration scale the individual data sets are reported on.

This represents an increase of 23 % between the beginning of 2010 and the end of 2017.

- 1) The cumulative global CO₂ equivalent of the PFCs discussed in the work are 23% higher in 2017 compared to 2010. We clarify it by rephrasing the sentence in question:

Original sentence: "This represents an increase of 23 % between the beginning of 2010 and the end of 2017."

Revised sentence: "This represents an increase **in the total global cumulative CO₂ equivalent** of 23% between the beginning of 2010 and the end of 2017. "

- 2) All measurement results are made publicly available through a DOI, in accordance with ACP guidelines. We have included a statement in the data availability section of the paper: “The measurement and modelling data presented in this work have been made available on Zenodo and can be publicly accessed using DOI 10.5281/zenodo.3519317, or by contacting e.droste@uea.ac.uk.”
- 3) The methods sections covers that n-C4F10, i-C6F14, n-C6F14, and n-C7F16 in this work have been re-calibrated in order to account for the separation of the isomers and that thus these compounds have a new calibration scale. It has also been stated that the re-calibration of c-C4F8 and n-C5F12 was deemed unnecessary, for reasons explained in the paper. The calibrations used for these compounds in this paper are thus the same as in previous work produced by our lab. We feel that the methods section makes this sufficiently clear. In response to an earlier comment, we have given the calibrations scales a clear label, i.e. UEA2010 and UEA2018.

1.5.31 Table 1, footnote a). State somehow that the assumption made on lifetime is one made

in the present work, and not in Myhre et al.

Done. “The lifetime for i-C6F14 in this work is here assumed to be the same as ...”

1.5.32 Table 4: 1) What are the analytical precisions of the calibrations exactly? 2) Is there a reason

they are given as ranges, and not as mean value? It is difficult to understand for several reason, one because there is not a clear mentioning of how many primary calibration standards are made, if and how these are propagated (to what) and how many working standards are used. 3) Also, mixing ratios in the primary calibration mixtures should be given. 4) Explain ‘accuracy for CFC-11’ more in detail. Why isn’t this simply a deviation (ratio) between the UEA primary calibration CFC-11 and that of NOAA? 5) Again, why ranges? 6) Also, ranges are given in an inconsistent way, sometimes from a small number to a large number (-1.4 to 2.8) and sometimes from a large number to a small number (-1.78 to -5.47). 7) Footnote a) I don’t understand the second part of the sentence (by calibrating pure compounds). 8) I don’t understand footnote b), please rephrase.

- 1) The analytical precision of the calibration refers to the 1-sigma standard deviation of the same working standard that was run several times before and after each calibration run in the same manner as the analytical precision for the samples is determined. As each sample was calibrated three times, the range for the precisions are given in this table. We have updated Table 4 by adding the average analytical precisions for the calibrations and keeping the ranges in brackets.

The following line has been added on line 25 on page 7:

“The latter is the relative 1-sigma standard deviation of the compound signal in multiple working standard runs analysed on the day of each calibration.”

The caption of Table 4 has been updated:

Original caption: “Mixing ratios determined in the working standard, precisions of the calibrations, and accuracies of CFC-11 calibrations compared to NOAA scales. For details on the calibration of c-C4F8 and n-C5F12, consult Oram et al. (2012) and

Laube et al. (2012)”

Revised caption: “Mixing ratios determined in the working standard, average analytical precisions of the calibrations, and measures of accuracies of CFC-11 calibrations expressed as the average relative differences compared to NOAA scales ((UEA-NOAA)/UEA). The analytical precision is the relative 1 sigma standard deviation of the compound signal in multiple working standard runs analysed on the day of each calibration. The ranges of analytical precisions and differences to NOAA are shown here for each compound in brackets and include all three calibrations done in this work for that compound. For details on the calibration of c-C4F8 and n-C5F12, consult Oram et al. (2012) and Laube et al. (2012).”

- 2) By addressing comment 1.3.17, we have already added the information on how many calibrations were done per compound. In the text (line 25, page 7) we do indeed write that we are reporting average precisions in Table 4. We have decided that we will show the average precisions in the table, along with the range in brackets.
- 3) We have created a table (new Table S1) with this information and have appended it into a new section within the Supplement, named “Additional Calibration Details”. Please see comment 1.3.17.
- 4) Please see the response to comment 1.3.18.
- 5) It was chosen to show ranges in order to stay consistent with the accuracy reported in Laube et al. 2012, which is also done in ranges. However, we agree that it would be clearer to show the average offsets to NOAA as well and have added them in Table 4. Caption has been edited to be consistent with the changes to the table (see point 1 of this comment).
- 6) Ranges changed to be consistent (smaller to larger).
- 7) Original sentence: “Mixing ratios determined in working standard by calibrating pure compounds.”
Rephrased sentence: “New calibration (UEA2018).”
- 8) As described in the text, some PFCs were not re-calibrated for the working standard used in this study as they do not have isomers that significantly affect the signal of the peak of the isomer in question.

Original sentence: “Mixing ratios determined in working standard by converting calibrated mixing ratios in the previous working standard to current working standard.”

Revised sentence: “Old calibration (UEA2010)”

1.5.33 Figure 2: 1) Contribution of what? 2) Spelling mistake in legend (Cenral China)

1) Original sentence: “Regions for which the contribution to the footprint simulated by the NAME model is quantified.”

Rephrased to: “**Regions used in the NAME model to quantify the simulated contributions to particle densities in Taiwan.**”

2) The typo in legend has been corrected. Double check size of figure after recompiling file.

1.5.34 Figure 5. It is very difficult to quickly get a good overview on this plot. The comment on the second-ary axis does not help much to directly understand, which of the two axes belongs to which com-pound. Suggest to extend '(blue circles)' by '(blue circles, left axis)', and correspondingly for '(green circles)', and then delete the sentence 'Note that : : :.'. Also, it would help a lot of the upper three sym-bols and descriptions would correspond to the upper part of the plot, i.e. suggest to put the three i-C6F14 legend entries on top (the current reversed way is the part that confuses most in this plot) (see Fig 4 where this is done correctly). Or split the legend in two. It would help to color-code the axis number and labels according to the plot colors. Lastly, it would also help if the left axis numbers stopped at the maximum values of the concentrations, i.e. at around 0.08 ppt. The sentence 'Data pri-or to 2010 : : :.' is incorrect, there are open circles up to about 2013. There is either no light blue or no dark blue shaded area visible on this plot. The symbol plot colors are difficult to distinguish and in some cases of similar tone for the two different compounds. The legend symbol size should be made larger (on a printed copy, they can hardly be distinguished in their colors). Suggest to set the left x axis limit somewhat prior to 1978 to show the 1978 results in full (there seems to be one green circle at 1978. No blue circle?). Space required before '[ppt]' for n-C6F14 for both main and inset axis. Some of these comments apply to some of the other figures.

We thank the reviewer for these useful suggestions and have implemented all of them apart from the following:

- Changing the order of the symbols in the legend. We have instead followed the alternative suggestion to split the legend.
- Limiting the (originally) left axis scale to the maximum values of the concentrations. The scales of the y axes are chosen in a way that the curves will not overlap in the figure.
- Changing the symbol plot colours. The colours in all figures have been carefully chosen as to be clearly distinguishable, by colour-blind people as well as on a printed grayscale copy.
- Shifting the left x axis limit. Our time series starts in 1978. We would like to keep consistency in all our graphs.

We recognised that the plot was difficult to quickly interpret, which is why we have also made the following additional changes in order to improve it:

- Switched the y axes so that the upper curve (now n-C6F14) is plotted on the left y axis, i.e. the one that it is closest to.
- Switched the colour coding of the two isomers to match the change above.
- Slightly enlarged the size of all markers in the plots to improve visibility.
- Removed the gridlines in response comment 2.4.19.
- We made changes to the caption in order to make it consistent with the changes in the plot (as outlined above). These also include the comments made in 1.5.34.

Original caption: “A) Mixing ratios at Cape Grim of i-C6F14 (blue circles) and n-C6F14 (green circles) between 1978 and 2018. Note that data for n-C6F14 are plotted on a secondary axis. Data prior to 2010 are shown as empty symbols (Laube et al., 2012), while data from samples collected after 2010 are shown as filled symbols to illustrate the part of the time series that is extended in the current work. Note that the data from Laube et al. have been converted to a new and improved calibration scale. The atmospheric trends simulated by the model are represented by the red line for i-C6F14 and by magenta line for n-C6F14. Total uncertainties (light blue for i-C6F14, light green for n-C6F14) and trend uncertainties (dark blue for i-C6F14, dark green for n-C6F14) are indicated with the shaded areas along the trend line. B) i-C6F14 mixing ratios after 2010 for Cape Grim (blue circles), for Tacolneston (orange diamonds), and Taiwan (light blue squares); n-C6F14 mixing ratios after 2010 for Cape Grim (green circles), for Tacolneston (light green diamonds), and Taiwan (magenta squares). The red and magenta lines indicate the modelled Southern Hemisphere baseline trend at Cape Grim for i-C6F14 and n-C6F14, respectively; while the dashed red and magenta lines indicate the modelled trend for mixing ratios at Tacolneston for i-C6F14 and n-C6F14, respectively. Total and trend uncertainties are indicated with the shaded grey areas along the Tacolneston dashed-trend lines for both i-C6F14 and n-C6F14.”

Revised caption: “A) Mixing ratios at Cape Grim of **n-C6F14 (blue circles, left axis) and i-C6F14 (green circles, right axis)** between 1978 and 2018. Data prior to 2010 are shown as empty symbols (Laube et al., 2012), while data from samples collected after 2010 are shown as filled symbols to illustrate the part of the time series that is extended in the current work. Note that the data from Laube et al. have been converted to a new and improved calibration scale. The atmospheric trends simulated by the model are represented by the red line for **n-C6F14** and by **magenta line for i-C6F14**. Total uncertainties (**light blue for n-C6F14, light green for i-C6F14**) and trend uncertainties (**dark blue for n-C6F14, dark green for i-C6F14**) are indicated with the shaded areas along the trend line. **Note that there is only a very small difference between the trend and total uncertainties and thus the latter is difficult to distinguish.** B) **n-C6F14** mixing ratios after 2010 (**left axis**) for Cape Grim (blue circles), for Tacolneston (orange diamonds), and Taiwan (light blue squares); **i-C6F14** mixing ratios after 2010 (**right axis**) for Cape Grim (green circles), for Tacolneston (light green diamonds), and Taiwan (magenta squares). The red and magenta lines indicate the modelled Southern Hemisphere baseline trend at Cape Grim **for n-C6F14 and i-C6F14**, respectively; while the dashed red and magenta lines indicate the modelled trend for mixing ratios at Tacolneston **for n-C6F14 and i-C6F14**, respectively. Total and trend uncertainties are indicated with the shaded grey areas along the Tacolneston dashed-trend lines for both **n-C6F14 and i-C6F14**.”

1.6.35 1) Fig. 7: Add the Muhle et al. 2019 emission results to this graph. 2) Fig 7 – 9: Colors are difficult to distinguish. Use methods to better distinguish the various lines. E.g. in Fig. 7, the Oram et al. results aren't visible for most of the record.

- 1) Done.
- 2) Done. The emission data from Laube et al. is now plotted in the same colour as the emission data from the current work (although the different line styles makes clear

distinctions between them). The emission data from Ivy et al. for C5F12 in figure 8 has been plotted in a different colour to make a clear distinction with the plotted data from Ivy et al for C4F10. The line styles have also been changed to make the distinction clearer. For Figure 9 specifically, we have changed the line style and colour for the curve illustrating the sum of emission estimates of the two C6F14 isomers.

Inspired by the suggestions made in comment 1.6.34 for the trend plots, we have made minor changes to the legends in the emission plots: we split the legend between symbols belonging to two different PFCs whenever we plot the emission estimates for more than one PFC in the same graph.

Captions of all emission plot figures have been updated accordingly. We hope that these changes have improved the emission plots.

1.6.36 References: p. 24, l. 18: capitalize 'US'.

Done.

1.6.37 Fig. S1. Section reference missing (currently ??).

Done.

1.6.38 1) Fig. S2. Line 2. 'samples collected after 2005'? or 'Samples measured after 2005'? Why? 2) There is a large difference between the ion ratios for the calibration standard and the tank samples, why? This large difference implies that there is still some kind of a co-elution on the column used in the present work. Perhaps an integration problem? 3) Mention here or elsewhere in the text, what mixing ratios the 'new' calibration standard has, and perhaps here, what the differences in peak sizes are typically for the CGAA samples and for the cal standard.. 4) Also, for some compounds, the ion ratio of the 'old' Laube 2012 calibration scales could be added to here.

- 1) Samples collected after 2005. This has been corrected.
- 2) This point has been addressed in our response to comment 1.3.15.
- 3) The mixing ratios determined for each PFC are already recorded in Table 4. The mixing ratios of the diluted pure compounds used in the calibration procedures are included into a separate table (Table S1) in the supplementary material. As the peak sizes in the CGAA samples substantially change over time, there is not "typical" difference with the working standard. We would be happy to provide these technical details on request, but this information is not relevant for any of the scientific messages in this paper.
- 4) The purpose of this particular graph is to show that the ion ratio in the calibration standards and the Cape Grim samples are consistent and not changing over time. We feel that adding outdated ion ratios would only confuse the reader.

Responses to Referee #2

General Comments:

2.2.1 Near where the isomers are first mentioned in the Introduction, it might be worth providing a paragraph that has a little more background on isomers (e.g., definition, explain the nomenclature n-isomer, i-isomer), and bringing this together with explanation of the significance of measuring the different isomers. The potential for distinguishing different source types is mentioned on page 4, line 23 and the different radiative efficiency is mentioned on page 4, line 9, and there is some discussion of the implications of separation of isomers from a measurement point of view elsewhere, but these points are interspersed with lots of other details, risking losing the overall significance of the work. A paragraph that discusses the significance of isomers in general, before going on with the details of this study, would be beneficial.

We agree with the referee that including more introductory details would be beneficial to the paper. We have added the following to the introduction (page 3 line 20):

Previous line: Previously reported PFC trends in the atmosphere include CF₄, C₂F₆, octafluoropropane (C₃F₈), cyclic-octafluorobutane (c-C₄F₈), decafluorobutane (C₄F₁₀), dodecafluoropentane (C₅F₁₂), tetradecafluorohexane (C₆F₁₄), hexadecafluoroheptane (C₇F₁₆), and octadecafluorooctane (C₈F₁₈) (Laube et al., 2012; Ivy et al., 2012a; Oram et al., 2012; Mühle et al., 2010; Mühle et al., 2019)."

New text added to the end of the paragraph: "No isomers of these PFC species have been reported in the atmosphere before. As the GWPs and atmospheric lifetimes can differ substantially between isomers (Bravo et al., 2010), it is important to ascertain the full analytical separation and quantification of such isomers."

2.2.2 A clearer description of uncertainties is needed in Section 2.5. 1) E.g., page 8, line 31 - what is the "averaged model-fit uncertainty of the Cape Grim trend" and how is it calculated? 2) page 9, line 9 - "After these uncertainties were calculated" - uncertainties in what, PFC trends? Page 9, line 9 - "the model was re-run" - the inversion for emissions? 3) I don't really understand this paragraph (lines 9-14). I do understand why you would want trend uncertainties without calibration uncertainty, it is the details of the description that I believe should be improved.

1) We have added more information on what the model-fit uncertainty entails and made a reference to an earlier section that covers the analytical uncertainty on page 8 line 32 : "The analytical uncertainty is described in Section 2.2. The model-fit uncertainty is the average relative difference between the observed mixing ratio and the simulated mixing ratio."

The average analytical uncertainty and average best-fit uncertainty have been added to (what is now) Table S1.

2) We have improved our explanation of how the emission uncertainties are determined:

Original sentence: "After these uncertainties were calculated, the model was re-run using the best fit of the observed mixing ratios adjusted by the uncertainties to estimate the maximum and minimum emissions."

Rephrased: “The “trend uncertainty” and the “total uncertainty” for each PFC were used to determine the respective uncertainty bands around the observed mixing ratio trend. The model was then re-run to find the emissions that fitted the simulated maximum and minimum mixing ratios best. The result is the minimum and maximum emissions according to both types (“trend” and “total”) of uncertainties.”

- 3) Lines 9 to 10 have been rephrased in point 2. Lines 10-14 (see below) have been moved to the end of section 2.2, because we decided that even though these lines discuss the errors/uncertainty in the measurements, it makes more sense to keep this information with the section that actually discusses the measurements.

Lines 10-14: “Measurement errors (indicated by the error bars on the observational data points) consist of a combination of the 1 sigma standard deviations of the working standard and sample replicates on the same analysis day. For samples that have been analysed against the previous working standard, the uncertainties include the aforementioned internal conversion accounted for as the 1 sigma standard deviation of the peak ratio on inter-comparison days (n=8).”

The title of section 2.5 has subsequently been changed from “Uncertainties” to “Trend and Emission Uncertainties” to make this distinction clear.

2.2.3 I am confused about the conclusion regarding the interhemispheric gradient of n-C6F14 and i-C6F14 (last sentence of section 3.1.3). Around page 13, line 7, I thought the authors were saying that the observations were close to or slightly exceeding a ratio of N:S mixing ratio the same as c-C4F8 (1.05), but that the measurement uncertainties were too large to discern the interhemispheric gradient. The conclusion at page 13, line 20 says that the NH sources are not as substantial - is this referring to NH sources relative to SH sources, and therefore influencing the interhemispheric gradient? We know that the recent total emissions for c-C4F8 are around 10 times the emissions of n-C6F14 and i-C6F14, so it is perhaps not surprising that the interhemispheric gradient will be small in an absolute sense, but that doesn't tell us about the relative sense. But I don't think we can conclude anything about the N-S distribution of emissions due to the N-S mixing ratio difference expected for typical N-S emissions distribution, relative to the measurement uncertainty.

We were indeed comparing the NH sources of the isomers of C6F14 to those for c-C4F8 in a relative sense. However, the comment made here is very valid and we have adjusted lines 18-20 on page 13:

Original sentence: “Even though a large range of mixing ratios is observed at Tacolneston and in Taiwan for both compounds, the lack of a discernible interhemispheric gradient (given the measurement uncertainties) suggests that the Northern Hemispheric sources are not as substantial as they are for, for example, c-C4F8.”

Revised sentence: "Even though substantial variability of mixing ratios above the Cape Grim baseline for both C6F14 isomers is observed at Tacolneston and in Taiwan, the low absolute mixing ratios in both hemispheres combined with the measurement uncertainties do not allow for any further conclusions on the hemispheric distribution of their emissions."

Specific Comments:

2.3.4 page 3, line 4 - "As a result" - of what? Provide a better link to the previous sentence.

Original sentence: "... by their strong infra-red absorption properties and inertness. As a result, PFCs can have global warming potentials (GWPs) of ..."

Revised sentence: "... by their strong infra-red absorption properties and inertness. As a result of these physical and chemical properties, PFCs can have ..."

2.3.5 page 3, line 13 - "Other sources include ..." is this still talking about the low mass PFCs? Maybe "Other sources of PFCs include..."

Done.

2.3.6 page 10, line 16 - perhaps replace 'sources' by 'pieces' or 'lines', and leave the word 'sources' to describe emissions to the atmosphere. Same on line 19.

Done. "Sources of evidence" on these two lines has been replaced by "pieces of evidence".

2.3.7 page 10, line 21 - "This is slightly less..." - what is? The 2017 value is slightly less?

The reviewer is correct. Please see our response to comment 1.4.23, where we have rephrased the sentence.

2.3.8 page 12, line 2 - specify whether this is the interhemispheric ratio of emissions or mixing ratio

This refers to the IH ratio of mixing ratio. This is now made explicit in the text.

Original sentence: "If the interhemispheric ratio for n-C4F10 and n-C5F12 were to be similar to that of c-C4F8, then the differences between the Cape Grim and Tacolneston data would have to be at least 0.01 ppt."

Revised sentence: "If the interhemispheric ratios of the mixing ratios of n-C4F10 and n-C5F12 were to be similar to that of c-C4F8, then the differences between the Cape Grim and Tacolneston data for these two PFCs would have to be at least 0.01 ppt. "

2.3.9 page 12, line 22 - "The trends are somewhat similar" - to what? Each other? Another PFC?

Original sentence: "The trends of i-C6F14 and n-C6F14 are somewhat similar. "

Rephrased to: "The trends of i-C6F14 and n-C6F14 are somewhat similar to each other."

2.3.10 page 12, line 23 - The fastest increase occurred in the mid to late 1990s.

Original sentence: "Its fastest increase in atmospheric abundance occurred in the 1990s and has since slowed down."

Revised sentence: "The fastest increase in atmospheric abundance occurred in the 1990s and has since slowed down."

2.3.11 page 13, line 4 - I would add the years, i.e. "Mixing ratios in Taiwan in 2015 and 2016 are again ..."

Done.

2.3.12 page 15, line 21 - change to "for n-C4F10 (Fig. 8) and n-C5F12 (emissions < 5.3x10⁻⁵ Gg/yr)." as only emissions for n-C4F10 are shown in Fig 8. I know this is specified in the caption, but simpler for the reader to also specify here.

Done.

2.3.13 page 16, line 4 - Add "Cape Grim" as follows: "However the Cape Grim data in this time period"

Done.

2.3.14 1) page 16, line 15 - "although within the uncertainties of the early data set this is not a significant difference" - isn't it the sparsity of the data (i.e. timing of the increase depends on one sample, around 1996) rather than the data uncertainties as indicated in the figure that mean we can't be conclusive about the timing of each increase? 2) Is there a clue to the timing (of the n-C6F14 increase, at least) from the Ivy measurements of the Cape Grim air archive, as these are more dense in time?

- 1) We agree with the referee. The scarcity of the data is certainly the main reason we cannot be conclusive about the timing of the emissions increase. We have therefore revised our statement in the text.

Original text: "In contrast with n-C6F14, emission rates for i-C6F14 are estimated to have started increasing in 1992 (rather than in 1994, as estimated for n-C6F14, although within the uncertainties of the early data set this is not a significant difference) and its initial rate of increase is not as fast. It reaches a maximum of 0.25±0.02 Gg yr⁻¹ in 1996-1997, which is when n-C6F14 emissions reach their maximum values as well."

Revised text: "Emission rates for i-C6F14 are estimated to have started increasing in 1992. This is in contrast to 1994, which is what was estimated for the onset of significant n-C6F14 emissions. However, the measurement uncertainties and especially the sparsity of the early data set do not allow for any further conclusions on the exact timing of the onset of emission increases for both isomers. i-C6F14 emissions increase at a slower rate than those for the n-isomer and reach a maximum of 0.25±0.02 Gg yr⁻¹ in 1996-1997, which is when n-C6F14 emissions reach their maximum values as well."

- 2) Since Ivy et al. measurements represent a mixture of the C6F14 isomers, they cannot provide unequivocal determination of the timing of the onset of the emission increases of the individual isomers. This is especially the case since our data allow for the possibility of a difference in the timing of onset of increased emissions for the two isomers.

2.4.15 page 16, line 16 - What does 'It' refer to? i-C6F14 emissions, presumably, but please specify.

i-C4F14 emissions. Done (see revised sentence as part of our response to comment 2.4.15, point 1).

2.4.16 page 16, line 29 - 'peak emission rates have increased' - please be clear what you are comparing here (n-C6F14 alone and the sum n-C6F14 + i-C6F14?)

Done.

Revised: "Two, peak emission rates of the sum of the C6F14 isomers have increased from ..."

2.4.17 page 16, line 33 – 1) what is being compared to EDGAR emissions here? Are you comparing the black dashes with the red dots? 2) Do they agree exceedingly well?

- 1) We are indeed comparing the EDGAR emissions (black dashes) with the red dots (i.e. the sum of the emissions of the two isomers of C6F14. This is explained in the legend and caption of Fig. 9. Note that the colour for this curve has been changed in the revised version, as part of our response to comment 1.6.35).
- 2) Given that all other PFC emissions do not compare well with the EDGAR emissions at all (i.e. differ several orders of magnitude), the sum of the emissions of the C6F14 isomers does indeed compare extremely well in a relative sense to the EDGAR emissions from 1999 onwards. We have revised the statement (see below).

Original sentence: "Three, the sum of the estimated emission rates of both C6F14 isomers agrees exceedingly well with the EDGARv4.2-reported values from 1999 onwards."

Revised sentence: "Three, **the estimated emission rates of the sum of both C6F14 isomers agree exceedingly well (relative to all other PFCs reported here)** with the EDGARv4.2-reported values from 1999 onwards."

2.4.18 page 18, line 1 and Table S4 - is this talking about the correlation with CO described at the end of page 9? Or just footprints? Please explain what this is.

The correlations referred to here in this sentence are those between PFC mixing ratios and the particle density footprints. The correlations with CO mixing ratios are only used to identify possible source types of PFCs measured in Taiwan. We have clarified this in the following way:

Original sentence(page 18, line 1): "Generally, the PFCs correlate less with any of the 15 regions used to quantify sources of particle densities used in the dispersion modelling, although sample numbers limit the statistics (Table S4)."

Revised sentence: "When PFC mixing ratios are correlated to the 15 regions used to quantify sources of particle densities used in the dispersion modelling, the R-squared values are generally much smaller, although sample numbers limit the statistics (Table S4)."

Original sentence (page 18, line 10): “All PFCs correlate well with energy industry and domestic sources, which is linked to population density (Table S5).”

Revised sentence: “**When using simulated CO mixing ratios as a tracer for source types**, all PFCs correlate well with energy industry and domestic sources, which is linked to population density (Table S5).”

2.4.19 Fig 5 - I found this figure confusing because it is combined, and I think it would be less confusing if it were split into two panels. It is the use of different axes I found most confusing - it gives the wrong impression of the relative magnitude of the two isomers. I had to keep checking the caption/legend to remember which axis to use, and which isomer was which, as I came back to the plot a number of times as I read through the paper. The gridlines (although faint) don't match the right axis. The one advantage of combining the plots is that it is easy to compare the timing of the increase around 1995 for the two isomers, but this could also be done with one plot above the other. If the plot is to remain combined, I suggest plotting the different isomers on the same y-axis. Alternatively, if the different axis ranges are to be maintained then color the axis tick labels and text blue and green to correspond to the colors of the symbols and shaded areas of each isomer, as in Fig 8. You could also put 'i-C6F14' in blue text near the i-C6F14 curve, and similar for n-C6F14 (green text). I think would still prefer it split into 2 panels.

We thank the reviewer for the helpful suggestions in improving this figure. We have implemented these, except for the following:

- We chose not to plot the two isomers on the same axis or to adjust the scale of the secondary y-axis, because the trend of i-C6F14 would not be visible anymore. We agree that splitting the plot would be an alternative solution. However, to minimise the space used by the figures and to allow for a direct comparison of the C6F14 isomer trends, we decided to keep plotting the data for these two isomers in one graph.
- We did not add the names of the isomers in a text box next to the trends, because we instead changed the colours of the axes and axes labels to match the colours of the trend lines.

We have made further improvements to the figure, as has been outlined in our response to comment 1.5.34.

2.4.20 Fig 5 - as the i-C6F14 data only begin around 1987, should the figure only show the red line and blue band from then? Otherwise it gives the impression that mixing ratio is known before 1987, but it isn't here.

We agree with this suggestion and have adjusted both the trend and emission plots for i-C6F14.

2.5.21 Fig 7 - could color the right y-axis text and the EDGAR data as a color other than black, to emphasise that it is on the secondary axis.

The EDGAR data is already distinguishable with the different line style, which is also used for the secondary y-axis. We decided not to change the colour in order to keep all emissions plots consistent with each other. We believe that consistency also helps the reader to interpret the graphs. We chose not to use a different colour for the EDGAR data in all emission plots, because it would be confusing in subsequent plots where various colour schemes are already used.

2.5.22 Fig 9 - it is hard to distinguish the red and magenta dotted lines on my printed copy - I suggest using a more different color or line type.

We have made changes to the colour scheme and line styles in order to make it easier to distinguish between the different lines, also on printed, grayscale copies. Please see our response to comment 1.6.35.

2.5.23 Figures - it might be good to combine the mixing ratio and emissions figures for each PFC, for example combine Figs 3 and 7 as two panels in the same figure, Figs 4 and 8 etc. I found I wanted to look at the mixing ratio plot when I was reading about the emissions and looking at the emissions plot, and combining them would remove the need for flicking back and forth. The text could still remain in the same order, just describe the top (mixing ratio) panels first and come back to the lower (emissions) panels.

Implementing this suggestion would result in mixing ratio trends being less easy to compare between species and would additionally mean that the reader would have to flick back and forth when reading the emission section. We have therefore decided to leave the figures as they are (apart from changes mentioned in responses to previous comments).

2.5.24 The measurements should be made available in a data archive or as downloadable tables in the Supplement.

See our response to comment 1.5.30.

Technical corrections:

2.5.25 page 12, line 18 - Hemisphere
Done.

2.5.26 page 12, line 19 - add 'is' after 'This'
Done.

2.5.27 page 16, line 26 - add 's' to 'emissions'
Done.

2.5.28 page 18, line 1 - with with
Done.

2.5.29 page 20, line 13 - exist, not exists
Done.

2.5.30 Supplement page 2, line 3 - Section ??
Done.

Responses to Referee #3

General Comments:

NA

Specific Comments:

3.1.1 P6 LN 14-16: Since the update of the calibration scale was suggested as one of the key purposes for this article, the absolute calibration procedure needs to be overviewed more in detail than in the current version, and thus readers don't have to search for and read through previous studies cited here.

We understand the concern of the reviewer. However, the calibration methods and procedures are exactly the same as described for the work of Laube et al. (2010). Additionally, if we were to include the absolute calibration procedure into our publication, then it would be put into the Supplement and readers would have to be referred to that too. Since the absolute calibration procedure is thoroughly described in detail in Laube et al.'s (2010) Supplement, the readers are referred to their work, as done in the revised text:

Original text: "The absolute calibration method has been described in detail in Laube et al. (2010) and has been described specifically in Oram et al. (2012) for c-C4F8 and in Laube et al. (2012) for C4F10, C5F12, C6F14 and C7F16, including linearity of the detector response and identification."

Revised text: "The absolute calibration method has been described in detail in Laube et al. (2010) and has been described specifically in Oram et al. (2012) for c-C4F8 and in Laube et al. (2012) for C4F10, C5F12, C6F14, and C7F16, including linearity of the detector response and identification. **For a detailed description and assessment of the calibration procedure and system we refer the reader to the Supplement of Laube et al. (2010). The only procedural difference for the calibrations here is the temperature of the system (100 °C instead of 80 °C).**"

3.2.2 P 7, LN 8: Clarify that the combined influence is <2.8%. Is it a relative difference between the n-C4F10 background concentrations determined based on the two different scales?

We explicitly state that the combined influence of the i-isomer and the leak-tightness of the calibration system is less than 2.8% (page 7, line 7-8). In the subsequent sentence, we have rephrased our explanation of how we arrived at this number and in which we refer to added details in the Supplement:

Original sentence: "This has been determined by comparing the old and the new calibration scale for n-C4F10."

Revised sentence: "This value has been determined by calculating the relative difference of the n-C4F10 mixing ratio in the working standard using the two different (UEA2010 versus UEA2018) calibration scales (see more details in the Supplement)."

3.2.3 P 7, LN 14: What does the ion ratio means? Is it a ratio of peak heights for two chromatograms of m/z=219 and 169? Or a ratio of peak areas?

The ion ratio refers to the ratio of peak areas determined for ions with $m/z = 219$ and $m/z = 169$. This has been clarified in the text as so:

Original text: “The confidence in the complete separation of all isomers for C6F14 and C7F16 is based on the ratio of the two most abundant ions into which these compounds are ionised during mass spectrometry: (mass-to-charge (m/z) ratios 219.0 and 169.0).”

Revised text: “The confidence in the complete separation of all isomers for C6F14 and C7F16 is based on the ratio of the peak areas of the two most abundant ions into which these compounds are ionised during mass spectrometry: (mass-to-charge (m/z) ratios 219.0 and 169.0).”

3.2.4 P 7, LN 14: Fig. S2 was shown earlier than Fig. S1 in the text.

Corrected.

3.2.5 P 7, LN 25: the accuracy derived from the CFC-11 reference compound seems to imply only an accuracy of the dilution process, not “the accuracy of the calibrations” that stated in the text. Otherwise more clarification is needed.

We have clarified that what we originally referred to as the “accuracy” is actually the offset between the CFC-11 calibration and NOAA values, which we use as a measure of accuracy (see our response to comment 1.3.18). We disagree with the referee that our measure of accuracy only represents the accuracy of the dilution process, as it also includes the accuracy of the entire pre-concentration and measurement process.

3.2.6 P 7, LN 30: How was the uncertainty of 0.3% determined? Was it 1-sigma? Then how many data were analyzed ($n=?$)?

It is indeed 1-sigma. $N = 3$. Please see our response to comment 1.3.17, in which we explain how this information has been incorporated into the text.

3.2.7 P 7, LN 31: How could the ranges (4.0-7.8%, and -5.5-2.8%) of calibration accuracy be determined? More detailed explanation should be given.

We have addressed this in our response to comment 1.3.17. Comment 1.5.31 enquired about the decision to report the range instead of the average. We decided to keep the range in brackets and add the average value.

3.2.8 P 7, LN 34: Again, please describe how the overestimation by 20% and 11% could be determined?

Please see our response to comment 1.3.20 by referee #1.

3.2.9 P 8, LN 15-19: The emission distribution for all PFCs seems to be based on the global distribution of C6F14 emissions recorded in the EDGAR database. The figures 7-10 showed the individual EDGAR emission estimate for each PFCs. Then authors need to discuss about how different (or consistent) the emission modeling results would be if the EDGAR emission estimate for each compound were used, instead of the C6F14 emissions record.

To clarify: the input to the model are the annual global emissions. The output is the mixing ratio per atmospheric layer per zonal band. We determine the annual global emissions per

compound by iteratively changing the emission input depending on how well the model subsequently simulates the mixing ratios compared to the mixing ratios observed at Cape Grim. This is explained in Section 2.4 and references therein.

If the EDGAR emission estimates were used as input to the model, as is suggested in this comment, then the result is simply that the simulated mixing ratios will be a lot lower than what we simulate with our emission results, because the EDGAR emissions are a lot lower (except for C6F14).

However, we think that the referee meant us to discuss what the emission modelling results would be if we were to use the emission *distribution* of the EDGAR record for each PFC instead of the emission distribution of C6F14, which we opted to use and apply to all PFC runs.

This is indeed an interesting discussion, because there is a lot about the actual global emission distribution that we do not know. We did not strictly test using each PFC's EDGAR distribution in the model runs, because of the obvious incompleteness of the EDGAR database. For example, in the EDGAR database, all emission sources for n-C5F10 and C7F16 came exclusively from Romania and Japan, respectively. However, we did test a number of different emission distributions to see what the effect would be on the simulated mixing ratios. These emission distributions had in common that 99% of the emissions occurred in the Northern Hemisphere, but they differed in the fraction of global emissions per latitudinal band. The conclusion from these runs is that, given the same global annual emissions, the simulated mixing ratios in the latitudinal band for Cape Grim (SH) are not affected by these variations in distribution. In contrast, the simulated mixing ratios for the latitudinal band for Tacolneston is affected due to the proximity of this latitudinal band to the emission sources.

Thus, even though we did not directly test the suggestion in this comment by the referee, we can say that if the emission distribution based on the EDGAR database for any PFC besides C6F14 is used, then the simulations for the mixing ratio at Cape Grim (which is used to compare to the observations at Cape Grim to obtain the global emission estimate) would not be significantly different compared to using the C6F14 emission distribution, but the simulated mixing ratios at Tacolneston would be impacted.

Nevertheless, we feel that this topic has sufficiently been discussed on page 11, lines 5 to 17. Thus, we have decided not to include any further elaboration.

3.2.10 P 9, LN 6-8: This statement conflicts with a previous comment in page 7 (lines 8- 10):

“Due to the leak-tightness of the system and a lack of observed isomers, a revision of the calibration scales for c-C4F8 and n-C5F12 was deemed unnecessary. If within the calibration uncertainty, their re-calibration was not necessary, why an additional uncertainty besides the calibration uncertainty should be added for these compounds?”

We do not agree that this is a conflicting statement. We justify that a re-calibration of c-C4F8 and n-C5F12 is unnecessary. The additional uncertainty that we attribute to these two particular compounds is not a calibration uncertainty, but an uncertainty in the determination of the mixing ratio in our current internal working standard. Each internal working standard has a different concentration. C-C4F8 and n-C5F12 had been calibrated for an internal working standard that we were using previously, so in order to obtain the mixing ratio of these PFCs in our current internal working standard, we converted the mixing ratio of the former to the latter by using the ratio in the signal of both internal working standards. This ratio carries an uncertainty, which is the uncertainty in question.

3.3.11 P 10, LN 6-11: Explain more in detail how a certain correlation between modeled CO and the PFC mixing ratio can represent which emission source is more associated with PFCs and what extent as well?

We have substituted line 31 on page 9 to line 11 on page 10 by the following:

“For the purpose of identifying the possible sources of PFCs, the NAME footprints were used to calculate the mixing ratio of a tracer at the Taiwan measurement site, given emissions from a range of different emission sectors. Carbon monoxide (CO) was chosen as the tracer because it is emitted from a number of different emission sources and because widely used and tested bottom-up emission estimates of CO are available from the Representative Concentration Pathway 8.5 (RCP 8.5) inventory (Riahi et al., 2011; Van Vuuren et al., 2011) (<http://tntcat.iiasa.ac.at:8787/RcpDb/dsd?Action=htmlpage&page=welcome>). Moreover, the RCP8.5 CO emissions are divided into various emission sectors (industry, power plants, solvents, agricultural waste burning, waste, forest burning, grassland burning, residential, international shipping, surface transportation, and agriculture), allowing us to test whether there was a correlation between the observed PFC mixing ratios and whether the air modelled to have arrived at the measurement site had likely been subject to emissions from any particular sector.

The NAME footprints were combined individually with the distribution of CO emissions from each sector to calculate a modelled mixing ratio of the emitted species at the measurement site (see Supplementary Material Section S5). Emissions were taken for the year 2010, for the timescale of each footprint (12 days) (more details can be found in Oram et al. (2017)). A correlation analysis was performed between the modelled CO from each sector and the measured PFC mixing ratios. Industry (combustion and processing) and solvent applications are expected to show some correlations with PFC mixing ratios, as they are most closely associated with PFC sources and so we would expect their emissions to be co-located. Results of these analyses are found in Section 3.3.”

We have also included an explanation about how the CO emissions per economic sector are calculated in the Supplementary Material (new Section S5).

3.3.12 P 10, LN 28: Clarify where the number of 1.05 came from.

Done.

Original sentence: “... , equivalent to an interhemispheric ratio of 1.05.”

Revised sentence: “... , equivalent to an interhemispheric ratio of 1.05 (**average enhancement of Tacolneston mixing ratio measurements against the background trend at Cape Grim**).”

3.3.13 P 10, LN 29-32: Please compare the current c-C4F8 measurements in Tacolneston with those from Mace Head in Muhle et al. (2019) and discuss and justify the statement of “the lack of variability in the data suggests that Tacolneston is not in close proximity to any major sources of c-C4F8. When considering the simulated atmospheric trend from the emission model for Tacolneston, it can be noted that it overestimates the observed concentrations, despite the well-fitted Southern Hemispheric trend.”

We have already included a comparison of the c-C4F8 Cape Grim time series to the Southern Hemisphere results in Muhle et al. (2019). From this comparison, it was concluded that there is no simple conversion factor between the two data sets. In turn, that means that we cannot use our Tacolneston and Muhle et al.'s Mace Head data to make any further statements on regional emissions. Please see our response to comment 1.4.23.

In addition, we have also modified our statement in lines 29-32 on page 10:

Original sentence: "... the lack of variability in the data suggests that Tacolneston is not in close proximity to any major sources of c-C4F8. When considering the simulated atmospheric trend from the emission model for Tacolneston, it can be noted that it overestimates the observed concentrations, despite the well-fitted Southern Hemispheric trend."

Revised sentence: "... the lack of variability in the data suggests that Tacolneston is not in close proximity to any major sources of c-C4F8. **Such a proximity of sources should cause multiple occurrences of substantially higher mixing ratios, as can be seen in the Taiwan data (discussed below).** When considering the simulated atmospheric trend from the emission model for Tacolneston, it can be noted that it overestimates the observed concentrations, despite the well-fitted Southern Hemispheric trend. "

3.3.14 P 11, LN 6-8: Are they based on the current simulation? Otherwise, add the correspond references.

They are indeed based on the current simulation and therefore no additional reference is necessary.

3.3.15 P 11, LN 30-31: Please discuss how authors could exclude a possibility that the found similarity in the mixing ratio trends between n-C4F10 and n-C5F12 might be due to the fact that they were determined using a same m/z (119).

n-C4F10 and n-C5F12 elute at different times and therefore enter the mass spectrometer at a different time. Specifically, the retention time (i.e. the time after injection when the maximum of the signal peak appears on the chromatogram) for n-C4F10 on ion m/z 119 is 14.04 minutes, while for n-C5F12 on ion m/z 119 it is at 17.62 minutes. This is what distinguishes their peaks from each other, even though they're analysed on the same m/z ion. We do not feel that it is necessary to include this information in the paper.

3.3.16 P 142, LN 18: Much lower mixing ratio elevations were observed where? In Taiwan.

Original sentence: "Much lower mixing ratio elevations for both n-C4F10 and n-C5F12 were observed in 2015."

Sentence rephrased: "Much lower mixing ratio elevations for both n-C4F10 and n-C5F12 were observed in Taiwan in 2015 **compared to 2014 and 2016.**"

3.3.17 P 12, LN 33 – P 13, LN 2: 1) Please explain how author can confirm the ratio shift from 2003-2008 to 2013-2018 periods was statistically significant. How was the uncertainty

of +/-0.01 determined? 2) Are there any possibility that the ratio shift could be related with the re-calibration after 2010?

- 1) We are giving the 1 sigma standard deviations of the ratios for these periods. This has been clarified in the text by adding it in brackets.
- 2) All samples have been re-measured (as described in Section 2.2), so this is not a possibility.

3.3.18 P 13, LN 10-11: For the observed high mixing ratio, authors need to examine their trajectories to argue an influence of a pollution plume.

Only two data points differ from the simulated Tacolneston by more than the 1-sigma measurement uncertainty. Both of these data points would agree within 2-sigma. We have therefore modified the statement as follows:

Original text: "Mixing ratios occasionally exceed the modelled uncertainty envelopes for Tacolneston, such as in 2015. This might imply a plume at the time of sampling. The simulated trend for the Tacolneston data corresponds well with the lower end of the variability in the observations."

Revised text: "Mixing ratios occasionally exceed the modelled uncertainty envelopes for Tacolneston, such as in 2015, **but none of these excursions exceeded the 2-sigma measurement uncertainties.** The simulated trend for the Tacolneston data corresponds well with the lower end of the variability in the observations."

3.4.19 P 18, LN 1: remove the first "with".

Done.

3.4.20 P 18, LN 10-17: Authors should describe much more in detail about the correlation analysis between PFCs mixing ratio versus CO mixing ratio derived CO source type, which was not given even in the Supplementary information. How can the CO mixing ratio be distinguished by the sources? The description and resulting discussion should be provided in the main text.

We have addressed this in our response to comment 3.3.11.

Marked-Up Manuscript Version

The marked-up versions of the manuscript and the Supplementary Material, according to all responses and outlined changes described above, have been attached below.

Trends and Emissions of Six Perfluorocarbons in the Northern and Southern Hemisphere

Elise S. Droste¹, Karina E. Adcock¹, Matthew J. Ashfold², Charles Chou³, Zoë Fleming^{4,*}, Paul J. Fraser⁵, Lauren J. Gooch¹, Andrew J. Hind¹, Ray L. Langenfelds⁵, Emma Leedham Elvidge¹, Norfazrin Mohd Hanif^{1,6}, Simon O'Doherty⁷, David E. Oram^{1,8}, Chang-Feng Ou-Yang⁹, Marios Panagi⁴, Claire E. Reeves¹, William T. Sturges¹, and Johannes C. Laube^{1,10}

¹Centre for Ocean and Atmospheric Sciences, School of Environmental Sciences, University of East Anglia, Norwich, NR4 7TJ, UK

²School of Environmental and Geographical Sciences, University of Nottingham Malaysia, 43500 Semenyih, Malaysia

³Research Center for Environmental Changes, Academia Sinica, Taipei 11529, Taiwan

⁴National Centre for Atmospheric Science (NCAS), Department of Chemistry, University of Leicester, UK

⁵Commonwealth Scientific and Industrial Research Organisation, Oceans and Atmosphere, Climate Science Centre, Aspendale, Australia

⁶School of Environmental and Natural Resource Sciences, Faculty of Science and Technology, Universiti Kebangsaan Malaysia, 43600 Bangi, Selangor, Malaysia

⁷Department of Chemistry, University of Bristol, Bristol, UK

⁸National Centre for Atmospheric Science, School of Environmental Sciences, University of East Anglia, Norwich, NR4 7TJ, UK

⁹Department of Atmospheric Sciences, National Central University, Taoyuan, Taiwan

¹⁰Institute of Energy and Climate Research – Stratosphere (IEK-7), Forschungszentrum Jülich GmbH, Jülich, Germany

* now at Center for Climate and Resilience Research (CR2), University of Chile, Santiago, Chile

Correspondence: E. S. Droste (e.droste@uea.ac.uk)

Abstract. Perfluorocarbons (PFCs) are potent greenhouse gases with Global Warming Potentials up to several thousand times greater than CO₂ on a 100-year time horizon. The lack of any significant sinks for PFCs means that they have long atmospheric lifetimes on the order of thousands of years. Anthropogenic production is thought to be the only source for most PFCs. Here we report an update on the global atmospheric abundances of the following PFCs, most of which have for the first time been [analytically](#) separated according to their isomers: *c*-octafluorobutane (*c*-C₄F₈), *n*-decafluorobutane (*n*-C₄F₁₀), *n*-dodecafluoropentane (*n*-C₅F₁₂), *n*-tetradecafluorohexane (*n*-C₆F₁₄), and *n*-hexadecafluoroheptane (*n*-C₇F₁₆). Additionally, we report the first data set on the atmospheric mixing ratios of ~~perfluoro(2-methylpentane)~~ ([perfluoro-2-methylpentane](#) (*i*-C₆F₁₄)). The existence and significance of PFC isomers has not been reported before, due to the analytical challenges of separating them. The time series spans a period from 1978 to the present. Several datasets are used to investigate temporal and spatial trends of these PFCs: time series of air samples collected at Cape Grim, Australia, from 1978 to the start of 2018; a time series of air samples collected between July 2015 and April 2017 at Tacolneston, UK; and intensive campaign-based sampling collections from Taiwan. Although the remote "background" Southern Hemispheric Cape Grim time series indicates that recent growth rates of most of these PFCs are lower than in the 1990s, we continue to see significantly increasing mixing ratios that are between 6 % to 27 % higher by the end of 2017 compared to abundances measured in 2010. Air samples from Tacolneston show

a positive offset in PFC mixing ratios compared to the Southern Hemisphere baseline. The highest mixing ratios and variability are seen in air samples from Taiwan, which is therefore likely situated much closer to PFC sources, confirming predominantly Northern Hemispheric emissions for most PFCs. Even though these PFCs occur in the atmosphere at levels of parts per trillion molar or less, their total cumulative global emissions translate into 833 million metric tonnes of CO₂ equivalent by the end of 5 2017, 23 % of which has been emitted ~~in the last eight years. since 2010.~~ Almost two-thirds of the CO₂ equivalent emissions within the last decade are attributable to c-C₄F₈, which currently also has the highest emission rates that continue to grow. ~~Despite this, the sources~~ Sources of all PFCs covered in this work remain poorly constrained and reported emissions in global databases do not account for the abundances found in the atmosphere.

1 Introduction

Perfluorocarbons (PFCs) are fully fluorinated hydrocarbon chemicals that occur ubiquitously in the atmosphere. Even though the magnitude of their mixing ratios are on the order of parts per trillion molar (ppt) or less, monitoring their atmospheric concentrations is highly warranted by their strong infra-red absorption properties and inertness. As a result [of these physical and chemical properties](#), PFCs can have global warming potentials (GWPs) of several thousands on a 100-year time horizon and extremely long atmospheric lifetimes (Bravo et al., 2010; Hartmann et al., 2013) (Table 1). Even though their low abundances mean that their contribution to radiative forcing is relatively minor at present, their continued accumulation in the atmosphere might result in a significant contribution to climate change by the end of the century (Zhang et al., 2011). Previous studies have shown the emergence of atmospheric PFCs in the 1960s based on firm air samples and a subsequent accelerated increase in the 1990s (Worton et al., 2007; Mühle et al., 2010; Ivy et al., 2012a; Laube et al., 2012; Oram et al., 2012; Trudinger et al., 2016). With the exception of tetrafluoromethane (CF₄) (Harnisch et al., 1996; Deeds et al., 2008; Mühle et al., 2010), all known PFCs are thought to be almost exclusively anthropogenic in origin (EDGAR, 2014). For the lowest molecular weight PFCs, such as CF₄ and hexafluoroethane (C₂F₆), emissions from aluminium production are one of the largest sources. Other sources [of PFCs](#) include the use in chemical vapour deposition (CVD) chamber cleaning, plasma etching, refrigerants, fire protection, fluoropolymer production, and - especially for the higher molecular weight PFCs, such as n-C₆F₁₄ and n-C₇F₁₆ - use as heat transfer fluids and solvents (Robin and Iikubo, 1992; Mazurin et al., 1994; Beu, 2005; EPA, 2008; Hartmann et al., 2013; EDGAR, 2014; Mühle et al., 2019). Atmospheric trends vary, but mixing ratios are increasing for all known PFCs. Previously reported PFC trends in the atmosphere include CF₄, C₂F₆, octafluoropropane (C₃F₈), cyclic-octafluorobutane (c-C₄F₈), ~~decofluorobutane~~ [decafluorobutane](#) (C₄F₁₀), dodecafluoropentane (C₅F₁₂), tetradecafluorohexane (C₆F₁₄), ~~hexodecafluoroheptane~~ [hexadecafluoroheptane](#) (C₇F₁₆), and octadecafluorooctane (C₈F₁₈) (Laube et al., 2012; Ivy et al., 2012a; Oram et al., 2012; Mühle et al., 2010; Mühle et al., 2019). [No analytically separated isomers of these PFC species have been reported in the atmosphere before. As the GWPs and atmospheric lifetimes can differ substantially between isomers \(Bravo et al., 2010\), it is important to ascertain the full analytical separation and quantification of such isomers.](#)

The current work focuses on six PFC isomers: c-C₄F₈, n-C₄F₁₀, n-C₅F₁₂, n-C₆F₁₄, i-C₆F₁₄ (perfluoro-2-methylpentane), and n-C₇F₁₆. Even though all but one of these PFCs have been reported before, this is the first time that we report on their separated isomers, except for c-C₄F₈ and n-C₅F₁₂, for which we are updating and expanding our previously reported data set (Laube et al., 2012; Oram et al., 2012). The GWPs on a 100-year time horizon of ~~these compounds range between 7820 (n-C₇F₁₆)~~ [all six compounds studied in this manuscript range between 7370 \(i-C₆F₁₄\)](#) and 9540 (n-C₄F₁₀) (Table 1) (Bravo et al., 2010; Hartmann et al., 2013). To assess the recent changes in atmospheric abundances of these PFCs, this work aims to achieve the following objectives:

1. To extend the 1978-2010 PFC records from Cape Grim, Australia (Oram et al., 2012; Laube et al., 2012) into early 2018. The air sampled at Cape Grim under baseline conditions has typically travelled over the open ocean many days prior and is known to be very well-mixed (Fraser et al., 1999). The Cape Grim time series is therefore an important data set used to study Southern Hemisphere baseline trends of various trace gases (Oram et al., 1995; Langenfelds et al., 1996;

Fraser et al., 1999; Reeves et al., 2005; Laube et al., 2012; Adcock et al., 2018). The global trend between 1978 and 2010 for $c\text{-C}_4\text{F}_8$ has been discussed in Oram et al. (2012) and most recently in Mühle et al. (2019), while those for $n\text{-C}_4\text{F}_{10}$, $n\text{-C}_5\text{F}_{12}$, $n\text{-C}_6\text{F}_{14}$, and $n\text{-C}_7\text{F}_{16}$ have previously been investigated in Laube et al. (2012) and Ivy et al. (2012a). Data acquired since then allows for a re-analysis of the conclusions, given the most recent trends.

- 5 2. To transfer some measurements to a new calibration scale. Re-calibration of the PFCs was necessary, as a number of PFC isomers have recently been identified in our laboratory at the University of East Anglia (UEA), including two isomers of C_4F_{10} ($n\text{-CF}_3(\text{CF}_2)_2\text{CF}_3$ and $i\text{-CF}(\text{CF}_3)_3$), two isomers of C_6F_{14} ($n\text{-CF}_3(\text{CF}_2)_4\text{CF}_3$ and $i\text{-CF}_3(\text{CF}_2)_2\text{CF}(\text{CF}_3)_2$), and three isomers of C_7F_{16} , of which one is the n -isomer ($\text{CF}_3(\text{CF}_2)_5\text{CF}_3$). The chemical structure of the other two isomers is still unknown. A suspicion that the chromatogram peaks previously reported for C_6F_{14} and C_7F_{16} consisted of more
10 than one isomer had already been expressed by Laube et al. (2012). Since then, a new gas-chromatography method reported here (Section 2.2) has been developed that led to the separation of these isomers, consequently increasing the accuracy of the measurements.
- 15 3. To study the atmospheric trend and abundance of $i\text{-C}_6\text{F}_{14}$ for the first time. The separation of isomers allows for more accurate estimations of the impact on the atmospheric radiative forcing, especially since $i\text{-C}_6\text{F}_{14}$ has a different radiative efficiency than $n\text{-C}_6\text{F}_{14}$ (Bravo et al., 2010).
- 20 4. To compare the abundance and variability of PFCs between the well-mixed, unpolluted air in the Southern Hemisphere, which are well represented by the Cape Grim data, and the Northern Hemisphere, where most of the emissions occur. Regarding the latter, this study presents recent observations from air samples collected in Tacolneston, United Kingdom, and in Taiwan. Neither of these sites necessarily represent average abundances for the Northern Hemisphere, but the
25 variability in the observations gives information on the geographical distance of these sites to potential sources. This leads to the final objective:
5. To estimate the global emissions of these six PFCs and compare them to emissions reported in the EDGARv4.2 database (EDGAR, 2014). PFCs are a part of the 1997 Kyoto Protocol and are covered in the 2014-revised F-Gas regulation of the European Union (EU), which will be a part of the Nationally Determined Contribution of the EU to the Paris Agreement. However, substantial discrepancies have been found between emissions derived from atmospheric background measurements and reported emissions (specifically for the compounds focused on in this study, see Laube et al. (2012), Oram et al. (2012), Ivy et al. (2012b), Mühle et al. (2019)). The gas-chromatographic separation of isomers is a useful development that may give some insight into, for example, the identity and potential commonality of sources and possibly a better understanding of the changes of sources with time.

The methods are discussed in Section 2, including sampling, analysis, emission modelling, uncertainties, and air mass trajectory modelling. The results are split up into three sections. The first section (Section 3.1) presents the Cape Grim observations and trends since 1978 for each PFC, with a focus on data since 2010. These are then compared to measurements from Tacolneston and Taiwan. The second section (Section 3.2) discusses the emissions based on the emission modelling and compares

5 these to the emissions from the emission report-based EDGARv4.2 database. The third section of the results (Section 3.3) covers potential source regions and types based on air mass trajectories simulated by the NAME model for the Taiwan samples. Implications of the findings are outlined in Section 4. Section 5 summarises the main conclusions.

2 Methods

2.1 Sampling and Measurement Sites

10 The surface air samples from Cape Grim, Tacolneston, and two sites in Taiwan have been collected over different periods of time and at different frequencies (Table 2).

1. Air samples collected at Cape Grim Baseline Air Pollution Station, Tasmania, since 1978 have been analysed regularly at UEA since the early 1990s. Between 1978 and 1994 and again since 2012, samples were collected as sub-samples from parent air archive tanks. Between 1995 and 2011, the majority of samples were collected directly in UEA flasks
15 (3 L) and only six samples were sub-sampled from parent air archives. Sampling procedures for this period are outlined in Langenfelds et al. (1996), Oram et al. (1995), and Fraser et al. (1999), and confidence in the stability of the PFCs in the archive is justified in Oram et al. (2012). A selection of these samples have been re-analysed using an updated method in order to revise the n-C₄F₁₀, n-C₆F₁₄, and n-C₇F₁₆ mixing ratios previously published in Laube et al. (2012) (see Section 2.2). Samples for UEA have been collected since 1994 in electropolished stainless steel canisters (Rasmussen) until 2000
20 and in silcosteel-treated stainless steel canisters (Restek Corp.) since 2001 (Laube et al., 2012; Oram et al., 2012). ~~Air samples collected for the Cape Grim Air Archive and UEA represent well-mixed, clean, Southern Hemispheric air, as the sampled air masses originate from the long trajectories over the Southern Ocean. Hence, the trace gas abundances in these samples can be considered as mid-latitude Southern Hemispheric background levels.~~

2. Samples from Tacolneston, United Kingdom, have been collected on a near bi-weekly basis between July 2015 and April
25 2017 (Stanley et al., 2018; Adcock et al., 2018). Samples were collected in Silcosteel-treated stainless steel canisters (Restek Corp.).

3. In Taiwan, air samples were collected between 2013 and 2016, in March and April each year. The collection site alternated each year between a site in the north (Cape Fuguei) and in the south of Taiwan (Hengchun), starting in the south in
30 2013 (Laube et al., 2016; Oram et al., 2017; Adcock et al., 2018). Sample collection was aimed at the winter monsoon flow from the north. Even though Hengchun is in the south and air at this time of year travels primarily from the north over Taiwan, the air at Hengchun has a similar trace gas composition as air in Cape Fuguei. This is because Taiwan's topography re-directs the northern winds along the eastern side of the mountains where the population is sparse and thus does not pick up additional anthropogenic PFC emissions before it arrives at Hengchun. Due to local PFC contamination issues during sampling, measurements taken in 2013 have been excluded.

2.2 Analytical Methods

5 All air samples were analysed using an Agilent 6890 Gas Chromatograph coupled to a Waters AutoSpec magnetic sector mass spectrometer (AutoSpec GC-MS). An in-house built cryo-trapping system pre-concentrates 200-300 mL of the air sample at -78 °C in a HayeSep D-filled loop (80/100 mesh) after passing through a magnesium perchlorate ($\text{Mg}(\text{ClO}_4)_2$) drier to remove any water vapour. Two columns are routinely used as part of AutoSpec analysis at UEA: a GS-GasPro column (length ~30-50 m; ID: 0.32 mm) and a KCl-passivated CP-PLOT Al_2O_3 column (length: 50 m; ID: 0.32 mm). As many samples as possible are analysed on both columns to provide a large suite (50+ compounds) of trace gas measurements (e.g. Adcock et al., 2018; Laube et al., 2016; Leedham Elvidge et al., 2018) (Table 2). For the current work, the CP-PLOT column is the most relevant, as it has the ability to separate the higher molecular weight PFCs and their isomers based on their boiling point and symmetry. For compounds analysed on the CP-PLOT column, an Ascarite (NaOH-coated silica) trap is included before the magnesium perchlorate trap to remove CO_2 , which can otherwise distort or reduce the signal of a number of compounds, including those 15 discussed in this study. The sample is injected into the GC at 100 °C. Instrumental drift was accounted for by bracketing samples with calibrated working standards (see Section 2.3).

The Taiwan samples collected in 2014 were analysed on the GS-GasPro column only, using a method optimised for a particular set of trace gases that does not include isomers of C_6F_{14} and C_7F_{16} . Taiwan samples collected in 2015 and 2016, as well as all Tacolneston samples, are measured on the CP-PLOT column.

20 The dry air mole fractions are measured and the mixing ratios (in units of parts per trillion, ppt) reported in this study are used as an equivalent to picomole per mole. The absolute calibration method has been described in detail in Laube et al. (2010) and has been described specifically in Oram et al. (2012) for $\text{c-C}_4\text{F}_8$ and in Laube et al. (2012) for C_4F_{10} , C_5F_{12} , C_6F_{14} and C_7F_{16} , including linearity of the detector response and identification. The For a detailed description and assessment of the calibration procedure and system we refer the reader to the Supplement of Laube et al. (2010). The only procedural difference 25 for the calibrations here is the temperature of the system (100 °C instead of 80 °C). The ions (m/z) used for the quantification of $\text{c-C}_4\text{F}_8$, $\text{n-C}_4\text{F}_{10}$, and $\text{n-C}_5\text{F}_{12}$ are: 131.0, 119.0, and 119.0, respectively. $\text{i-C}_6\text{F}_{14}$, $\text{n-C}_6\text{F}_{14}$, and $\text{n-C}_7\text{F}_{16}$ have been analysed on both quantifying ions (m/z) 169.0 and 219.0. Ion m/z 169 is used for trend analysis, unless a baseline distortion occurred in the chromatogram, in which case the 219 ion is used. Other studies that used the same set-up and method include Laube et al. (2016) and Adcock et al. (2018).

30 Even though two isomers of C_4F_{10} , two isomers of C_6F_{14} , and three isomers of C_7F_{16} have been identified with the current analytical method, the current study only focuses on a selection of these ($\text{n-C}_4\text{F}_{10}$, $\text{i-C}_6\text{F}_{14}$, $\text{n-C}_6\text{F}_{14}$, $\text{n-C}_7\text{F}_{16}$) for the following reasons. The main signal of the quantifying ion for $\text{i-C}_4\text{F}_{10}$ (m/z 131.0) is not well separated from the larger $\text{n-C}_4\text{F}_{10}$ peak on that same ion. Nevertheless, it is still possible to determine the n -isomer for C_4F_{10} on a different quantifying ion, which we confirm to be unaffected by the i -isomer (see Section 2.3). Regarding the isomers of C_7F_{16} , two out of the three isomers have very small signals resulting in bad precisions. Additionally, these two smallest peaks are not well separated from each other (but are well separated from the main isomer peak) and the number of possible isomers with very similar mass spectra 5 is too high to allow for a high-confidence identification. Therefore, their current quantification is too inaccurate and imprecise.

However, it is possible to quantify the n-isomer of C₇F₁₆ with sufficient precision, because it has a larger signal. For the same reasons, both isomers of C₆F₁₄ are quantified here.

Measurement errors (indicated by the error bars on the observational data points) consist of a combination of the 1σ standard deviations of the working standard and sample replicates on the same analysis day. For samples that have been analysed against the previous working standard, the uncertainties include the aforementioned internal conversion accounted for as the 1σ standard deviation of the peak ratio on inter-comparison days (n=8).

2.3 Calibrations

The mixing ratios in the samples are determined based on a secondary calibration standard, which we refer to as the working standard. Our working standard consists of clean Northern Hemispheric air, which therefore contains all relevant PFCs. For many gases, the mixing ratios in the working standard have been calibrated by NOAA. As certified values do not exist for the relevant PFCs, we calibrate them at UEA using an independent calibration scale (see more details in the Supplement).

The previously reported calibration scales (Laube et al., 2012) (now referred to as UEA2010) were revised to accommodate the separated isomers. The ~~calibration~~-new calibration scale is referred to as UEA2018. The calibration procedure has been described in Laube et al. (2010) and has undergone little alteration. High purity compounds for n-C₄F₁₀, n-C₆F₁₄, i-C₆F₁₄, and n-C₇F₁₆ were diluted to ppt levels in a two-step static dilution series using Oxygen Free Nitrogen (OFN) gas (British Oxygen Company). This calibration procedure was repeated three times for each compound and for a range of dilutions (Table S1). All pure compounds had a 98 % purity or higher at time of acquisition and were subsequently further purified in our lab by subjecting each to three repeated freeze-heating cycles. We used the same compounds as in Laube et al. (2012) for n-C₄F₁₀ and n-C₆F₁₄, for which we now confirm their isomeric purity. For i-C₆F₁₄ and n-C₇F₁₆ we used newly purchased pure compounds, which were also confirmed to be isomerically pure. In addition, for n-C₇F₁₆ this represents a significant improvement to Laube et al. (2012), as the latter used a technical mixture with an 85 % n-isomer content.

The OFN was filtered to remove small amounts of trace gas contaminations by flowing the gas through 60 cm $\frac{1}{4}$ " stainless-steel tubing filled with HayeSep D, which was submersed in an ethanol-dry-ice cold trap (-78 °C). The calibration system operates under low pressures (<300 mbar) and high temperatures (100 °C). This results in insignificant virial coefficients, and thus the dry-air mole fractions could be calculated using the ideal gas law (Laube et al., 2010).

n-C₄F₁₀ was re-calibrated to rule out any bias from the observed i-C₄F₁₀ isomer (a small side peak of which was observed in both the working standard and atmospheric samples), and to confirm the leak-tightness of the calibration system (Laube et al., 2016). The combined influence of the i-isomer and the leak-tightness of the calibration system is <2.8 %. This value has been determined by ~~comparing the old and the new calibration scale for calculating the relative difference of n-C₄F₁₀ mixing ratio in the working standard using the two (UEA2010 versus UEA2018) calibration scales (see more details in the Supplement).~~ Due to the leak-tightness of the system and a lack of observed isomers, ~~a revision of the calibration scales for of c-C₄F₈ and n-C₅F₁₂ in the working standard and atmospheric samples, a revision of the calibration scales~~ was deemed unnecessary for these two compounds. Note that the data for c-C₄F₈, n-C₄F₁₀, and n-C₅F₁₂ in Oram et al. (2012) and Laube et al. (2012) are included in the current work.

The confidence in the complete separation of all isomers for C_6F_{14} and C_7F_{16} is based on the ratio of the [peak areas of the](#) two most abundant ions into which these compounds are ionised during mass spectrometry: (mass-to-charge (m/z) ratios 219.0 and 169.0). A comparison of the 219:169 ion ratio is made between the Cape Grim air samples and the calibrations done (Fig. [S2S1](#)). Since the calibration samples are based on dilutions of high purity isomer compounds (>98 %), a significant deviation from the ion ratios in the air samples compared to the ion ratios in the calibration samples might suggest that the peak measured in the chromatogram for the air samples actually consists of more than one isomer. In turn, if the ion ratios measured in the air samples are similar to the ion ratios measured in the calibration samples, then confidence can be attributed within the uncertainties that the signal measured in the air samples is for one particular isomer only. For i- C_6F_{14} , n- C_6F_{14} , and n- C_7F_{16} , the ion ratio in the Cape Grim samples did not differ significantly from the ion ratio in the calibrations [within 1 \$\sigma\$ measurement uncertainty](#) (Fig. [S2S1](#)). It should be noted that even if other isomers do exist and co-elute, they a) likely do not have a trend that is substantially different from any of the C_6F_{14} and C_7F_{16} isomers discussed here and b) currently have mixing ratios that are extremely small compared to those of the main isomers.

Calibrated mixing ratios for the working standard (i.e. unpolluted Northern Hemispheric air from 2017) are given in Table 3, along with the average analytical precision per compound. ~~To determine the~~ [The latter is the relative 1 \$\sigma\$ standard deviation of the compound signal in multiple working standard runs analysed on the day of each calibration. To obtain a measure of](#) accuracy of the calibrations [\(as in Laube et al. \(2010, 2012\)\)](#), trichlorofluoromethane (CFC-11) was diluted along with the pure PFCs as a reference compound, as our working tank has been calibrated by the globally recognised ~~CMD (Global Measurement~~ [GMD \(Global Monitoring](#) Division) of the NOAA-ESRL (National Oceanic and Atmospheric Administration - Earth System Research Laboratory) for CFC-11. For all UEA calibrations, the average ~~difference-offset~~ with values determined by NOAA show that the UEA calibrated concentrations for CFC-11 are consistently slightly lower by on average 4.2 % \pm 0.3 %. To put the accuracy of these calibrations into perspective, the accuracies of calibrations for the PFCs in common with Ivy et al. (2012a) and Laube et al. (2012) are between 4.0 % and 7.8 % and between -5.5 % and 2.8 %, respectively.

The improvement of the new calibration scale by separating the isomers of C_6F_{14} and C_7F_{16} is substantial. Even though the n-isomer of both C_6F_{14} and C_7F_{16} is dominant for both PFCs, the old calibration scale would have overestimated the mixing ratios of these n-isomers by 20 % and 11 %, respectively. [These levels of improvement in the UEA2018 calibration scale are determined based on the relative difference in concentration determined for the respective n-isomers in the working standard between using the UEA2010 and the UEA2018 calibration scales.](#) The new UEA calibration scale thus allows for a more accurate analysis of atmospheric mixing ratios of these PFCs.

2.4 Emission Modelling

The annual global emissions are derived using a 2-D global atmospheric chemistry-transport model (run using the software Facsimile, version 7, also see Laube et al. (2012); Oram et al. (2012); Reeves et al. (2005); Fraser et al. (1999)). The model domain consists of 24 equal-area, zonally averaged latitudinal bands, which ~~have twelve horizontal layers~~ [each have twelve atmospheric layers between the surface and the maximum altitude represented in the model.](#) Each layer is attributed with a height of 2 km, resulting in a total altitude of 24 km.

Due to the high stability of the C-F bonds, PFCs are considered to be chemically inert and thus the model is set to have no chemical or photolytic loss for these compounds. Photolytic loss would only be relevant at ~~stratospheric and~~ mesospheric altitudes (Morris et al., 1995), which are not ~~fully~~ represented in the model domain. The only sink for PFCs in the model is the diffusive loss at the top boundary of the model domain, where the diffusive loss is controlled by a fixed ratio of the mixing ratio of the PFC in the top atmospheric layer to the layer above the model domain, thereby creating a gradient. If there is no gradient, i.e. the ratio is equal to 1, then there is no diffusive loss. The upper boundary ratio used for each modelled gas is set such that the diffusive loss replicates the lifetime of the gas in the upper atmosphere (i.e. above the model domain). For the PFCs, this is effectively their atmospheric lifetime. As PFCs have lifetimes that are much longer than the time period studied, the gradient out of the model is set very low (i.e. ratio of 0.997; Laube et al. (2012)).

The emission distribution is based on the global distribution of reported C₆F₁₄ emissions in the EDGARv4.2 data set in 2005. This set-up is kept the same as in Laube et al. (2012), because the EDGARv4.2 emission distribution for C₆F₁₄ between 2005 and 2010 has not changed significantly and also does not significantly affect the simulated mixing ratios. The reason the EDGARv4.2 data for C₆F₁₄ is used for all PFCs is that the discrepancy between atmospherically-derived and reported emissions is smallest for C₆F₁₄ (Laube et al., 2012). In the model, PFC emissions are set to occur 99 % in the northern mid-latitudes. This is a realistic assumption according to reported emissions recorded in the EDGARv4.2 database, which indicate that 98 % to 100 % of the PFC emissions occur in the Northern Hemisphere, depending on the PFC compound (EDGAR, 2014).

Model runs start in 1934 and end in 2018. The annual emissions are iteratively altered to obtain a best fit of the modelled mixing ratios to the observed mixing ratios at Cape Grim (located within the latitudinal band spanning 35.7 °S to 41.8 °S). The earliest annual PFC emissions set in the model start in the 1950s, when certain PFCs were first detected above detection limits in firm air (Laube et al., 2012). The best fit is determined by minimising the sum of least squares between the modelled and observed Cape Grim mixing ratios (Table [S2S3](#)).

2.5 [Trend and Emission Uncertainties](#)

Two versions of uncertainties have been computed for the model-derived PFC trends for Cape Grim and Tacolneston data (visualised as the shaded envelopes in the figures). The first version will be referred to as the “trend uncertainty”, which consists of the annually averaged analytical uncertainty, the averaged model-fit uncertainty of the Cape Grim trend, and a 5 % modelling uncertainty (Table [S1S2](#)). The [analytical uncertainty is described in Section 2.2. The model-fit uncertainty is the average relative difference between the observed mixing ratio and the simulated mixing ratio.](#) The modelling uncertainty accounts for uncertainties regarding the model transport scheme and is the error in simulating the concentration at Cape Grim of a long-lived gas that is emitted primarily in the Northern Hemisphere at a well known rate (Reeves et al., 2005). Lifetime uncertainties are not included, because they are too long for the time period studied here and would not have a significant effect on the results. Note that the trend uncertainty does not include the calibration uncertainty. Even though it is important to consider the calibration uncertainty in order to evaluate the complete uncertainty of the model simulation, it does not affect the trend. However, to give an overview of all uncertainties, the calibration is included in the “total uncertainty”, which is the

second type of uncertainty referred to in this work (Table S1S2). An additional uncertainty for the trends of $n\text{-C}_2\text{-C}_4\text{F}_{10-8}$ and $n\text{-C}_5\text{F}_{12}$ is added in the total uncertainty, which is the error in the conversion of the mixing ratio between internal working standards, as these two PFCs have not been re-calibrated for the current study (see Section 2.3).

10 ~~After these uncertainties were calculated, the model was~~ The "trend uncertainty" and the "total uncertainty" for each PFC
were used to determine their respective uncertainty bands around the observed mixing ratio trend. The model was then re-run
~~using the best fit of the observed mixing ratios adjusted by the uncertainties to estimate the maximum and minimum emissions.~~
~~Measurement errors (indicated by the error bars on the observational data points) consist of a combination of the 1 σ standard~~
~~deviations of the working standard and sample replicates on the same analysis day. For samples that have been analysed~~
15 ~~against the previous working standard, the uncertainties include the aforementioned internal conversion accounted for as the 1 σ~~
~~standard deviation of the peak ratio on inter-comparison days (n=8)~~ to find the emissions that fitted the simulated maximum
and minimum mixing ratios best. The result is the minimum and maximum emissions according to both types ("trend" and
"total") of uncertainties.

2.6 NAME Modelling

20 This work used the UK Met Office's Lagrangian particle dispersion model, Numerical Atmospheric Modelling Environment (NAME) (Jones et al., 2007), for tracking and understanding the origin of air masses arriving at Taiwan. The model was run in the backward mode for 12-day long simulations to generate the footprints of where the air sampled during the campaigns had previously been close to the Earth's surface (see Fig. 1). The analysis begins by releasing batches of 30 000 inert backward particles over a three hour period encompassing the collection time of each sample. Over the course of the 12-day travel time,
25 the locations of all particles within the lowest 100 m of the model atmosphere were recorded every 15 minutes on a grid with a resolution of 0.25° longitude and 0.25° latitude. The trajectories were calculated using three-dimensional meteorological fields produced by the UK Met Office's Numerical Weather Prediction tool, the Unified Model (UM). These fields have a horizontal grid resolution of 0.23° longitude by 0.16° latitude and 59 vertical levels below ~ 30 km.

In order to quantify the contribution of various regions to each footprint, the domain was divided into 15 regions using shape
30 files produced by ArcGIS, a geographic information system (GIS) for working with maps and geographic information (Fig. 2). The segregation of China from the East Asia region category has enabled a more detailed analyses to be conducted to determine which specific Chinese sub-regions could contribute to the variations in the PFCs mixing ratios in Taiwan. The contribution of each region is quantified by summing the particle concentration (gsm^{-3}) in each grid cell within each shape file (see Fleming et al. (2012) and O'Shea et al. (2017)).

For the purpose of identifying the possible sources of PFCs, ~~carbon monoxide (CO) emission data were used along with the~~
~~NAME footprints to calculate a modelled~~ were used to calculate the mixing ratio of CO a tracer at the Taiwan measurement
~~site. This modelled CO only takes into account the CO that has been emitted during the 12-day simulation in the NAME~~
5 ~~model domain (more details can be found in Oram et al. (2017)). CO was used,~~ given emissions from a range of different
emission sectors. Carbon monoxide (CO) was chosen as the tracer because it is ~~a tracer of anthropogenic emissions and its~~
~~lifetime of 1–2 months is long enough to track pollution plumes on the regional scale of this study. Additionally, reasonable~~

~~bottom-up emissions of CO also exist and are emitted from a number of different emission sources and because~~ widely used and tested. ~~The inventory of CO emissions was taken~~ bottom-up emission estimates of CO are available from the Representative Concentration Pathway 8.5 (RCP 8.5) (Riahi et al., 2011; Van Vuuren et al., 2011) for the year 2010. ~~More information and access to the database can be found on the RCP 8.5 website~~ inventory (Riahi et al., 2011; Van Vuuren et al., 2011) (<http://tntcat.iiasa.ac.at:8787/RcpDb/dsd?Action=htmlpage&page=welcome>). ~~The CO emission inventory is~~ Moreover, the RCP8.5 CO emissions are divided into various emission sectors: (industry, power plants, solvents, agricultural waste burning, waste, forest burning, grassland burning, residential, international shipping, surface transportation, and agriculture). ~~A correlation analysis was performed between the modelled CO and the measured~~), allowing us to test whether there was a correlation between the observed PFC mixing ratios in air samples collected in Taiwan in order to assess the extent to which these categories of emissions might be related to the and whether the air modelled to have arrived at the measurement site had likely been subject to emissions from any particular sector.

The NAME footprints were combined individually with the distribution of CO emissions from each sector to calculate a modelled mixing ratio of the emitted species at the measurement site (see Supplementary Material). Emissions were taken for the year 2010, for the time scale of each footprint (12 days) (more details can be found in Oram et al. (2017)). A correlation analysis was performed between the modelled CO from each sector and the measured PFC mixing ratios in these air masses. Industry (combustion and processing) and solvent applications are expected to show some correlations with PFC concentrations mixing ratios, as they are the most closely associated with PFC sources. ~~This approach sheds some light on the potential sources of PFCs.~~ and so we would expect their emissions to be co-located. Results of these analyses are found in Section 3.3.

3 Results and Discussion

3.1 Atmospheric abundances

3.1.1 c-C₄F₈ Trends

Out of all PFC compounds reported in this work, c-C₄F₈ is the most abundant. c-C₄F₈ seems to still have substantial Northern Hemispheric emissions, for which the measured abundances provide three potential ~~sources~~ pieces of evidence: 1) a considerable, and even accelerating, rate of increase in concentration over time, 2) the existence of a relatively large interhemispheric gradient given its long atmospheric lifetime, and 3) large variations above background levels at Northern Hemispheric sites. Each of these ~~sources~~ pieces of evidence will be illustrated with the Cape Grim, Tacolneston, and Taiwan observations, respectively.

The c-C₄F₈ mixing ratio in the Southern Hemisphere increased from 0.31 ppt in 1978 to 1.52 ppt by the end of 2017 (Fig. 3). ~~This is slightly less than the mixing ratios of ~1.6 ppt reported in the recent work of Mühle et al. (2019) with the difference most likely being due to the two independent absolute calibration scales.~~ As reported previously by Oram et al. (2012), the mixing ratios seemed to stabilise in the 1990s, but picked up again in the 2000s. The extended time series since 2008 indicate a continuing increasing trend similar to the one pre-1990, totalling in a 27 % enhancement in the last eight years

(2010-2018). In fact, atmospheric c-C₄F₈ abundances show accelerating growth in recent years, potential reasons for which are explored in Section 3.2.1. Mühle et al. (2019) reported a slightly higher mixing ratio of 1.61 ppt at the end of 2017 in the high latitude Southern Hemisphere. Since Mühle et al. (2019) already compared their Southern Hemisphere time series to ours until 2008 (published in Oram et al. (2012)), we here focus our comparison on the extended part of the record, i.e. from 2008 until 2017. The average difference of annual mixing ratios for this part of the time series is 0.09 ± 0.01 ppt (1σ). This difference, which is equivalent to an average of 7 %, is to some degree likely due to the two different independent absolute calibration scales. However, since the difference is clearly not constant over time (see Fig. 3), which has also been discussed in Mühle et al. (2019), no simple conversion factor can be derived for the two data sets.

The mixing ratios at Tacolneston, UK, seem to have a consistent offset compared to the observations at Cape Grim on average of 0.07 ppt (based on monthly averages; Fig. 3), equivalent to an interhemispheric ratio of 1.05 (average enhancement of Tacolneston mixing ratio measurements against the background trend at Cape Grim). Note that mixing ratios at Tacolneston have not been shown to be representative of Northern Hemisphere background mixing ratios. However, the lack of variability in the data suggests that Tacolneston is not in close proximity to any major sources of c-C₄F₈. Such a proximity of sources should cause multiple occurrences of substantially higher mixing ratios, as can be seen in the Taiwan data (discussed below). When considering the simulated atmospheric trend from the emission model for Tacolneston, it can be noted that it overestimates the observed concentrations, despite the well-fitted Southern Hemispheric trend. The difficulty in validating trace gas trends for Tacolneston is three-fold. 1) The time series for Tacolneston only covers the time period between 2015 and 2017, which does not enable a validation of the atmospheric trends over the period during which c-C₄F₈ has been emitted. 2) The model is 2-dimensional and as such represents zonal averages. In reality, emissions will occur at specific longitudes, which leads to heterogeneity in atmospheric concentrations at the latitudes of the emissions, even for these very long-lived compounds. This is clearly illustrated by the Taiwan data (see below). 3) The mixing ratios simulated by the model are dependent on a given global distribution of emissions, which harbours a substantial amount of uncertainty. Varying the distribution of the 99 % of global emissions within the Northern Hemisphere does not significantly affect the simulated mixing ratios for Cape Grim, but naturally it does for Northern Hemispheric sites, such as Tacolneston. It is likely that the distribution for c-C₄F₈ in the Northern Hemisphere requires revision to include, for example, a distribution that changes over time rather than a fixed distribution (e.g. see a similar discussion for CFC-113a in Adcock et al., 2018). It is not unrealistic to consider a Northern Hemispheric distribution that moves from higher to lower latitudes over time, as the industries that utilise PFCs and other halocarbons, such as the electronics industry, have moved from more northern latitudes to regions such as South-East Asia (Montzka et al. (2009) for hydrochlorofluorocarbons). However, available information on regions that are sources of c-C₄F₈ (and other PFCs in general) provide insufficient evidence to base a well-founded emission distribution on (see Section 3.2). The global emission distribution for c-C₄F₈ is thus kept consistent with that for the other PFCs discussed in this work, for which the simulated Tacolneston trend compares reasonably well with the observations, i.e. within the measurement and modelling uncertainties.

The c-C₄F₈ mixing ratios observed in samples collected in Taiwan are contrasting to those at Cape Grim and Tacolneston because of their large day-to-day variability (Fig. 3 B). The maximum measured mixing ratios for each year in Taiwan are on

average 17 % higher than the average simulated mixing ratio in the respective year. This strongly suggests a close proximity to one or more PFC sources. Considering that much of the air sampled in Taiwan during the campaigns has been transported from the direction of China (Laube et al., 2016; Adcock et al., 2018) and that Taiwan itself has a major semi-conductor industry as well (Saito et al., 2010), it is not surprising to find such high levels of c-C₄F₈ at these sites.

3.1.2 n-C₄F₁₀ and n-C₅F₁₂ Trends

Between 1978 and 2018, the background mixing ratios for n-C₄F₁₀ and n-C₅F₁₂ at Cape Grim have increased from 0.02 ppt to 0.18 ppt and from 0.02 ppt to 0.15 ppt, respectively (Fig. 4). In contrast to c-C₄F₈, n-C₄F₁₀ and n-C₅F₁₂ seem to have much smaller Northern Hemispheric sources at the present time. First of all, the Southern Hemispheric mixing ratio growth rate has declined since ~ 2000. n-C₄F₁₀ and n-C₅F₁₂ mixing ratios at Cape Grim have only increased by 9 % and 6 % between 2010 and 2018, respectively. Even though growth rates are currently slower than they were in the 1990s, the continuing increasing mixing ratios shown in the extended time series indicate that sources still exist. The similarity in the trends of n-C₄F₁₀ and n-C₅F₁₂ suggests that these sources might be similar or common. The ratio between n-C₄F₁₀ and n-C₅F₁₂ has remained relatively stable between 1978 and 2018 at an average of about 1.3±0.07.

Second of all, as would be expected from a slowly increasing trace gas – and based on the samples collected at Tacolneston and at Cape Grim (Fig. 4) – there does not seem to be an interhemispheric gradient for these PFCs that is discernible given the measurement uncertainties. This is also captured in the simulated mixing ratios for both sites by the model. If the interhemispheric ~~ratio for~~ ratios of the mixing ratios of n-C₄F₁₀ and n-C₅F₁₂ were to be similar to that of c-C₄F₈, then the differences between the Cape Grim and Tacolneston data for these two PFCs would have to be at least 0.01 ppt. This is not the case, but even so, these differences in mixing ratios are too small to discern given the measurement uncertainty.

With the current measurement precisions and low growth rates, the data allow no detailed conclusions on the appropriateness of the global emission distributions used for the model simulations of these two gases. As the Cape Grim observations are representative of the well-mixed Southern Hemispheric air, the similarity in abundances between the Tacolneston and Cape Grim observations might mean that the Tacolneston site is situated relatively far away from n-C₄F₁₀ and n-C₅F₁₂ sources. Additionally, it indicates that the emissions of n-C₄F₁₀ and n-C₅F₁₂ occur at a low rate, which means that these PFCs will be relatively well-mixed in the Northern Hemisphere. Note that the n-C₄F₁₀ data at Tacolneston do display some scatter, but it is well within the uncertainties of the Cape Grim record.

Third of all, smaller Northern Hemispheric sources of n-C₄F₁₀ and n-C₅F₁₂ compared to c-C₄F₈ are reflected by the smaller elevations of their mixing ratios measured in Taiwan relative to those of c-C₄F₈, despite their enhancement compared to Cape Grim measurements (Fig. 4). Maximum values are around 0.25 ppt for n-C₄F₁₀ and 0.20 ppt for n-C₅F₁₂. On average, the mixing ratios measured in Taiwan are 5 % higher than the average mixing ratios simulated in the respective year for Cape Grim for both n-C₄F₁₀ and n-C₅F₁₂. Even though this provides some evidence that there are sources of n-C₄F₁₀ and n-C₅F₁₂ in East- and South-East Asia, these sources do not appear to have a large impact on the interhemispheric ratio between the unpolluted Northern Hemisphere and Southern ~~Hemisphere~~ Hemisphere sites. Much lower mixing ratio elevations for both n-C₄F₁₀ and

n-C₅F₁₂ were observed in ~~2015. This~~ Taiwan in 2015 compared to 2014 and 2016. This is likely related to different air mass origins of samples collected in this particular year (see also Oram et al. (2017); Adcock et al. (2018)).

10 3.1.3 i-C₆F₁₄ and n-C₆F₁₄ Trends

The trends of i-C₆F₁₄ and n-C₆F₁₄ are somewhat similar to each other. n-C₆F₁₄ (~~CF₃(CF₂)₄CF₃)~~ mixing ratios at Cape Grim have increased from 0.01 ppt in 1978 to 0.22 ppt in 2018 (Fig. 5). ~~Its~~ The fastest increase in atmospheric abundance occurred in the 1990s and has since slowed down. Mixing ratios appear to be approaching stabilisation, but have still increased by about 9 % since 2010. Observed long-term trends are similar for i-C₆F₁₄ (~~CF₃(CF₂)₂CF(CF₃)₂)~~, although its atmospheric abundance is much lower (Fig. 5). This points towards commonality or co-location in sources with n-C₆F₁₄. i-C₆F₁₄ mixing ratios were <0.01 ppt before 1987, but reached 0.07 ppt by 2018 (note that the earliest observation for i-C₆F₁₄ shown within the Cape Grim archive is in 1987, due to limited precision of measurements on samples collected prior to that year). In the current work, it is the PFC with the lowest atmospheric abundance throughout the Cape Grim record. Despite the similarities between these two isomers, a notable difference is observed in their recent rate of change: the relative growth rate of i-C₆F₁₄ since 2010 (~ 19 %) is double that of n-C₆F₁₄. Given their similar physico-chemical properties it is likely that these two isomers are emitted to the atmosphere by the same anthropogenic processes. If their production has not changed much over time, the i-C₆F₁₄ :n-C₆F₁₄ ratio is expected to remain relatively stable over that same time period. However, the i-C₆F₁₄ :n-C₆F₁₄ ratio has increased from an average of 0.26±0.01 (1σ standard deviation) between 2003 and 2008 to an average of 0.3±0.01 between 2013 and 2018 (~~Fig-S1~~1σ)(Fig. S2). This might indicate a shift in production method or new sources that emit these isomers in different ratios.

Observed Tacolneston mixing ratios for n-C₆F₁₄ and i-C₆F₁₄ in 2015 and 2016 compared to those at Cape Grim in the same years show no clear interhemispheric gradient (Fig. 5). The average monthly difference between the observations at these two sites is 0.008 ppt and 0.005 ppt for n-C₆F₁₄ and i-C₆F₁₄, respectively, which approaches or even exceeds the differences in mixing ratio one would expect if the interhemispheric ratio was at least that of c-C₄F₈ (0.01 ppt for n-C₆F₁₄ and 0.003 for i-C₆F₁₄). However, such differences in mixing ratios are too small compared to the measurement uncertainties and thus no interhemispheric gradient is discernible based on these data.

The mixing ratios at Tacolneston for the isomers of C₆F₁₄ have greater variability in observed mixing ratios compared to those of the other PFCs discussed in this work. Mixing ratios occasionally exceed the modelled uncertainty envelopes for Tacolneston, such as in ~~2015. This might imply a plume at the time of sampling~~2015, but none of these excursions exceeded the 2σ measurement uncertainties. The simulated trend for the Tacolneston data corresponds well with the lower end of the variability in the observations.

No measurements of either n-C₆F₁₄ or i-C₆F₁₄ were made for Taiwan samples taken in 2014, as these samples were analysed on a GC-column that did not allow for a separation of these isomers (see Section 2.2). Mixing ratios in Taiwan in 2015 and 2016 are again extremely variable on short time scales and reach higher abundances than at Cape Grim or Tacolneston, ranging between 0.21-0.47 ppt for n-C₆F₁₄ and between 0.06-0.13 ppt for i-C₆F₁₄ (Fig. 5). On average, the mixing ratios measured for both n-C₆F₁₄ and i-C₆F₁₄ are 9 % higher in Taiwan than at Cape Grim.

Even though ~~a large range substantial variability~~ of mixing ratios above the Cape Grim baseline for both C₆F₁₄ isomers is observed at Tacolneston and in Taiwan ~~for both compounds, the lack of a discernible interhemispheric gradient (given the low absolute mixing ratios in both hemispheres combined with the measurement uncertainties) suggests that the Northern Hemispheric sources are not as substantial as they are for, for example, c-C₄F₈ do not allow for any further conclusions on the hemispheric distribution of their emissions.~~

3.1.4 n-C₇F₁₆ Trends

Similarly to c-C₄F₈, n-C₇F₁₆ shows substantial sources in the Northern Hemisphere, as is suggested by its rate of change, interhemispheric gradient, and large variations above background levels in Taiwan (Fig. 6 A, B). Mixing ratios of n-C₇F₁₆ at Cape Grim increased from 0.01 ppt in 1978 to 0.11 ppt in 2018. Its trend is different from those of the other PFC compounds reported here, as its mixing ratios have been continuously increasing at an approximately constant rate since 1985. Between 2010 and 2018, atmospheric background levels in the Southern Hemisphere have increased by 21 % and show no signs of slowing down. Two statistical outliers appear in measurements on samples collected in 1988 and 1992.

Observations at Tacolneston and Cape Grim together display an interhemispheric gradient for n-C₇F₁₆ of 1.04, which is captured by the model. However, even though this interhemispheric gradient is comparable to that for c-C₄F₈, the measurement uncertainties are too large to be able to conclude based on these data that the interhemispheric gradient is clearly discernible. The Taiwan measurements range between 0.10 ppt and 0.22 ppt, which is consistent with the large variability seen at Taiwan's measurement sites for all other PFCs analysed in this work. Mixing ratios in Taiwan are on average 15 % higher than at Cape Grim. Having discussed the atmospheric trends, the next step is to investigate how global emissions changed over time and what their current status is.

3.2 Global Emissions

3.2.1 c-C₄F₈ Emissions

The model-derived global c-C₄F₈ emissions have changed substantially over time (Fig. 7). An increase in emission rates occurred in the 1980s, peaking around 1.7 Gg yr⁻¹ (gigagrams per year) in 1986. A possible contributing source to these emissions might have been the increasing use of liquid PFC coolants in temperature control units within semiconductor processing. The design of these temperature control units, which was initially made to be used with water and glycol, was inadequate to prevent any leakage of the replacement PFCs from the pumps and seals (Tuma and Knoll, 2003; EPA, 2008). The following rapid decrease in emissions between 1985 and 1995 despite the growing demand in the semiconductor industry remains unexplained (Oram et al., 2012), especially because it precedes the Kyoto Protocol and any formal initiative taken by the semiconductor industry to reduce PFC emissions.

Emissions have subsequently continued to increase from the 1990s minimum. The global emission trend is consistent up to 2006 with our previously reported data by Oram et al. (2012) and agree well on average with the most recent results of Mühle et al. (2019), although our data show larger variability for some periods. However, the extended time series reveals that

emission rates do not show any signs of stabilisation and have instead continued to increase, and even accelerate after ~ 2012 . Annual emission are now approaching rates of 2.0 Gg yr^{-1} , which are, within uncertainties, comparable to rates determined for the mid-1980s. This compares quite well with the estimated global emissions of 2.2 Gg yr^{-1} in 2017 by the recent work of Mühle et al. (2019). The average difference between Mühle et al. (2019)'s and our emission estimates for 2008-2017 is $0.17 \pm 0.09 \text{ Gg yr}^{-1}$ (1σ). However, the two data sets agree within the uncertainty ranges. Emission rates have increased by approximately 50 % since 2010. The increasing emissions are interesting especially in the light of the substantial PFC emission-reduction efforts by the semiconductor industry since 1999 by means of process optimisation, alternative chemistries, PFC recovery, and abatement (Beu, 2005). The report by the International Sematech Manufacturing Initiative (ISMI) refers to effective and successful reduction efforts for all PFCs by the semiconductor industry, explicitly describing those for CF_4 , C_2F_6 , C_3F_8 , and $\text{c-C}_4\text{F}_8$ (Beu, 2005). Giving credibility to these reduction efforts by the World Semiconductor Council (WSC), it is perhaps unexpected that $\text{c-C}_4\text{F}_8$ emissions are increasing at their current rate. However, the list of WSC members is not exclusive to all major semiconductor manufacturers in the world and while technology is becoming more efficient, demand within the electronics industry may be offsetting PFC reduction efforts. Additionally, $\text{c-C}_4\text{F}_8$ is one of the candidates as a replacement for lower molecular weight PFCs, such as CF_4 and C_2F_6 , which have longer atmospheric lifetimes and higher GWPs (Tsai et al., 2002). Finally, the results of Mühle et al. (2019) point toward fluoropolymer production as another major source of atmospheric $\text{c-C}_4\text{F}_8$.

An enormous discrepancy is evident between $\text{c-C}_4\text{F}_8$ emissions based on reported production (bottom-up) in the EDGARv4.2 data base and emissions derived based on the model simulations of the atmospheric mixing ratios (top-down). This finding continues a trend noted for our earlier measurements (Oram et al., 2012). The $\text{c-C}_4\text{F}_8$ emission rates from the EDGARv4.2 database are lower than model-derived values by two orders of magnitude. This reveals the continued lack of reporting by nations on PFC production and emissions. However, a fraction of the discrepancies between atmospherically-derived and report-derived emissions is possibly attributable to inadvertent PFC production and emission, despite efforts to reduce PFC release into the atmosphere through leakage (Beu, 2005). Some of these inadvertent PFC sources may remain unidentified, complicating attempts to locate source regions and source types. Even the recent evidence towards fluoropolymer production sources by Mühle et al. (2019), which is consistent with their much larger observational data set for $\text{c-C}_4\text{F}_8$, still remains somewhat speculative on a global scale.

3.2.2 $\text{n-C}_4\text{F}_{10}$ and $\text{n-C}_5\text{F}_{12}$ Emissions

Emission rates for $\text{n-C}_4\text{F}_{10}$ and $\text{n-C}_5\text{F}_{12}$ are comparable to each other both in terms of trend and magnitude, which is consistent with previous work (Laube et al., 2012; Ivy et al., 2012b) (Fig. 8). Emissions of both compounds initially rise steadily to peak at around 0.30 Gg yr^{-1} in the mid-1990s, after which they decrease. $\text{n-C}_4\text{F}_{10}$ and $\text{n-C}_5\text{F}_{12}$ are used in refrigeration technology and fire extinguishing methods (Robin and Iikubo, 1992; Mazurin et al., 1994; EDGAR, 2014). The upward emission trend prior to the mid-1990s may be attributed to the growth of the electronics industry, which required cooling technology, and the substitution of ozone-depleting chlorofluorocarbons (CFCs) in refrigeration and fire extinguishing applications. Subsequent

replacement strategies of PFC applications after the signing of the Kyoto Protocol in 1997, such as substitution by alternative chemistries, may have triggered the decline in these emissions.

Maximum emission rates reported in Laube et al. (2012) are 0.27 Gg yr^{-1} for $n\text{-C}_4\text{F}_{10}$ and 0.31 Gg yr^{-1} $n\text{-C}_5\text{F}_{12}$, which agrees within the uncertainties of the current work. A similar conclusion is valid for the maximum emissions rates in Ivy et al. (2012) (Fig. 8). In order to fit the observed mixing ratios, emission rates are required to have stabilised in the last decade. In the current work, $n\text{-C}_4\text{F}_{10}$ stabilises at lower emission rates than in the late 1970s. These trends are also qualitatively comparable to the work by Ivy et al. (2012b). Laube et al. (2012) already suspected a stabilisation in emission rates, which is supported by the extended data set presented in the current study. This low emission rate is consistent with 1) the low NH-SH gradient seen in the Cape Grim and Tacolneston observations, and 2) the Taiwan data only showing moderately elevated mixing ratios.

As with $c\text{-C}_4\text{F}_8$, it is apparent that top-down and the bottom-up approaches estimate very different annual global emissions for $n\text{-C}_4\text{F}_{10}$ (Fig. 8) and $n\text{-C}_5\text{F}_{12}$ (Fig. 8 emissions $< 5.3 \times 10^{-5} \text{ Gg yr}^{-1}$). It is important to note that data reported in the EDGARv4.2 database do not distinguish between different isomers. Hence, the reported emissions in the EDGARv4.2 database are likely a combination of various isomers. Nevertheless, it is still worthwhile comparing these data on reported emissions to the modelled emissions for the n -isomers in the current study, because the abundance of other isomers besides the n -isomer is very low for C_4F_{10} and not detectable for C_5F_{12} . The discrepancy between the modelled emissions for the isomers in the current study and the total reported emissions in the EDGARv4.2 database is around two orders of magnitude for C_4F_{10} and four orders of magnitude for C_5F_{12} , with maximum EDGARv4.2 emission rates of 0.02 Gg yr^{-1} (C_4F_{10}) and of $5.26 \times 10^{-5} \text{ Gg yr}^{-1}$ (C_5F_{12}) (EDGARv4.2 data for $n\text{-C}_5\text{F}_{12}$ is not shown) (Fig. 8).

25 3.2.3 $i\text{-C}_6\text{F}_{14}$ and $n\text{-C}_6\text{F}_{14}$ Emissions

One of the most striking features of the top-down derived emission trend for $n\text{-C}_6\text{F}_{14}$ is the sudden increase in emissions in the mid-1990s (Fig. 9). Emission rates are estimated to be constant at less than 0.2 Gg yr^{-1} up until ~ 1994 , but then increase by a factor of six to reach $1.21 \pm 0.10 \text{ Gg yr}^{-1}$ by ~ 1997 . $n\text{-C}_6\text{F}_{14}$ is liquid at room temperature and thus has widely used applications as a heat transfer fluid. As described in section 3.2.1, the switch to using PFCs as heat transfer fluids was rapid due to their effectiveness at regulating heat which was necessary to cope with the increasing demand of the semiconductor manufacturing industry. This development could be an explanation for the rapid onset of $n\text{-C}_6\text{F}_{14}$ emissions. Additionally, the onset roughly follows the signing of the Montreal Protocol in 1987 and may have triggered the replacement of some CFCs, such as CFC-113, which also had applications in equipment cooling (EPA, 2008). However, the Cape Grim data in this time period are relatively scarce and thus the exact timing of the increase in emissions is not well constrained. By 2013, emission rates have decreased to below 0.2 Gg yr^{-1} again. This reduction in emissions may partly be attributable to the substitution of $n\text{-C}_6\text{F}_{14}$ as heat-transfer fluid by hydrofluoroethers, which have some superior properties compared to most liquid PFCs (Tuma and Tousignant, 2001).

5 The effect of separating the C_6F_{14} isomers on the estimated emissions is apparent when comparing them to emission estimates in Laube et al. (2012) where the isomers are not separated (Fig. 9); the emission trend for $i\text{-C}_6\text{F}_{14}$ is disaggregated from that of the actual $n\text{-C}_6\text{F}_{14}$ emission trend. Observations presented in Laube et al. (2012) led $n\text{-C}_6\text{F}_{14}$ emission rate estimates

to increase earlier and more gradually and to decline more gradually as well, underestimating the maximum emissions in the late 1990s compared to those in EDGARv4.2 (although they are comparable within the uncertainties) (Fig. 9).

10 ~~In contrast with n-C₆F₁₄, emission~~ Emission rates for i-C₆F₁₄ are estimated to have started increasing in ~~1992 (rather than~~
~~in 1992. This is in contrast to~~ 1994, ~~as estimated for~~ which is what was estimated for the onset of significant n-C₆F₁₄ ~~;~~ although
~~within the uncertainties~~ emissions. However, the measurement uncertainties and especially the sparsity of the early data set ~~this~~
~~is not a significant difference) and its initial rate of increase is not as fast. It reaches a~~ do not allow for any further conclusions
15 on the exact timing of the onset of emission increases for both isomers. i-C₆F₁₄ emissions increase at a slower rate than those
for the n-isomer and reach a maximum of 0.25 ± 0.02 Gg yr⁻¹ in 1996-1997, which is when n-C₆F₁₄ emissions reach their
maximum values as well. i-C₆F₁₄ emissions subsequently decrease gradually and stabilise at about 0.09 ± 0.007 Gg yr⁻¹ by
2005. Interestingly, global emissions for i-C₆F₁₄ are constant since ~ 2004, but emissions for n-C₆F₁₄ seem to continue to
decrease until about 2012 (Fig. 5). This is consistent with the increasing i-C₆F₁₄ : n-C₆F₁₄ ratio in the last two decades (Section
3.1.3).

20 The current study has shown that the i-isomer of C₆F₁₄ is clearly present and increasing in the atmosphere (Section 3.1.3).
The emissions reported in Laube et al. (2012) and Ivy et al. (2012a) (which are based on dilutions of the n-isomer calibrated
against a working tank containing compressed, unpolluted air that inevitably contains both isomers) cannot be directly com-
pared to the emissions derived here for the isomers separately. Similarly, due to the fact that EDGARv4.2 does not distinguish
PFC isomers, caution must be taken when comparing the emission estimates for the C₆F₁₄ isomers from the model to the
25 ~~emission~~ emissions reported for the C₆F₁₄ compound in EDGARv4.2.

Thus, it would be more accurate to compare the sum of the observation-derived emissions of the separate isomers of C₆F₁₄
to the reported EDGARv4.2 data. This results in three major improvements. One, it reduces the gap between derived emissions
and EDGARv4.2 emissions prior to 1995, as seen for n-C₆F₁₄ emission estimates. Two, peak emission rates of the sum of the
C₆F₁₄ isomers have increased from 1.21 ± 0.1 Gg yr⁻¹ for n-C₆F₁₆ alone to 1.46 ± 0.12 Gg yr⁻¹ for the two isomers combined
30 and thereby exceed EDGARv4.2 values. However, given that reported emission rates in EDGARv4.2 inherently also have an
uncertainty that is not shown here and that it is more likely that nations under-report emissions, this increase in peak emissions
is probably realistic. Three, the ~~sum of the~~ estimated emission rates of the sum of both C₆F₁₄ isomers ~~agrees exceedingly well~~
agree exceedingly well (relative to all other PFCs reported here) with the EDGARv4.2-reported values from 1999 onwards.

3.2.4 n-C₇F₁₆ Emissions

Emission rate estimates for n-C₇F₁₆ increase from 0.05 ± 0.003 Gg yr⁻¹ in 1980 to a maximum of 0.18 ± 0.01 Gg yr⁻¹ in 1985.
Emissions remain stable at this emission level until 2017 (Fig. 10), despite emission-reduction efforts for higher molecular
5 weight PFCs as heat transfer fluids by leak proofing pumps and applying alternative chemistry (EPA, 2008). This suggests that
n-C₇F₁₆ either has properties and/or applications that are challenging to substitute and/or unknown atmospheric sources.

Similar to Laube et al. (2012), model-based emission estimates are higher compared to the EDGARv4.2 reported values
before 1990 and after 1999, and are lower in between. Maximum emission rates for n-C₇F₁₆ derived by Laube et al. (2012)
are 0.23 ± 0.1 Gg yr⁻¹. This slightly higher maximum as compared to the results in this work are likely due to calibration

10 differences as a) at least two minor isomers of C_7F_{16} are present in the atmosphere and were not chromatographically separated by Laube et al. and b) the n- C_7F_{16} calibration in Laube et al. was not based on a pure isomer, but a technical mixture of isomers. The uncertainties are larger in the work by Laube et al., due to the additional uncertainty that had to be attributed based on the limited purity of C_7F_{16} used for the calibration.

The estimated emissions have a distinctly different trend compared to those in Ivy et al. (2012b), which seem to be in better agreement with the peak seen in the 1990s in the EDGARv4.2 data. Their larger data set, which also included time series in both the Northern and Southern Hemisphere, is able to better constrain their model. This results in more detailed features in the simulated atmospheric trends. However, to assume that the measured signal for C_7F_{16} in previous work only consists of the n- C_7F_{16} isomer would overestimate n- C_7F_{16} mixing ratios by an unknown amount (~~our calibration changed by 11 %, see Section 2.3~~see Section 2.3), because ~~even though previous work diluted high purity compounds in calibration work, the amount of likely unseparated isomers present in their the signal for C_7F_{16} in the working standard tanks and samples remains unknown in the air samples is not exclusive to the n-isomer, as isomers were not separated in the earlier studies.~~

Observations of the continuing increasing background mixing ratios in the Southern Hemisphere strongly suggest that global emissions of n- C_7F_{16} persist at an approximately constant rate. These conclusions remains consistent with those made in Laube et al. (2012) and Ivy et al. (2012b) for C_7F_{16} .

25 3.3 Possible Source Regions and Source Types

The high variability of the PFC mixing ratios in Taiwan described in this work suggests that these measurement sites are close to major PFC sources. The fact that these sampled air masses are not yet well mixed offers the possibility to investigate the following questions: 1) Which PFCs are likely co-emitted and have similar sources? 2) What are likely source regions for these PFCs within Asia? 3) And what are likely source types of the PFCs measured in Taiwan? To pursue the answers to these, the air measurements are combined with the NAME model data, as described in ~~section~~Section 2.4.

The similarity of sources among the PFCs can be studied by looking at the inter-species correlations (Fig. S3). These results show that all PFCs, including C_2F_6 and C_3F_8 (CF_4 was not measured), are significantly correlated with each other, with squared Spearman coefficients ranging from 0.14 to 0.68 (Table ~~S3~~S4). The best correlations are observed between C_2F_6 and C_3F_8 (in contrast to what was reported by Zhang et al. (2017)) and between c- C_4F_8 and n- C_4F_{10} (Table 4). i- C_6F_{14} and n- C_6F_{14} are not very well correlated, which supports the hypothesis of at least partly independent sources. Some correlation plots seem to show bifurcation within the scattered data (most notably in the correlations of most PFCs with C_3F_8), suggesting that multiple source signatures may exist (Fig. S3).

~~Generally, the PFCs correlate less with with any of~~ When PFC mixing ratios are correlated to the 15 regions used to quantify sources of particle densities used in the dispersion modelling, the R-squared values are generally much smaller, although sample numbers limit the statistics (Table ~~S4~~S5). The best correlations are observed for East China for all compounds with the highest squared Spearman rank coefficients found for n- C_7F_{16} (0.49) and n- C_5F_{12} (0.47) (Table 4). Significant correlations are also found for all PFC species with the East China Sea, which can be explained by the fact that air masses from East China travel over the East China Sea before they reach Taiwan.

All When using simulated CO mixing ratios as a tracer for source types, all PFCs correlate well with energy industry and domestic sources, which is linked to population density (Table S5S6). Other best coefficients are found either with the signature of power plants (C_2F_6 , C_3F_8 , $c-C_4F_8$, $i-C_6F_{14}$, $n-C_6F_{14}$) or solvents ($n-C_4F_{10}$, $n-C_5F_{12}$, $n-C_7F_{16}$) (Table 4). ~~Some correlation plots seem to show bifurcation within the scattered data (most notably in the correlations of most PFCs with C_3F_8), suggesting that multiple source signatures may exist (Fig. S3).~~

The combination of the NAME modelling work and air measurements shows potential to identify and quantify regional PFC sources and source types. However, the interpretation of the results may be challenging, such as the possibility of the heterogeneity in emissions over time (e.g. discontinuous emissions may lead to two similar particle density signatures linked to two very different atmospheric concentrations measured in Taiwan). The collection of air samples at the sites in Taiwan is ongoing. New data in addition to the current dataset can be used to inspect PFC source regions and types more rigorously, including the significance of the initial signs of any bifurcation in the correlations between PFCs and CO concentrations that share source types. Nevertheless, this regional study on Taiwan is indicative of the relation between measured atmospheric PFC concentrations and important economic sectors, which feeds back to the implications on rising global PFC trends.

25 4 Implications

The changing trends and emissions of six PFCs have been thoroughly discussed in Sections 3.1 and 3.2, but since these greenhouse gases only occur at very low ppt and sub-ppt levels in our atmosphere, the significance of their influence on our climate system needs further clarification. In order to gain more insight into this matter, the annual global emission rates of all six PFCs covered in this work have been converted to the equivalent of CO_2 by using the updated GWPs from the latest IPCC report (Myhre et al., 2013) (Table 1). As isomers have the same molecular mass, the GWP for $i-C_6F_{14}$ is estimated based on the GWP reported for $n-C_6F_{14}$ (7910; (Myhre et al., 2013) and scaled with the ratio of the radiative efficiencies of $i-C_6F_{14}$ ($0.41 \text{ Wm}^{-2} \text{ ppbv}^{-1}$; Bravo et al. (2010)) and $n-C_6F_{14}$ ($0.44 \text{ Wm}^{-2} \text{ ppbv}^{-1}$; (Myhre et al., 2013)). PFCs have extremely long atmospheric lifetimes, and thus their CO_2 equivalents are calculated here as accumulating over time (Fig. 11) (Laube et al., 2012). By 2017, the cumulative global emissions of $c-C_4F_8$, $n-C_4F_{10}$, $n-C_5F_{12}$, $i-C_6F_{14}$, $n-C_6F_{14}$, and $n-C_7F_{16}$ amounted to 833 million metric tonnes of CO_2 equivalents. This represents an increase in the total global cumulative CO_2 equivalent of 23 % between the beginning of 2010 and the end of 2017. 61 % of the total CO_2 equivalent is attributable to $c-C_4F_8$. The difference between the total CO_2 equivalent by the end of 2009 reported in Laube et al. (2012) (~ 750 million metric tonnes CO_2 equivalent) and in the current work (~ 678 million metric tonnes CO_2 equivalent) is partly the result of the separation of isomers, but mostly due to the updated global warming potentials (Myhre et al., 2013).

The importance of PFCs extends beyond the scope of climate in the troposphere. The inert nature and continuously-increasing concentrations in the troposphere of PFCs over time make them interesting as potential new age-of-air (AoA) tracers. AoA tracers are crucial for research on stratospheric circulation (e.g., Engel et al., 2017) and troposphere-stratosphere fluxes (e.g., Bönisch et al., 2009), which enables further understanding of threats to the ozone layer. SF_6 and CO_2 are among the most commonly used AoA tracers, but have limitations that significantly compromise conclusions on dynamic and chemi-

cal stratospheric processes (Stiller et al., 2012; Ray et al., 2017; Leedham Elvidge et al., 2018). Some of the lower molecular weight PFCs, such as CF_4 , C_2F_6 , C_3F_8 , have already been shown to be suitable age tracers (Leedham Elvidge et al., 2018).
15 Considering all PFCs presented in the current work, $\text{c-C}_4\text{F}_8$ has a particular potential to be an excellent age tracer for three reasons: 1) It has a well-constrained time series from 1978 to the present. 2) It still has a sufficiently fast tropospheric growth rate ($3.2 \pm 0.2\%$ on average between 2010 and 2018). 3) Observations for background $\text{c-C}_4\text{F}_8$ levels in the Southern Hemisphere have an average measurement uncertainty of about 1 % ($1.0 \pm 0.7\%$). The other PFCs presented in this work are currently not suitable as AoA tracers as their annual growth rates since 2010 ($\sim 0.8\text{-}2.9\%$) do not exceed their average measurement
20 precisions ($\sim 3.1\text{-}7.3\%$).

5 Conclusions

This work has extended existing time series on observations at Cape Grim, Australia, for atmospheric mixing ratios of $\text{c-C}_4\text{F}_8$, $\text{n-C}_4\text{F}_{10}$, $\text{n-C}_5\text{F}_{12}$, $\text{n-C}_6\text{F}_{14}$, and $\text{n-C}_7\text{F}_{16}$ from 2010 to 2018 and converted it onto an improved calibration scale. The calibration scale is improved due to the separation of isomers, which leads to a more accurate analysis of tropospheric trends.
25 Moreover, the background trend in $\text{i-C}_6\text{F}_{14}$ mixing ratios in the Southern Hemisphere is reported here for the first time and some of the other PFCs have been measured of the first time as discrete isomers.

The background mixing ratios for all six PFCs continue to increase and reached 1.51 ppt ($\text{c-C}_4\text{F}_8$), 0.18 ppt ($\text{n-C}_4\text{F}_{10}$), 0.15 ppt ($\text{n-C}_5\text{F}_{12}$), 0.07 ppt ($\text{i-C}_6\text{F}_{14}$), 0.22 ppt ($\text{n-C}_6\text{F}_{14}$), and 0.11 ppt ($\text{n-C}_7\text{F}_{16}$) by the end of 2017. An increasing trend is observed most clearly for atmospheric background concentrations of $\text{c-C}_4\text{F}_8$, $\text{i-C}_6\text{F}_{14}$, and $\text{n-C}_7\text{F}_{16}$, which have increased by
30 27 %, 19 %, and 21 % in the last eight years, respectively. Atmospheric mixing ratios for $\text{n-C}_4\text{F}_{10}$, $\text{n-C}_5\text{F}_{12}$, and $\text{n-C}_6\text{F}_{14}$ have increased by 9 %, 6 %, and 9 %, respectively.

Southern Hemispheric background trends are compared to mixing ratios in the Northern Hemisphere. Air samples from the Tacolneston site in the UK show an interhemispheric gradient for $\text{c-C}_4\text{F}_8$ and $\text{n-C}_7\text{F}_{16}$, indicating substantial emissions within the Northern Hemisphere. This is consistent with their faster (as compared to the other four PFCs) increasing atmospheric levels observed in unpolluted, Southern Hemispheric air.

All PFC mixing ratios in Taiwan air samples are extremely variable and show frequent enhancements. These observations show that the Taiwan measurement sites are in close proximity to substantial PFC sources, which is not surprising given the extensive presence of electronic manufacturing industry in East Asia, which is believed to be one of the main atmospheric
5 sources of these gases (Beu, 2005; Saito et al., 2010).

Finally, emission rate model-estimates generally agree well with previous modelling work. Most noteworthy is the continuation of the increasing trend for $\text{c-C}_4\text{F}_8$ emissions. This increase reflects an acceleration of mixing ratio increases in recent years. Our work provides an independent verification of the recent trend of that particular gas and is largely in agreement with the findings of the more extensive $\text{c-C}_4\text{F}_8$ -focused work of Mühle et al. (2019). For the longer-chain PFCs, differences with
10 results by Laube et al. (2012) are mainly due to the improved calibration scales. Especially the comparison for C_6F_{14} has improved as its two main isomers are now separated.

The current study demonstrates that for most of the six PFCs in this work, the emissions determined with the bottom-up approach of the EDGARv4.2 database are much lower than those determined by the top-down approach using observations of mixing ratios. This suggests that production and emissions of PFCs are going unreported, which demonstrates the need to better determine the locations of major PFC sources. Analysis of Taiwan PFC mixing ratios and simulated particle dispersion and CO concentrations by the NAME model indicate the potential of such regional studies in understanding the global trends. This analysis will gain statistical weight with more measurements added to the dataset each year and is therefore considered ongoing. Voluntary PFC reduction plans ~~exists~~ exist among semiconductor industry associations (Beu, 2005). Even though these may be adhered to, PFC emissions are not reported by most nations, including those in East Asia (Saito et al., 2010). Determining the contribution of various regions to rising PFC mixing ratios thus remains a challenge.

Monitoring and regulating PFC emissions is relevant to future climate, as illustrated by the cumulative CO₂ equivalents of over 830 million tonnes for all PFCs reported here (an increase of 155 million tonnes between the beginning of 2010 and the end of 2017), and the potential to be applied in other areas of atmospheric research, such as circulation and chemistry changes in the stratosphere.

Data availability. The measurement and modelling data presented in this work have been made available on Zenodo and can be publicly accessed using DOI 10.5281/zenodo.3519317, or by contacting e.droste@uea.ac.uk.

Author contributions. ESD led the manuscript writing process and carried out the emission modelling and some of the measurements. KEA, LYG, AJH, ELE and JCL also contributed to the measurements while CER, MJA, ZF, NMH, and MP contributed to the modelling parts of the study. CC, PJF, RLF, SO, DEO, CO and WTS contributed through the coordination and execution of the various sampling activities. JCL developed the concept for this study and all authors contributed to developing it further as well as to the manuscript.

Acknowledgements. This work was supported by the European Research Council's (ERC) funding for the EXC³ITE project (EXploring stratospheric Chemistry, Composition, and Circulation using Innovative TEchniques). The collection and curation of the Cape Grim Air Archive is jointly funded by CSIRO, the Bureau of Meteorology (BoM) and Refrigerant Reclaim Australia; BoM/CGBAPS staff at Cape Grim were/are largely responsible for the collection of archive samples and UEA flask air samples; the original (mid-1990s) subsampling of the archive for UEA was funded by AFEAS and CSIRO, with ongoing subsampling by CSIRO. Operation of Tacolneston is funded by the Department of Business, Energy & Industrial Strategy (BEIS) through contract TN 1537/06/2018. We would specifically like to thank Stephen Humphrey and Andy MacDonald for all their work collecting the samples at the Tacolneston site and transporting them to UEA. Taiwan-related work was supported by the NERC IOF award NE/I016012/1. This work used the NAME atmospheric dispersion model, for which the UK Met Office provided the NWP meteorological datasets. Karina E. Adcock's PhD is supported by the Natural Environment Research Council through the EnvEast Doctoral Training Partnership [PhD Studentship NE/L002582//1]. Norfazrin Mohd Hanif's PhD is supported by the Ministry of Education Malaysia (MOE) and Universiti Kebangsaan Malaysia (UKM). Johannes C. Laube and Lauren J. Gooch received funding from the UK Natural Environment Research Council (Research Fellowship NE/I021918/1 and studentship NE/1210143) and David E. Oram from the National Centre for Atmospheric Science. Lastly, we would like to thank our anonymous referees, whose detailed and constructive comments have helped to substantially improve this manuscript.

References

- Adcock, K. E., Reeves, C. E., Gooch, L. J., Leedham Elvidge, E. C., Ashfold, M. J., Brenninkmeijer, C. A., Chou, C., Fraser, P. J., Langenfelds, R. L., Mohd Hanif, N., et al.: Continued increase of CFC-113a (CCl_3CF_3) mixing ratios in the global atmosphere: emissions, occurrence and potential sources, *Atmospheric Chemistry and Physics*, 18, 4737–4751, <https://doi.org/10.5194/acp-18-4737-2018>, 2018.
- 30 Beu, L.: Reductions in Perfluorocompound (PFC) Emissions: 2005 State-of-the-Technology Report, International SEMATECH Manufacturing Initiative, 2005.
- Bönisch, H., Engel, A., Curtius, J., Birner, T., and Hoor, P.: Quantifying transport into the lowermost stratosphere using simultaneous in-situ measurements of SF_6 and CO_2 , *Atmospheric Chemistry and Physics*, 9, 5905–5919, <https://doi.org/10.5194/acp-9-5905-2009>, 2009.
- 35 Bravo, I., Aranda, A., Hurley, M. D., Marston, G., Nutt, D. R., Shine, K. P., Smith, K., and Wallington, T. J.: Infrared absorption spectra, radiative efficiencies, and global warming potentials of perfluorocarbons: Comparison between experiment and theory, *Journal of Geophysical Research: Atmospheres*, 115, <https://doi.org/10.1029/2010JD014771>, 2010.
- Deeds, D. A., Vollmer, M. K., Kulongoski, J. T., Miller, B. R., Mühle, J., Harth, C. M., Izbicki, J. A., Hilton, D. R., and Weiss, R. F.: Evidence for crustal degassing of CF_4 and SF_6 in Mojave Desert groundwaters, *Geochimica et Cosmochimica Acta*, 72, 999–1013, <https://doi.org/10.1016/j.gca.2007.11.027>, 2008.
- EDGAR: EDGAR: Emission Database for Global Atmospheric Research (EDGAR), release version 4.2, European Commission, Joint Research Centre (JRC)/Netherlands Environmental Assessment Agency (PBL), <http://edgar.jrc.ec.europa.eu>, last access: 31 August 2018, 2014.
- 5 Engel, A., Bönisch, H., Ullrich, M., Sitals, R., Membrive, O., Danis, F., and Crevoisier, C.: Mean age of stratospheric air derived from AirCore observations, *Atmospheric Chemistry and Physics*, 17, 6825–6838, <https://doi.org/10.5194/acp-17-6825-2017>, 2017.
- EPA: Uses and Emissions of Liquid PFC Heat Transfer Fluids from the Electronics Sector, 2008.
- 10 Fleming, Z. L., Monks, P. S., and Manning, A. J.: Untangling the influence of air-mass history in interpreting observed atmospheric composition, *Atmospheric Research*, 104, 1–39, <https://doi.org/10.1016/j.atmosres.2011.09.009>, 2012.
- Fraser, P., Oram, D., Reeves, C., Penkett, S., and McCulloch, A.: Southern Hemispheric halon trends (1978–1998) and global halon emissions, *Journal of Geophysical Research: Atmospheres*, 104, 15 985–15 999, <https://doi.org/10.1029/1999JD900113>, 1999.
- Harnisch, J., Borchers, R., Fabian, P., and Maiss, M.: Tropospheric trends for CF_4 and C_2F_6 since 1982 derived from SF_6 dated stratospheric air, *Geophysical Research Letters*, 23, 1099–1102, <https://doi.org/10.1029/96GL01198>, 1996.
- 15 Hartmann, D., Klein Tank, A., Rusticucci, M., Alexander, L., Brönnimann, S., Charabi, Y., Dentener, F., Dlugokencky, E., Easterling, D., Kaplan, A., Soden, B., Thorne, P., Wild, M., and Zhai, P.: Observations: atmosphere and surface, in: *Climate Change 2013: The Physical Science Basis. Contribution of Working Group I to the Fifth Assessment Report of the Intergovernmental Panel on Climate Change*, chap. 2, p. 159–254, Cambridge University Press, <https://doi.org/10.1017/CBO9781107415324.008>, 2013.
- 20 Ivy, D. J., Arnold, T., Harth, C. M., Steele, L. P., Mühle, J., Rigby, M., Salameh, P. K., Leist, M., Krummel, P. B., Fraser, P. J., et al.: Atmospheric histories and growth trends of C_4F_{10} , C_5F_{12} , C_6F_{14} , C_7F_{16} and C_8F_{18} , *Atmospheric Chemistry and Physics*, 12, 4313–4325, <https://doi.org/10.5194/acp-12-4313-2012>, 2012a.
- Ivy, D. J., Rigby, M., Baasandorj, M., Burkholder, J. B., and Prinn, R. G.: Global emission estimates and radiative impact of C_4F_{10} , C_5F_{12} , C_6F_{14} , C_7F_{16} and C_8F_{18} , *Atmospheric Chemistry and Physics*, 12, 7635–7645, <https://doi.org/10.5194/acp-12-7635-2012>, 2012b.
- 25 Jones, A., Thomson, D., Hort, M., and Devenish, B.: The UK Met Office’s next-generation atmospheric dispersion model, NAME III, in: *Air pollution modeling and its application XVII*, pp. 580–589, Springer, https://doi.org/10.1007/978-0-387-68854-1_62, 2007.

- Langenfelds, R., Fraser, P., Francey, R., Steele, L., Porter, L., and Allison, C.: The Cape Grim air archive: The first seventeen years, 1978–1995, <https://doi.org/20ed4c00-86d3-4d33-9604-4a514ebf4e35>, 1996.
- Laube, J., Hogan, C., Newland, M., Mani, F. S., Fraser, P., Brenninkmeijer, C., Martinerie, P., Oram, D., Röckmann, T., Schwander, J.,
30 et al.: Distributions, long term trends and emissions of four perfluorocarbons in remote parts of the atmosphere and firn air, *Atmospheric chemistry and physics*, 12, 4081–4090, <https://doi.org/10.5194/acp-12-4081-2012>, 2012.
- Laube, J. C., Martinerie, P., Witrant, E., Blunier, T., Schwander, J., Brenninkmeijer, C., Schuck, T. J., Bolder, M., Röckmann, T., Veen, C.,
et al.: Accelerating growth of HFC-227ea (1, 1, 1, 2, 3, 3, 3-heptafluoropropane) in the atmosphere, *Atmospheric chemistry and physics*,
10, 5903–5910, <https://doi.org/10.5194/acp-10-5903-2010>, 2010.
- 35 Laube, J. C., Mohd Hanif, N., Martinerie, P., Gallacher, E., Fraser, P. J., Langenfelds, R., Brenninkmeijer, C. A., Schwander, J., Witrant, E.,
Wang, J.-L., et al.: Tropospheric observations of CFC-114 and CFC-114a with a focus on long-term trends and emissions, *Atmospheric
Chemistry and Physics*, 16, 15 347–15 358, <https://doi.org/10.5194/acp-16-15347-2016>, 2016.
- Leedham Elvidge, E., Bönisch, H., Brenninkmeijer, C. A., Engel, A., Fraser, P. J., Gallacher, E., Langenfelds, R., Mühle, J., Oram, D. E.,
Ray, E. A., et al.: Evaluation of stratospheric age of air from CF₄, C₂F₆, C₃F₈, CHF₃, HFC-125, HFC-227ea and SF₆; implications for
the calculations of halocarbon lifetimes, fractional release factors and ozone depletion potentials, *Atmospheric Chemistry and Physics*,
18, 3369–3385, <https://doi.org/10.5194/acp-18-3369-2018>, 2018.
- Mazurin, I. M., Stolyarevsky, A. Y., Doronin, A. S., and Shevtsov, A. G.: Ozone-Friendly Working Mixture For Refrigeration Equipment,
5 european Patent 0676460A1, 1994.
- Montzka, S., Hall, B., and Elkins, J.: Accelerated increases observed for hydrochlorofluorocarbons since 2004 in the global atmosphere,
Geophysical Research Letters, 36, <https://doi.org/10.1029/2008GL036475>, 2009.
- Morris, R. A., Miller, T. M., Viggiano, A., Paulson, J. F., Solomon, S., and Reid, G.: Effects of electron and ion reac-
tions on atmospheric lifetimes of fully fluorinated compounds, *Journal of Geophysical Research: Atmospheres*, 100, 1287–1294,
10 <https://doi.org/10.1029/94JD02399>, 1995.
- Mühle, J., Ganesan, A., Miller, B., Salameh, P., Harth, C., Grealley, B., Rigby, M., Porter, L., Steele, L., Trudinger, C., et al.: Perfluorocarbons
in the global atmosphere: tetrafluoromethane, hexafluoroethane, and octafluoropropane, *Atmospheric Chemistry and Physics*, 10, 5145–
5164, <https://doi.org/10.5194/acp-10-5145-2010>, 2010.
- Mühle, J., Trudinger, C. M., Rigby, M., Western, L. M., Vollmer, M. K., Park, S., Manning, A. J., Say, D., Ganesan, A., Steele, L. P., Ivy,
15 D. J., Arnold, T., Li, S., Stohl, A., Harth, C. M., Salameh, P. K., McCulloch, A., O’Doherty, S., Park, M.-K., Jo, C. O., Young, D., Stanley,
K. M., Krummel, P. B., Mitrevski, B., Hermansen, O., Lunder, C., Evangelidou, N., Yao, B., Kim, J., Hmiel, B., Buizert, C., Petrenko,
V. V., Arduini, J., Maione, M., Etheridge, D. M., Michalopoulou, E., Czerniak, M., Severinghaus, J. P., Reimann, S., Simmonds, P. G.,
Fraser, P. J., Prinn, R. G., and Weiss, R. F.: Perfluorocyclobutane (PFC-318, *c*-C₄F₈) in the global atmosphere, *Atmospheric Chemistry
and Physics Discussions*, 2019, 1–44, <https://doi.org/10.5194/acp-2019-267>, <https://www.atmos-chem-phys-discuss.net/acp-2019-267/>,
20 2019.
- Myhre, G., Shindell, D., Bréon, F.-M., Collins, W., Fuglestedt, J., Huang, J., Koch, D., Lamarque, J.-F., Lee, D., Mendoza, B., Nakajima,
T., Robock, A., Stephens, G., Takemura, T., and Zhang, H.: Anthropogenic and natural radiative forcing, in: *Climate Change 2013: The
Physical Science Basis. Contribution of Working Group I to the Fifth Assessment Report of the Intergovernmental Panel on Climate
Change*, chap. 8, pp. 658–740, Cambridge University Press, 2013.
- 25 Oram, D., Reeves, C., Penkett, S., and Fraser, P.: Measurements of HCFC-142b and HCFC-141b in the Cape Grim air Archive: 1978–1993,
Geophysical Research Letters, 22, 2741–2744, <https://doi.org/10.1029/95GL02849>, 1995.

- Oram, D., Mani, F. S., Laube, J., Newland, M., Reeves, C., Sturges, W., Penkett, S., Brenninkmeijer, C., Röckmann, T., and Fraser, P.: Long-term tropospheric trend of octafluorocyclobutane (c-C₄F₈ or PFC-318), *Atmospheric Chemistry and Physics*, 12, 261–269, <https://doi.org/10.5194/acp-12-261-2012>, 2012.
- 30 Oram, D. E., Ashfold, M. J., Laube, J. C., Gooch, L. J., Humphrey, S., Sturges, W. T., Leedham Elvidge, E., Forster, G. L., Harris, N. R., Mead, M. I., et al.: A growing threat to the ozone layer from short-lived anthropogenic chlorocarbons, *Atmospheric Chemistry and Physics*, 17, 11 929–11 941, <https://doi.org/10.5194/acp-17-11929-2017>, 2017.
- O’Shea, S., Choulaton, T. W., Flynn, M., Bower, K. N., Gallagher, M., Crosier, J., Williams, P., Crawford, I., Fleming, Z. L., Listowski, C., et al.: In situ measurements of cloud microphysics and aerosol over coastal Antarctica during the MAC campaign, *Atmospheric Chemistry and Physics*, 17, 13 049–13 070, <https://doi.org/10.5194/acp-17-13049-2017>, 2017.
- 35 Ray, E. A., Moore, F. L., Elkins, J. W., Rosenlof, K. H., Laube, J. C., Röckmann, T., Marsh, D. R., and Andrews, A. E.: Quantification of the SF₆ lifetime based on mesospheric loss measured in the stratospheric polar vortex, *Journal of Geophysical Research: Atmospheres*, 122, 4626–4638, <https://doi.org/10.1002/2016JD026198>, 2017.
- Reeves, C., Sturges, W., Sturrock, G., Preston, K., Oram, D., Schwander, J., Mulvaney, R., Barnola, J.-M., and Chappellaz, J.: Trends of halon gases in polar firn air: implications for their emission distributions, *Atmospheric Chemistry and Physics*, 5, 2055–2064, <https://doi.org/10.5194/acp-5-2055-2005>, 2005.
- Riahi, K., Rao, S., Krey, V., Cho, C., Chirkov, V., Fischer, G., Kindermann, G., Nakicenovic, N., and Rafaj, P.: RCP 8.5—A scenario of 5 comparatively high greenhouse gas emissions, *Climatic Change*, 109, 33, <https://doi.org/10.1007/s10584-011-0149-y>, 2011.
- Robin, L. R. and Iikubo, Y.: Fire Extinguishing Methods Utilizing Perfluorocarbons, US Patent 5117917, 1992.
- Saito, T., Yokouchi, Y., Stohl, A., Taguchi, S., and Mukai, H.: Large emissions of perfluorocarbons in East Asia deduced from continuous atmospheric measurements, *Environmental science & technology*, 44, 4089–4095, <https://doi.org/10.1021/es1001488>, 2010.
- 785 Stanley, K. M., Grant, A., O’Doherty, S., Young, D., Manning, A. J., Stavert, A. R., Spain, T. G., Salameh, P. K., Harth, C. M., Simmonds, P. G., et al.: Greenhouse gas measurements from a UK network of tall towers: technical description and first results, *Atmospheric Measurement Techniques*, 11, 1437–1458, <https://doi.org/10.5194/amt-11-1437-2018>, 2018.
- Stiller, G., Clarmann, T. v., Haenel, F., Funke, B., Glatthor, N., Grabowski, U., Kellmann, S., Kiefer, M., Linden, A., Lossow, S., et al.: 790 Observed temporal evolution of global mean age of stratospheric air for the 2002 to 2010 period, *Atmospheric Chemistry and Physics*, 12, 3311–3331, <https://doi.org/10.5194/acp-12-3311-2012>, 2012.
- Trudinger, C. M., Fraser, P. J., Etheridge, D. M., Sturges, W. T., Vollmer, M. K., Rigby, M., Martinerie, P., Mühle, J., Worton, D. R., Krummel, P. B., et al.: Atmospheric abundance and global emissions of perfluorocarbons CF₄, C₂F₆ and C₃F₈ since 1800 inferred from ice core, firn, air archive and in situ measurements, *Atmospheric chemistry and physics*, 16, 11 733–11 754, <https://doi.org/10.5194/acp-16-11733-2016>, 2016.
- 795 Tsai, W.-T., Chen, H.-P., and Hsien, W.-Y.: A review of uses, environmental hazards and recovery/recycle technologies of perfluorocarbons (PFCs) emissions from the semiconductor manufacturing processes, *Journal of Loss Prevention in the Process Industries*, 15, 65–75, [https://doi.org/10.1016/S0950-4230\(01\)00067-5](https://doi.org/10.1016/S0950-4230(01)00067-5), 2002.
- Tuma, P. and Tousignant, L.: Reducing emissions of PFC heat transfer fluids, in: SEMI Technical Symposium, 3M Specialty Materials, pp. 1–8, 2001.
- 800 Tuma, P. E. and Knoll, S.: A comparison of fluorinated and DI/glycol heat transfer fluids, *Solid State Technology*, 9, 2003.
- Van Vuuren, D. P., Edmonds, J., Kainuma, M., Riahi, K., Thomson, A., Hibbard, K., Hurtt, G. C., Kram, T., Krey, V., Lamarque, J.-F., et al.: The representative concentration pathways: an overview, *Climatic change*, 109, 5, <https://doi.org/10.1007/s10584-011-0148-z>, 2011.

- Worton, D. R., Sturges, W. T., Gohar, L. K., Shine, K. P., Martinerie, P., Oram, D. E., Humphrey, S. P., Begley, P., Gunn, L., Barnola, J.-M., et al.: Atmospheric trends and radiative forcings of CF_4 and C_2F_6 inferred from firn air, *Environmental science & technology*, 41, 2184–2189, <https://doi.org/10.1021/es061710t>, 2007.
- 805
- Zhang, G., Yao, B., Vollmer, M. K., Montzka, S. A., Mühle, J., Weiss, R. F., O’Doherty, S., Li, Y., Fang, S., and Reimann, S.: Ambient mixing ratios of atmospheric halogenated compounds at five background stations in China, *Atmospheric environment*, 160, 55–69, <https://doi.org/10.1016/j.atmosenv.2017.04.017>, 2017.
- Zhang, H., Wu, J., and Shen, Z.: Radiative forcing and global warming potential of perfluorocarbons and sulfur hexafluoride, *Science China Earth Sciences*, 54, 764–772, <https://doi.org/10.1007/s11430-010-4155-0>, 2011.
- 810

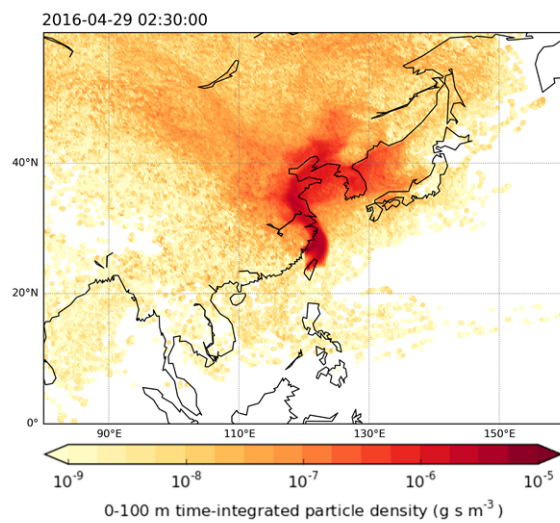


Figure 1. Example of the particle footprints, indicating where air sampled in Taiwan came from. The colour scale is logarithmic and represents the calculated time-integrated particle density (g s m^{-3}) within the surface layer (0-100 m) during 12 days prior to the sampling days given a point release at Taiwan of g s^{-1} . Darker colours indicate a greater influence of the region to the chemical composition of the air sampled in Taiwan compared to the lighter colours.

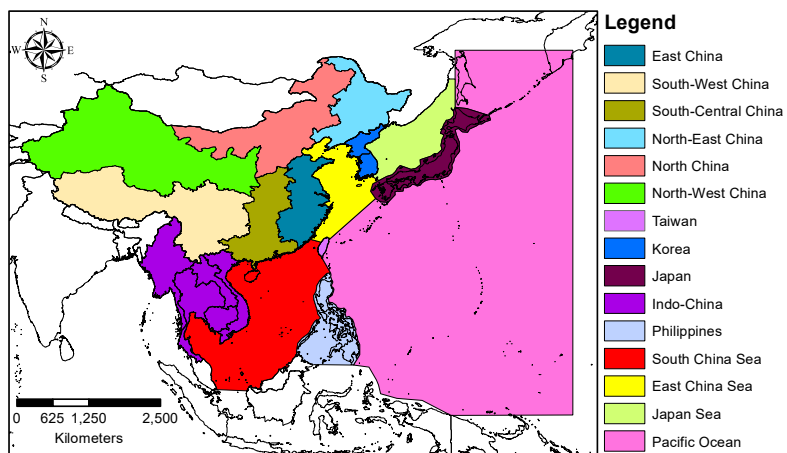


Figure 2. Regions ~~for which used in~~ the ~~contribution-NAME model~~ to ~~quantify~~ the ~~footprint-simulated~~ by the ~~NAME-model-is~~ ~~quantified~~ contributions to particle densities in Taiwan.

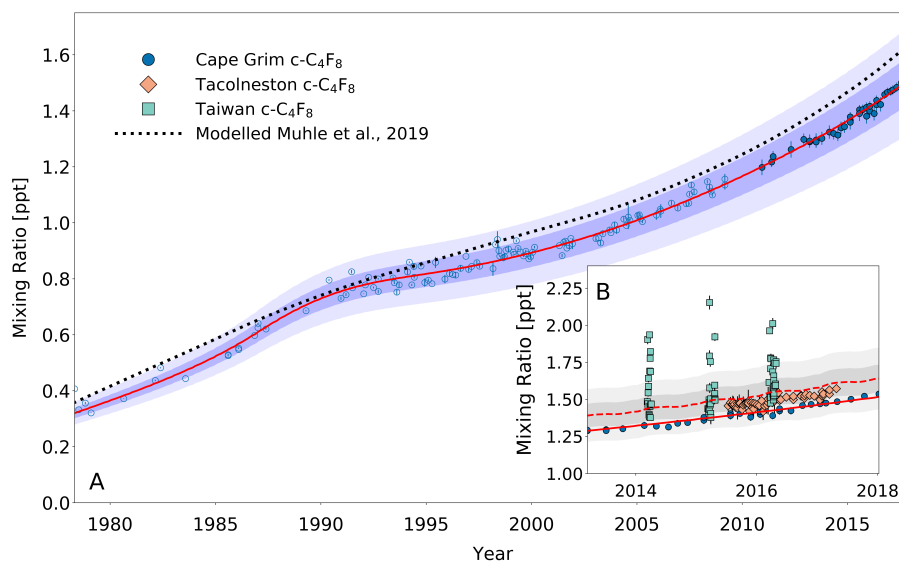


Figure 3. A) Mixing ratios at Cape Grim of c-C₄F₈ between 1978 and 2018–2018 (blue circles). Data prior to 2010 are shown as empty symbols-markers (Oram et al., 2012), while data from samples collected after 2010 are shown as filled symbols-markers to illustrate the part of the time series that is extended in the current work. The atmospheric trend simulated by the model is represented by the red line. Total uncertainties (light blue) and trend uncertainties (dark blue) are indicated with the shaded areas along the trend line. Results for the c-C₄F₈ trend published in Muhle et al. (2019) are shown in the dotted black line. B) Mixing ratios after 2010 for Cape Grim (circles), for Tacolneston (diamonds), and Taiwan (squares). The red line indicates the modelled Southern Hemisphere baseline trend at Cape Grim, while the dashed red line indicates the modelled trend for mixing ratios at Tacolneston. Total and trend uncertainties are indicated with the shaded grey areas along the Tacolneston dashed-trend line.

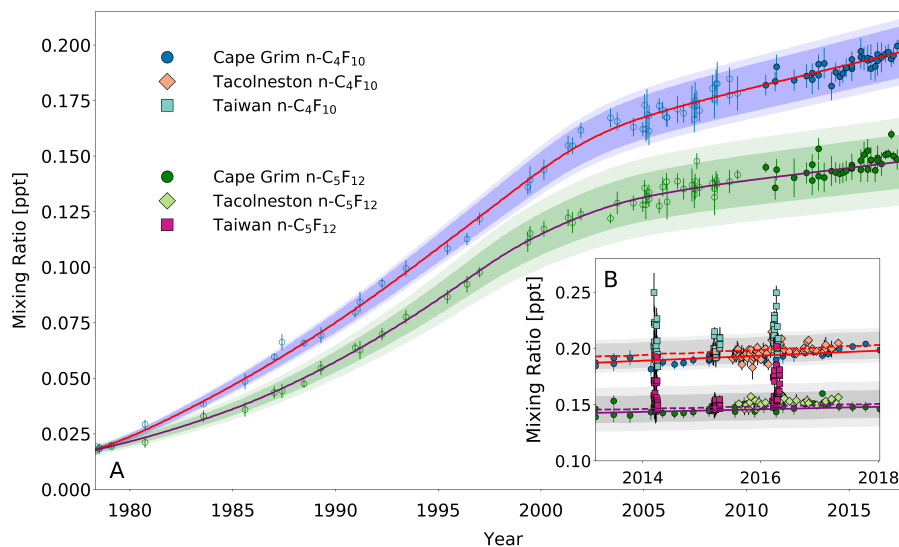


Figure 4. A) Mixing ratios at Cape Grim of n-C₄F₁₀ (blue circles) and n-C₅F₁₂ (green circles) between 1978 and 2018. Data prior to 2010 are shown as empty symbols (Laube et al., 2012), while data from samples collected after 2010 are shown as filled symbols to illustrate the part of the time series that is extended in the current work. Note that the data from Laube et al. have been converted to a new and improved calibration scale. The atmospheric trends simulated by the model are represented by the red line for n-C₄F₁₀ and by magenta line for n-C₅F₁₂. Total uncertainties (light blue for n-C₄F₁₀, light green for n-C₅F₁₂) and trend uncertainties (dark blue for n-C₄F₁₀, dark green for n-C₅F₁₂) are indicated with the shaded areas along the trend line. B) n-C₄F₁₀ mixing ratios after 2010 for Cape Grim (blue circles), for Tacolneston (orange diamonds), and Taiwan (light blue squares); n-C₅F₁₂ mixing ratios after 2010 for Cape Grim (green circles), for Tacolneston (light green diamonds), and Taiwan (magenta squares). The red and magenta lines indicate the modelled Southern Hemisphere baseline trend at Cape Grim for n-C₄F₁₀ and n-C₅F₁₂, respectively; while the dashed red and magenta lines indicate the modelled trend for mixing ratios at Tacolneston for n-C₄F₁₀ and n-C₅F₁₂, respectively. Total and trend uncertainties are indicated with the shaded grey areas along the Tacolneston dashed-trend lines for both n-C₄F₁₀ and n-C₅F₁₂.

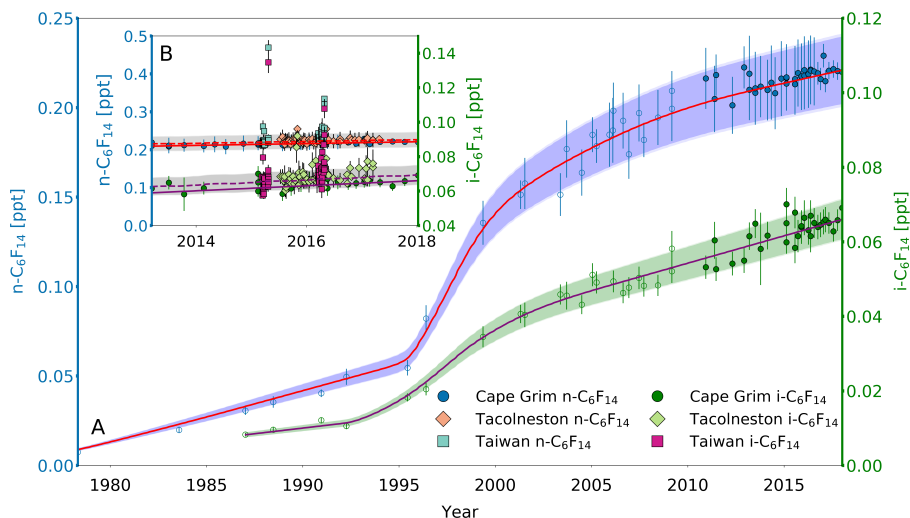


Figure 5. A) Mixing ratios at Cape Grim of $i\text{-C}_n\text{-C}_6\text{F}_{14}$ (blue circles, left axis) between 1978 and $n\text{-C}_6\text{F}_{14}$ (green circles, right axis) between 1978–1987 and 2018. Note that data for $n\text{-C}_6\text{F}_{14}$ are plotted on a secondary axis. Data prior to 2010 are shown as empty symbols (Laube et al., 2012), while data from samples collected after 2010 are shown as filled symbols to illustrate the part of the time series that is extended in the current work. Note that the data from Laube et al. have been converted to a new and improved calibration scale. The atmospheric trends simulated by the model are represented by the red line for $i\text{-C}_n\text{-C}_6\text{F}_{14}$ and by magenta line for $n\text{-C}_i\text{-C}_6\text{F}_{14}$. Total uncertainties (light blue for $i\text{-C}_n\text{-C}_6\text{F}_{14}$, light green for $n\text{-C}_i\text{-C}_6\text{F}_{14}$) and trend uncertainties (dark blue for $i\text{-C}_n\text{-C}_6\text{F}_{14}$, dark green for $n\text{-C}_i\text{-C}_6\text{F}_{14}$) are indicated with the shaded areas along the trend line. Note that there is only a very small difference between the trend and total uncertainties and thus the latter is difficult to distinguish. B) $i\text{-C}_n\text{-C}_6\text{F}_{14}$ mixing ratios after 2010 (left axis) for Cape Grim (blue circles, left axis), for Tacolneston (orange diamonds), and Taiwan (light blue squares); $n\text{-C}_i\text{-C}_6\text{F}_{14}$ mixing ratios (right axis) after 2010 for Cape Grim (green circles, right axis), for Tacolneston (light green diamonds), and Taiwan (magenta squares). The red and magenta lines indicate the modelled Southern Hemisphere baseline trend at Cape Grim for $i\text{-C}_n\text{-C}_6\text{F}_{14}$ and $n\text{-C}_i\text{-C}_6\text{F}_{14}$, respectively; while the dashed red and magenta lines indicate the modelled trend for mixing ratios at Tacolneston for $i\text{-C}_n\text{-C}_6\text{F}_{14}$ and $n\text{-C}_i\text{-C}_6\text{F}_{14}$, respectively. Total and trend uncertainties are indicated with the shaded grey areas along the Tacolneston dashed-trend lines for both $i\text{-C}_n\text{-C}_6\text{F}_{14}$ and $n\text{-C}_i\text{-C}_6\text{F}_{14}$.

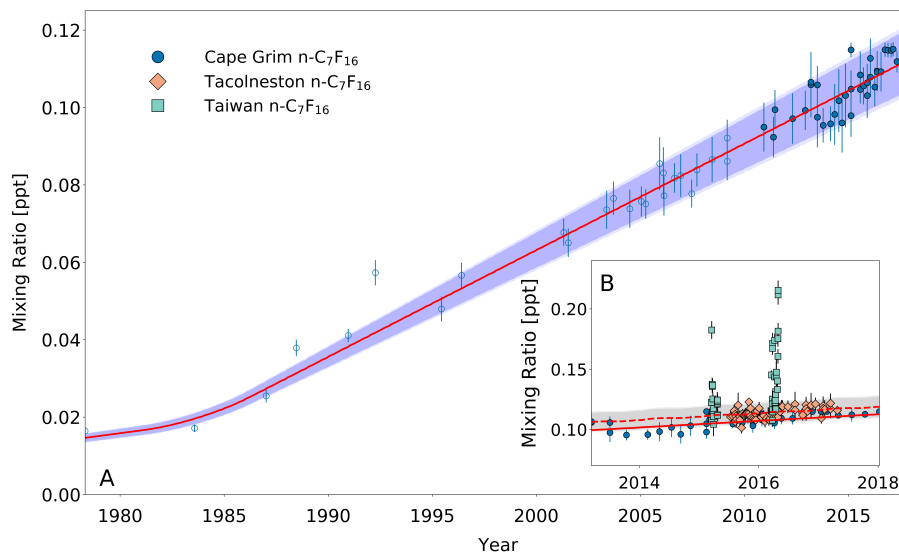


Figure 6. Same as Fig. 3, but for A) Mixing ratios at Cape Grim of n-C₇F₁₆ between 1978 and 2018 (blue circles). Data from Laube et al. (2012) prior to 2010 are plotted shown as empty markers, while data from samples collected after 2010 are shown as filled markers to illustrate the part of the time series that is extended in the current work. Note that the data from Laube et al. have been converted to a new and improved calibration scale. The atmospheric trend simulated by the model is represented by the red line. Total uncertainties (light blue) and trend uncertainties (dark blue) are indicated with the shaded areas along the trend line. B) Mixing ratios after 2010 for Cape Grim (circles), for Tacolneston (diamonds), and Taiwan (squares). The red line indicates the modelled Southern Hemisphere baseline trend at Cape Grim, while the dashed red line indicates the modelled trend for mixing ratios at Tacolneston. Total and trend uncertainties are indicated with the shaded grey areas along the Tacolneston dashed-trend line.

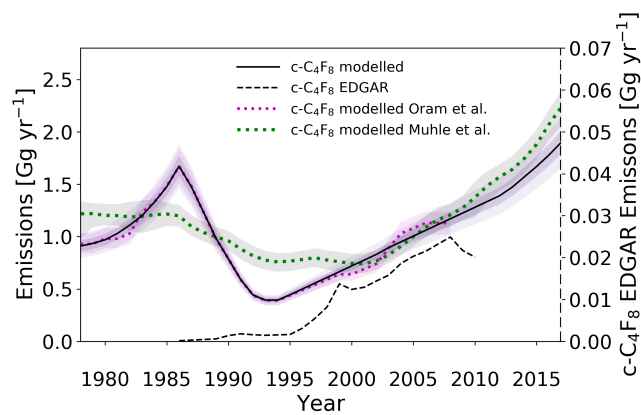


Figure 7. Estimated global emission rates for c-C₄F₈ in this study (full black line), in Oram et al. (2012) (dotted magenta line), [in Mühle et al. \(2019\) \(dotted green line\)](#), and as reported in the EDGARv4.2 database (dashed black line). Note that the EDGARv4.2 emission rates are plotted on the secondary axis. Uncertainty envelopes include contributions from measurements, modelling, and calibrations.

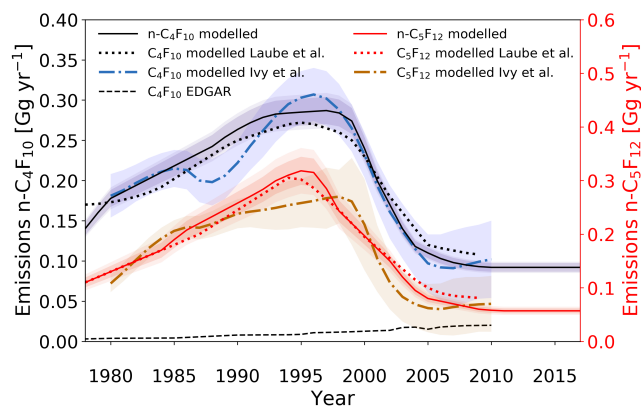


Figure 8. Estimated global emission rates for n-C₄F₁₀ and n-C₅F₁₂ (full red and black and red lines, respectively) in this study, global emission rates for C₄F₁₀ as reported in the EDGARv4.2 database (dashed black line; no distinction between isomers), modelled emissions by Ivy et al. (2012b) for C₄F₁₀ and C₅F₁₂ (dotted light dash-dotted blue and dark blue-hued brown lines, respectively; no distinction between isomers), and modelled emissions by Laube et al. (2012) for C₄F₁₀ and C₅F₁₂ (dotted red-black and magenta-red lines, respectively; no distinction between isomers). Note that the maximum EDGARv4.2 emission rate for n-C₅F₁₂ is less than 0.6×10^{-4} and is therefore not plotted here. Shadings illustrate the uncertainties.

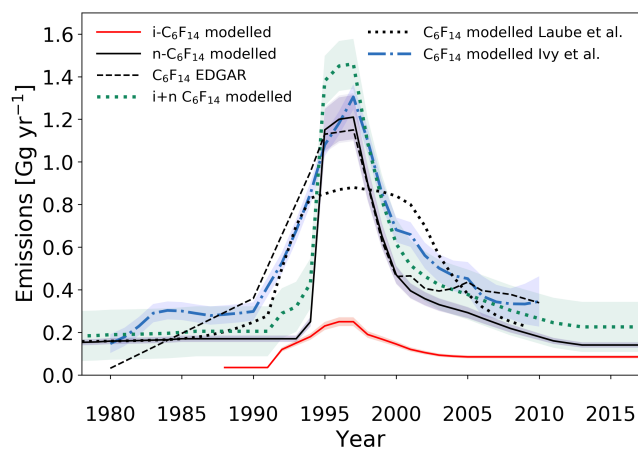


Figure 9. Estimated global emission rates for i-C₆F₁₄ and n-C₆F₁₄ in this study (full red and black lines, respectively); ~~and~~, global emission rates for C₆F₁₄ as reported in the EDGARv4.2 database (dashed black line; no distinction between isomers), by Ivy et al. (2012b) (~~dotted~~ dash-dotted blue line; no distinction between isomers), and by Laube et al. (2012) (dotted ~~magenta~~ black line; no distinction between isomers). The sum of the global emissions for the isomers of C₆F₁₄, as reported in the current work, is illustrated by the dotted ~~orange~~ green line. Shadings illustrate uncertainties.

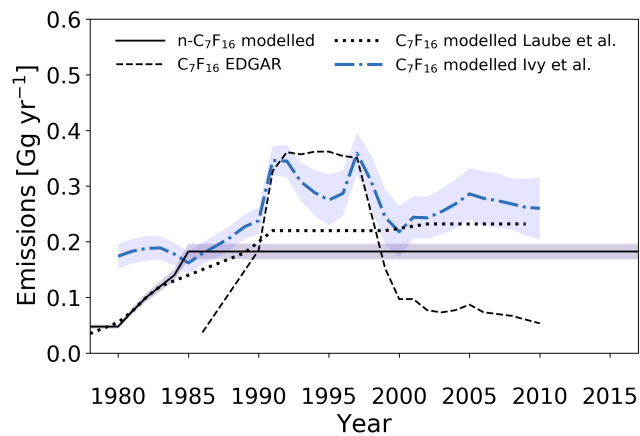


Figure 10. Estimated global emission rates for n-C₇F₁₆ in this study (full black line) and global emission rates for C₇F₁₆ as reported in the EDGARv4.2 database (dashed black line; no distinction between isomers), as reported in Ivy et al. (2012b) (dash-dotted blue line; no distinction between isomers), and as reported in Laube et al. (2012) (dotted black line; no distinction between isomers).

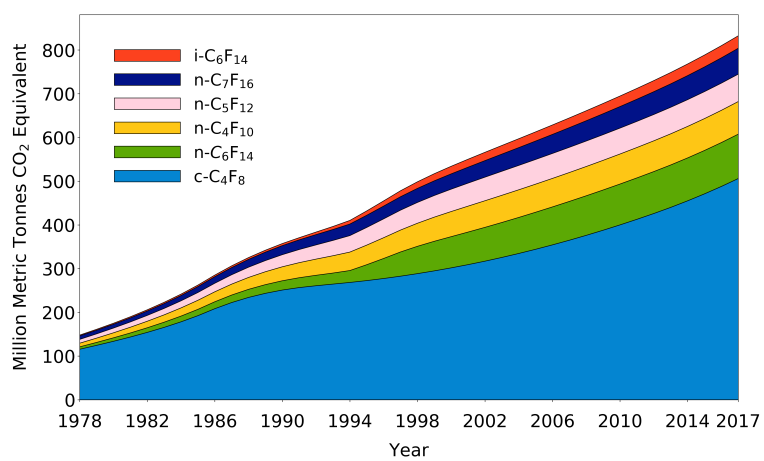


Figure 11. Cumulative CO₂ equivalent [million metric tonnes] of c-C₄F₈, n-C₄F₁₀, n-C₅F₁₂, i-C₆F₁₄, n-C₆F₁₄, n-C₇F₁₆ based on emissions between 1978 and 2017.

Table 1. Atmospheric lifetimes and global warming potentials (GWP) on a 100 year time horizon as reported in the 2013 Intergovernmental Panel on Climate Change (IPCC) report for all PFCs discussed here (Myhre et al., 2013).

PFC	Lifetime [yr]	GWP, 100 yr time horizon
c-C ₄ F ₈	3200	9540
n-C ₄ F ₁₀	2600	9200
n-C ₅ F ₁₂	4100	8550
i-C ₆ F ₁₄	3100 ^a	7370 ^b
n-C ₆ F ₁₄	3100	7910
n-C ₇ F ₁₆	3000	7820

^a The lifetime for i-C₆F₁₄ in this work is here assumed to be the same as for n-C₆F₁₄. ^b GWP for i-C₆F₁₄ is estimated based on the radiative efficiency reported in Bravo et al. (2010).

Table 2. Details on locations of sampling sites and dates, gas-chromatography columns used, and number of samples of which the measurements for each PFC compound are reported here. Differences among number of samples per compound are due to a combination of the length of the period during which the compound was measured, the chromatography method, and the precision of the measurement affected by baseline distortions.

Site	Location	Dates	CG Column	Compounds and Samples					
				c-C ₄ F ₈	n-C ₄ F ₁₀	n-C ₅ F ₁₂	i-C ₆ F ₁₄	n-C ₆ F ₁₄	n-C ₇ F ₁₆
Cape Grim	Tasmania, Australia, 41 °S, 145 °E	1978- January 2018	CP Plot	150	90	89	53	62	62
Tacolneston	Norfolk, UK, 52 °N, 1 °E, 185 m tower	July 2015 - April 2017	CP Plot	60	60	34	54	60	59
Taiwan	Cape Fuguei, 25 °N, 122 °E	March and April 2014, 2016	GasPro (2014), CP Plot (2016)	93	79	86	61	61	61
	Hengchun, 22 °N, 121 °E	March and April 2013, 2015	GasPro (2013), CP Plot (2015)						

Table 3. Mixing ratios determined in the working standard, average analytical precisions of the calibrations, and measures of accuracies of CFC-11 calibrations expressed as the average relative differences compared to NOAA scales ((UEA-NOAA)/UEA). The analytical precision is the relative 1 σ standard deviation of the compound signal in multiple working standard runs analysed on the day of each calibration. The ranges of analytical precisions and differences to NOAA are shown here for each compound in brackets and include all three calibrations done in this work for that compound. For details on the calibration of c-C₄F₈ and n-C₅F₁₂, consult Oram et al. (2012) and Laube et al. (2012).

<u>PFC</u>	<u>Mixing Ratio [ppt]</u>	<u>Analytical Precision [%]</u>	<u>CFC-11 Difference to NOAA [%]</u>	<u>Calibration Scale Uncertainty [%]</u>
<u>c-C₄F₈</u>	<u>1.565^b</u>	<u>-</u>	<u><4.60^c</u>	<u>7^c</u>
<u>n-C₄F₁₀</u>	<u>0.201^a</u>	<u>2.55 (0.61-5.04)</u>	<u>-4.66 (-5.47 - -4.19)</u>	<u>1.75</u>
<u>n-C₅F₁₂</u>	<u>0.152^b</u>	<u>-</u>	<u>(-1.4 - 2.8)^d</u>	<u>5.13^d</u>
<u>i-C₆F₁₄</u>	<u>0.067^a</u>	<u>0.7 (0.22-1.31)</u>	<u>-4.24 (-4.58 - -3.96)</u>	<u>0.52</u>
<u>n-C₆F₁₄</u>	<u>0.224^a</u>	<u>1.54 (1.06-2.41)</u>	<u>-3.72 (-5.47 - -1.78)</u>	<u>0.74</u>
<u>n-C₇F₁₆</u>	<u>0.115^a</u>	<u>2.13 (1.52-2.65)</u>	<u>-4.03 (-4.58 - -3.60)</u>	<u>1.02</u>

^aNew calibration (UEA2018). ^bOld calibration (UEA2010). ^c(Oram et al., 2012). ^d(Laube et al., 2012).

Table 4. An overview of the best Spearman rank correlations values (squared) for all PFCs measured in Taiwan and reported here, including C₂F₆ and C₃F₈, with PFC species, regions, and sources. EC: East China, ECS: East China Sea, SCC: South-central China. A complete overview of correlation coefficients can be found in the supplement.

Species	Best correlation (Spearman rank-squared) with					
	Species		Region		Source	
c-C ₄ F ₈	n-C ₄ F ₁₀ (0.62)	n-C ₅ F ₁₂ (0.56)	EC (0.33)	ECS (0.19)	Domestic (0.42)	Energy (0.41)
n-C ₄ F ₁₀	c-C ₄ F ₈ (0.62)	n-C ₅ F ₁₂ (0.56)	EC (0.20)	ECS (0.12)	Solvents (0.21)	Domestic (0.20)
n-C ₅ F ₁₂	c-C ₄ F ₈ (0.56)	n-C ₇ F ₁₆ (0.49)	EC (0.47)	ECS (0.33)	Solvents (0.50)	Domestic (0.45)
i-C ₆ F ₁₄	C ₂ F ₆ (0.52)	n-C ₆ F ₁₄ (0.40)	EC (0.33)	ECS (0.19)	Domestic (0.33)	Energy (0.31)
n-C ₆ F ₁₄	C ₂ F ₆ (0.52)	C ₃ F ₈ (0.50)	ECS (0.27)	EC (0.18)	Energy (0.26)	Domestic (0.22)
n-C ₇ F ₁₆	c-C ₄ F ₈ (0.55)	C ₂ F ₆ (0.54)	EC (0.49)	ECS (0.21)	Domestic (0.46)	Solvents (0.44)
C ₂ F ₆	C ₃ F ₈ (0.68)	n-C ₇ F ₁₆ (0.54)	EC (0.19)	SCC (0.13)	Energy (0.34)	Domestic (0.25)
C ₃ F ₈	C ₂ F ₆ (0.68)	n-C ₆ F ₁₄ (0.54)	EC (0.10)	ECS (0.07)	Energy (0.31)	Transport (0.19)

Mixing ratios determined in the working standard, precisions of the calibrations, and accuracies of CFC-11 calibrations compared to NOAA scales. For details on the calibration of c-C₄F₈ and n-C₅F₁₂, consult Oram et al. (2012) and Laube et al. (2012). PFC Mixing Ratio ppt Analytical Precision % Accuracy for CFC-11 % Calibration Scale Uncertainty % c-C₄F₈ 1.565^b < 4.60^c n-C₄F₁₀ 0.201^a 0.61-5.04 -4.19 -5.47 1.75 n-C₅F₁₂ 0.152^b 1.4 -2.8^d 5.13^d i-C₆F₁₄ 0.067^a 0.22-1.31-3.96 -4.58 0.52 n-C₆F₁₄ 0.224^a 1.06-2.41-1.78 -5.47 0.74 n-C₇F₁₆ 0.115^a 1.52-2.65 -3.60 -4.58 1.02

Trends and Emissions of Six Perfluorocarbons in the Northern and Southern Hemisphere: Supplementary Material

Elise S. Droste¹, Karina E. Adcock¹, Matthew J. Ashfold², Charles Chou³, Zoë Fleming^{4,*}, Paul J. Fraser⁵, Lauren J. Gooch¹, Andrew J. Hind¹, Ray L. Langenfelds⁵, Emma Leedham Elvidge¹, Norfazrin Mohd Hanif^{1,6}, Simon O'Doherty⁷, David E. Oram^{1,8}, Chang-Feng Ou-Yang⁹, Marios Panagi⁴, Claire E. Reeves¹, William T. Sturges¹, and Johannes C. Laube^{1,10}

¹Centre for Ocean and Atmospheric Sciences, School of Environmental Sciences, University of East Anglia, Norwich, NR4 7TJ, UK

²School of Environmental and Geographical Sciences, University of Nottingham Malaysia, 43500 Semenyih, Malaysia

³Research Center for Environmental Changes, Academia Sinica, Taipei 11529, Taiwan

⁴National Centre for Atmospheric Science (NCAS), Department of Chemistry, University of Leicester, UK

⁵Commonwealth Scientific and Industrial Research Organisation, Oceans and Atmosphere, Climate Science Centre, Aspendale, Australia

⁶School of Environmental and Natural Resource Sciences, Faculty of Science and Technology, Universiti Kebangsaan Malaysia, 43600 Bangi, Selangor, Malaysia

⁷Department of Chemistry, University of Bristol, Bristol, UK

⁸National Centre for Atmospheric Science, School of Environmental Sciences, University of East Anglia, Norwich, NR4 7TJ, UK

⁹Department of Atmospheric Sciences, National Central University, Taoyuan, Taiwan

¹⁰Institute of Energy and Climate Research – Stratosphere (IEK-7), Forschungszentrum Jülich GmbH, Jülich, Germany

* now at Center for Climate and Resilience Research (CR2), University of Chile, Santiago, Chile

Correspondence: E. S. Droste (e.droste@uea.ac.uk)

Contents

1	Perfluorocarbon Ratios <u>Additional Calibration Details</u>	2
2	Ion Ratios	3
3	<u>Perfluorocarbon Ratios</u>	5
5	4 Uncertainties	6
5	<u>NAME Footprints and CO Emissions</u>	7
6	Global Emission Rates	8
7	Correlations of PFC Mixing Ratios in Taiwan	9

1 Perfluorocarbon Ratios Additional Calibration Details

Ratio of $n\text{-C}_4\text{F}_{10}$: $n\text{-C}_5\text{F}_{12}$ (diamonds) and $i\text{-C}_6\text{F}_{14}$: $n\text{-C}_6\text{F}_{14}$ (circles) mixing ratios measured in Cape Grim samples between 1978 and 2018 (see Section ??). Error bars indicate propagated measurement uncertainties. Full orange and magenta lines illustrate respective five-year averages of the ratios, with error bars comprising the propagated measurement uncertainties.

- 5 Even though the current method has separated the isomers for C_4F_{10} , the $i\text{-C}_4\text{F}_{10}$ isomer can currently not be quantified yet, because, apart from having a very small signal, its main quantifying ion is not well separated from one of the quantifying ions for $n\text{-C}_4\text{F}_{10}$. Even if we were able to separate it completely, it would also have to be calibrated using a pure $i\text{-C}_4\text{F}_{10}$ reagent, which we were unable to acquire. Hence, we are unable to quantify what fraction of the 2.8% (which is the relative difference between the UEA2010 and UEA2018 calibration scales for $n\text{-C}_4\text{F}_{10}$) is due to leak-tightness and to the influence of $i\text{-C}_4\text{F}_{10}$.
- 10 The overall volume uncertainty of the sample loops that were filled with pure compounds during both dilution steps is 5%, as has been outlined in Laube et al. (2010). This is the likeliest and highest source of uncertainty in the entire calibration procedure. As has been shown in multiple previous papers (Laube et al., 2010, 2012, 2014, 2016; Oram et al., 2012; Kloss et al., 2014), the overall calibration uncertainty is very likely about 7%. Our measurements fall well within that envelope.

Table S1. Mixing ratios (in parts per trillion) determined for the diluted, high purity PFC compounds and CFC-11 as the reference compound.

<u>Calibration No.</u>	<u>$n\text{-C}_4\text{F}_{10}$ / CFC-11</u>	<u>$i\text{-C}_6\text{F}_{14}$ / CFC-11</u>	<u>$n\text{-C}_6\text{F}_{14}$ / CFC-11</u>	<u>$n\text{-C}_7\text{F}_{16}$ / CFC-11</u>
<u>1</u>	<u>9 / 24.7</u>	<u>5.9 / 22.3</u>	<u>7.1 / 27.3</u>	<u>5.8 / 23.6</u>
<u>2</u>	<u>8.6 / 29.3</u>	<u>8.9 / 25.3</u>	<u>5.0 / 24.7</u>	<u>6.8 / 25.3</u>
<u>3</u>	<u>9.8 / 22.4</u>	<u>5.1 / 22.4</u>	<u>8.9 / 25.3</u>	<u>4.8 / 29.3</u>

2 Ion Ratios

The ratio of the two main quantifying ions for C_6F_{14} and C_7F_{16} (m/z 169.0 and 219.0) is used to determine whether all isomers have been separated for a particular peak in the chromatograph. Deviation of the ratio measured in the Cape Grim samples from the ratio measured in the calibration samples, which are composed of highly purified isomers, indicates the possibility
5 that not all isomers have been separated during gas-chromatography.

For $i-C_6F_{14}$, the average ion ratio in the calibration is 0.89 ± 0.03 and Cape Grim air samples have an ion ratio that is on average 1.00 ± 0.07 (Fig. S1 A). The positive offset of the Cape Grim ion ratio to the calibration ion ratio for $i-C_6F_{14}$ seems to be consistent. $n-C_6F_{14}$ measured in air samples have an average ion ratio of 0.99 ± 0.03 , which is consistently - but not significantly - lower than the ion ratio for the calibrations (1.04 ± 0.07) (Fig. S1 B). Finally, $n-C_7F_{16}$ has an average ion ratio
10 of 1.00 ± 0.05 in the Cape Grim air samples, which agrees very well with the average ion ratio in its calibration: 1.02 ± 0.07 (Fig. S1 C). Overall, the difference between the ion ratios of the air samples and the calibrations is not significant within the uncertainties, especially for $n-C_6F_{14}$ and $n-C_7F_{16}$. Even though this means that it is highly likely that only one isomer is being measured instead of multiple under one peak, the possibility that not all isomers within this peak have been separated cannot be excluded.

15 A limitation is that a trend analysis of the ion ratio for these PFC isomers is not possible here, since problems with baseline distortions in the Cape Grim data resulted in a lack of samples before 2005 that have good precisions on both m/z 219.0 and 169.0 ions. This is especially the case for the m/z 219 ion, which generally exhibits smaller peaks than the m/z 169 ion and also has a noisier baseline in our analytical system.

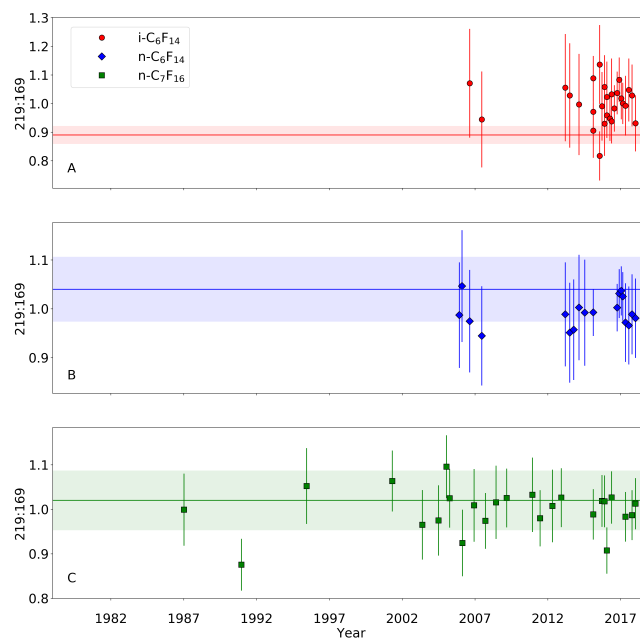


Figure S1. Ratios of ions m/z 219:169 for $i\text{-C}_6\text{F}_{14}$ (A), $n\text{-C}_6\text{F}_{14}$ (B), and $n\text{-C}_7\text{F}_{16}$ (C) for Cape Grim air samples between 1987 and 2018. Note that both ions could only be measured with high precision for samples [collected](#) after 2005 for $i\text{-C}_6\text{F}_{14}$ and $n\text{-C}_6\text{F}_{14}$. The horizontal line illustrates the average 219:169 ion ratio of the calibrations done in the current work. Shaded area indicates the propagated uncertainty of the average 219:169 ratio of the calibrations.

3 Perfluorocarbon Ratios

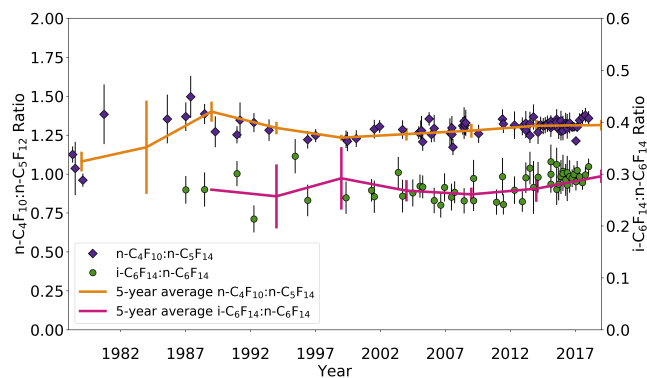


Figure S2. Ratio of n-C₄F₁₀ :n-C₅F₁₂ (diamonds) and i-C₆F₁₄ :n-C₆F₁₄ (circles) mixing ratios measured in Cape Grim samples between 1978 and 2018. Error bars indicate propagated measurement uncertainties. Full orange and magenta lines illustrate respective five-year averages of the ratios, with error bars comprising the propagated measurement uncertainties.

4 Uncertainties

Table S2. ~~Trend~~ Average analytical uncertainties, average model-fit uncertainties, calibration uncertainty, trend uncertainties (composed of the average analytical uncertainty, the average best-fit uncertainty, and the model transport uncertainty of 5 %) and total uncertainties (composed as the trend uncertainty and calibration uncertainty) for all PFCs. ~~PFC Trend Uncertainty % Total Uncertainty %~~ The total uncertainties for c-C₄F₈ 5.7-12.7 and n-C₄F₁₀ 5.9-7.6 n-C₅F₁₂ 8.2-13.4 i-C₆F₁₄ 8.0-8.5 n-C₆F₁₄ 8.5-9.3 n-C₇F₁₆ 7.2-8.2 also includes an uncertainty related to the error in the conversion of the mixing ratio between two internal working standards: 0.58 % and 1.98 %, respectively.

PFC	Average Analytical Uncertainty [%]	Average Model-Fit Uncertainty [%]	Calibration Uncertainty [%]	Trend Uncertainty [%]	Total Uncertainty [%]
c-C ₄ F ₈	0.94	0.64	7	5.7	12.7
n-C ₄ F ₁₀	3.08	0.10	1.75	5.9	7.6
n-C ₅ F ₁₂	3.74	0.09	5.13	8.2	13.4
i-C ₆ F ₁₄	6.27	0.09	0.52	8.0	8.5
n-C ₆ F ₁₄	6.92	0.42	0.74	8.5	9.3
n-C ₇ F ₁₆	5.07	0.89	1.02	7.2	8.2

5 NAME Footprints and CO Emissions

The following explains the calculations used to derive modelled CO mixing ratios, using the NAME model's footprints.

The dilution factor (n) is determined for air masses in each grid cell. The dilution factor relates to the amount of time that a particle spends in each grid cell for each 100 m of grid cell depth. Equation 1 shows how the dilution factor (unit: $s\ m^{-1}$) is
5 calculated:

$$n = \frac{P}{m} \cdot S \quad (1)$$

where P is the particle mass density residence time in $g\ s\ m^{-3}$, m is the mass of the particle emitted in g , and S is the surface area of each grid cell in m^2 . The modelled mixing ratios of CO are calculated by combining the output of Equation 1 (i.e. the dilution factor) with the distribution of the emissions, which are taken from the Representative Concentration Pathway
10 (Riahi et al., 2011; Van Vuuren et al., 2011) (<http://tntcat.iiasa.ac.at:8787/RcpDb/dsd?Action=htmlpage&page=welcome>). This is represented in Equation 2, where E is the emission estimates of CO in $g\ m^{-2}\ s^{-1}$, Z refers to any of the sectors applicable to this model (industry, power plants, solvents, agricultural waste burning, waste, forest burning, grassland burning, residential, international shipping, surface transportation, or agriculture), M_{CO} is the molar mass in $g\ mol^{-1}$, x is the number of grid cells, and CO_Z is the modelled concentration of CO emitted from sector Z in $mol\ m^{-3}$, which is converted to $mol\ mol^{-1}$ using the
15 gas law with temperature and pressure data.

$$\sum^x \frac{E_Z \cdot n}{M_{CO}} = CO_Z \quad (2)$$

Both E_Z and n match two dimensional (lat-lon) grids. For each grid cell, E_Z and n are combined to get a contribution to the modelled mixing ratio from emissions in that grid cell, which are converted to mixing ratios using the number of moles of air per volume. Those contributions are summed for all grid cells (x) to obtain CO_Z .

6 Global Emission Rates

Table S3. Global annual emission rates (Gg yr^{-1}) for all six PFCs used in the model simulations to obtain the best fit of the simulated model mixing ratios to the measured mixing ratios in Cape Grim.

Year	c-C ₄ F ₈	n-C ₄ F ₁₀	n-C ₅ F ₁₂	i-C ₆ F ₁₄	n-C ₆ F ₁₄	n-C ₇ F ₁₆
1978	0.910	0.140	0.110	0.030	0.153	0.048
1979	0.935	0.160	0.120	0.030	0.155	0.048
1980	0.970	0.178	0.130	0.030	0.159	0.048
1981	1.030	0.186	0.140	0.030	0.160	0.075
1982	1.110	0.194	0.150	0.030	0.162	0.100
1983	1.20	0.202	0.160	0.030	0.164	0.120
1984	1.328	0.210	0.170	0.030	0.166	0.140
1985	1.476	0.218	0.190	0.030	0.170	0.183
1986	1.673	0.226	0.208	0.035	0.170	0.183
1987	1.476	0.234	0.220	0.035	0.170	0.183
1988	1.230	0.242	0.233	0.035	0.170	0.183
1989	0.984	0.254	0.245	0.035	0.170	0.183
1990	0.787	0.264	0.258	0.035	0.170	0.183
1991	0.590	0.272	0.270	0.035	0.170	0.183
1992	0.443	0.279	0.284	0.119	0.170	0.183
1993	0.394	0.283	0.300	0.150	0.170	0.183
1994	0.394	0.284	0.310	0.180	0.250	0.183
1995	0.445	0.285	0.318	0.230	1.150	0.183
1996	0.500	0.286	0.315	0.250	1.200	0.183
1997	0.555	0.287	0.285	0.250	1.210	0.183
1998	0.610	0.284	0.243	0.190	0.900	0.183
1999	0.665	0.274	0.220	0.168	0.653	0.183
2000	0.720	0.240	0.197	0.145	0.470	0.183
2001	0.775	0.200	0.173	0.120	0.395	0.183
2002	0.830	0.170	0.150	0.105	0.358	0.183
2003	0.895	0.140	0.120	0.093	0.330	0.183
2004	0.950	0.118	0.095	0.088	0.311	0.183
2005	1.005	0.110	0.080	0.085	0.293	0.183
2006	1.060	0.103	0.075	0.085	0.267	0.183
2007	1.115	0.098	0.070	0.085	0.243	0.183
2008	1.170	0.095	0.065	0.085	0.218	0.183
2009	1.225	0.093	0.060	0.085	0.199	0.183
2010	1.280	0.092	0.058	0.085	0.179	0.183
2011	1.335	0.092	0.057	0.085	0.160	0.183
2012	1.390	0.092	0.057	0.085	0.150	0.183
2013	1.470	0.092	0.057	0.085	0.141	0.183
2014	1.570	0.092	0.057	0.085	0.141	0.183
2015	1.670	0.092	0.057	0.085	0.141	0.183
2016	1.779	0.092	0.057	0.085	0.141	0.183
2017	1.900	0.092	0.057	0.085	0.141	0.183

7 Correlations of PFC Mixing Ratios in Taiwan

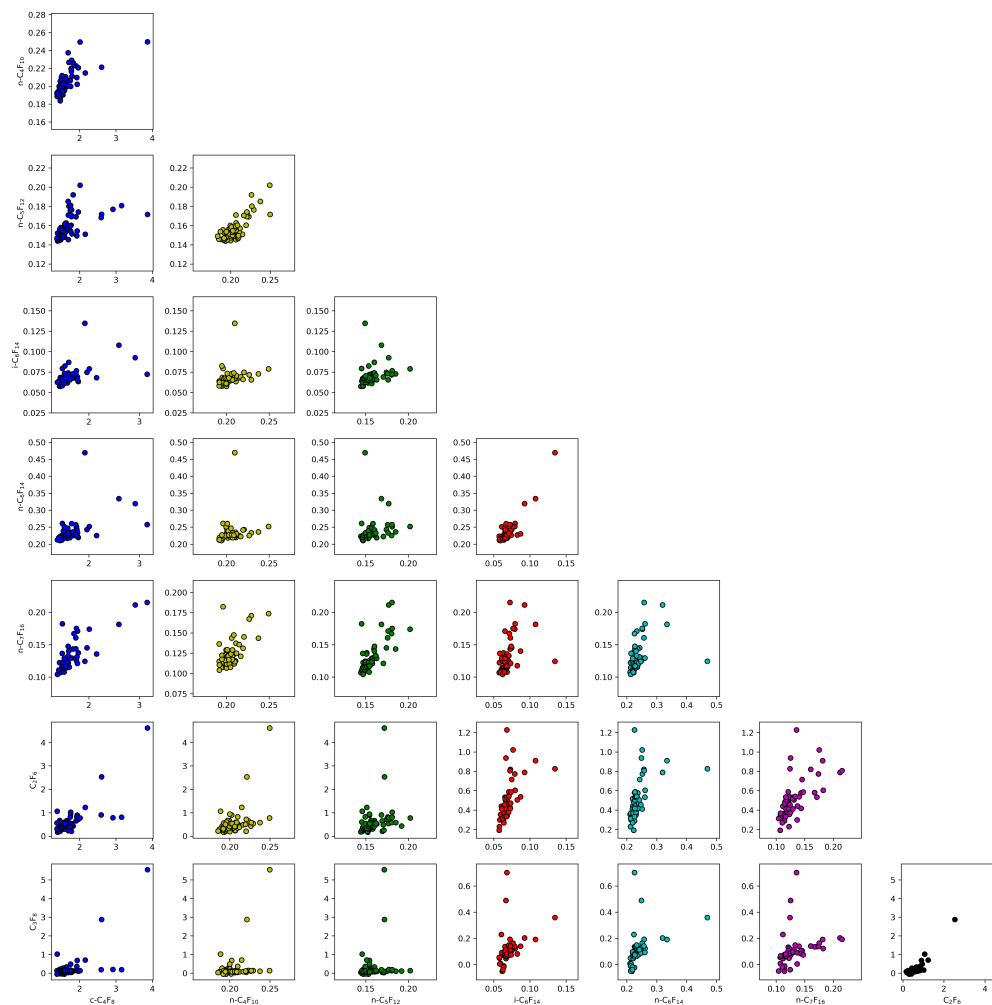


Figure S3. Correlations of all PFC mixing ratios (ppt) measured in Taiwan.

Table S4. R-squared Spearman correlation coefficients for correlation analysis between all PFCs in this study. All values are significant (p-value<0.05).

	c-C ₄ F ₈	n-C ₄ F ₁₀	n-C ₅ F ₁₂	i-C ₆ F ₁₄	n-C ₆ F ₁₄	n-C ₇ F ₁₆	C ₂ F ₆	C ₃ F ₈
n-C ₄ F ₁₀	0.62							
n-C ₅ F ₁₂	0.56	0.45						
i-C ₆ F ₁₄	0.35	0.20	0.32					
n-C ₆ F ₁₄	0.35	0.20	0.33	0.40				
n-C ₇ F ₁₆	0.55	0.23	0.49	0.33	0.39			
C ₂ F ₆	0.42	0.21	0.28	0.52	0.52	0.54		
C ₃ F ₈	0.35	0.14	0.20	0.39	0.50	0.46	0.68	

Table S5. R-squared Spearman correlation coefficients for correlation analysis between all PFCs in this study and the particle density per region derived from NAME model results. Significance is indicated by * (p-value<0.05).

	c-C ₄ F ₈	n-C ₄ F ₁₀	n-C ₅ F ₁₂	i-C ₆ F ₁₄	n-C ₆ F ₁₄	n-C ₇ F ₁₆	C ₂ F ₆	C ₃ F ₈
East China	0.33*	0.20*	0.47*	0.33*	0.19*	0.49*	0.19*	0.10*
North China	0.02*	0.03	0.10*	0.02	0.01	0.07*	0.00	0.00
North -East China	0.02	0.01	0.01	0.02	0.01	0.00	0.01	0.00
North-West China	0.06	0.00	0.00	0.06	0.01	0.01	0.00	0.03
South-Central China	0.14*	0.09*	0.21*	0.14*	0.07	0.11*	0.13*	0.05
South-West China	0.01	0.00	0.00	0.01	0.00	0.02	0.02	0.02
Indo-China	0.00	0.01	0.00	0.00	0.00	0.01	0.03	0.05*
Philippines	0.03	0.01	0.01	0.03	0.05	0.01	0.04	0.01
Taiwan	0.00	0.00	0.03	0.00	0.02	0.02	0.02	0.04
Japan	0.01	0.01	0.01	0.01	0.01	0.00	0.00	0.01
Korea	0.08*	0.00	0.01	0.08*	0.14*	0.06	0.07*	0.01
East China Sea	0.19*	0.12*	0.33*	0.19*	0.27*	0.21*	0.12*	0.07*
Japan Sea	0.05	0.00	0.00	0.05	0.06	0.02	0.03	0.00
Pacific Ocean	0.03	0.01	0.06*	0.03	0.02	0.05	0.00	0.01
South China Sea	0.03	0.00	0.00	0.03	0.00	0.00	0.06*	0.05*

Table S6. R-squared Spearman correlation coefficients for correlation analysis between all PFCs in this study and the CO mixing ratio derived from the NAME model results per CO source type. Significance is indicated by * (p-value<0.05). Industry includes combustion and processing; power plants include energy generation, energy conversion, and extraction; waste includes landfills, waste water, and waste incineration; residential includes domestic and commercial residences; and agriculture includes animal husbandry, rice crops, and soil.

	c-C ₄ F ₈	n-C ₄ F ₁₀	n-C ₅ F ₁₂	i-C ₆ F ₁₄	n-C ₆ F ₁₄	n-C ₇ F ₁₆	C ₂ F ₆	C ₃ F ₈
Industry	0.45*	0.21*	0.48*	0.34*	0.25*	0.48*	0.28*	0.21*
Power Plants	0.41*	0.13*	0.27*	0.31*	0.26*	0.37*	0.34*	0.31*
Solvents	0.39*	0.21*	0.50*	0.30*	0.20*	0.44*	0.19*	0.12*
Agricultural Waste Burning	0.33*	0.18*	0.41*	0.26*	0.18*	0.41*	0.18*	0.08*
Waste	0.04	0.00	0.00	0.03	0.14*	0.04	0.06*	0.01
Forest Burning	0.00	0.00	0.01	0.01	0.02	0.00	0.00	0.01
Grassland Burning	0.01	0.00	0.01	0.01	0.01	0.02	0.00	0.00
Residential	0.42*	0.2*	0.45*	0.33*	0.22*	0.46*	0.25*	0.17*
International Shipping	0.01	0.00	0.00	0.00	0.02	0.00	0.04	0.05*
Surface Transportation	0.16*	0.02	0.03	0.10*	0.08*	0.08*	0.17*	0.19*
Agriculture	0.00	0.01	0.01	0.00	0.00	0.01	0.00	0.01

References

- Kloss, C., Newland, M. J., Oram, D. E., Fraser, P. J., Brenninkmeijer, C. A. M., Röckmann, T., and Laube, J. C.: Atmospheric abundances, trends and emissions of CFC-216ba, CFC-216ca and HCFC-225ca, *Atmosphere*, 5, 420–434, <https://doi.org/10.3390/atmos5020420>, 2014.
- 5 Laube, J., Hogan, C., Newland, M., Mani, F. S., Fraser, P., Brenninkmeijer, C., Martinerie, P., Oram, D., Röckmann, T., Schwander, J., et al.: Distributions, long term trends and emissions of four perfluorocarbons in remote parts of the atmosphere and firn air, *Atmospheric chemistry and physics*, 12, 4081–4090, <https://doi.org/10.5194/acp-12-4081-2012>, 2012.
- Laube, J. C., Martinerie, P., Witrant, E., Blunier, T., Schwander, J., Brenninkmeijer, C., Schuck, T. J., Bolder, M., Röckmann, T., Veen, C., et al.: Accelerating growth of HFC-227ea (1, 1, 1, 2, 3, 3, 3-heptafluoropropane) in the atmosphere, *Atmospheric chemistry and physics*, 10, 5903–5910, <https://doi.org/10.5194/acp-10-5903-2010>, 2010.
- 10 Laube, J. C., Newland, M. J., Hogan, C., Brenninkmeijer, C. A. M., Fraser, P. J., Martinerie, P., Oram, D. E., Reeves, C. E., Röckmann, T., Schwander, J., et al.: Newly detected ozone-depleting substances in the atmosphere, *Nature Geoscience*, 7, 266–269, <https://doi.org/10.1038/ngeo2109>, 2014.
- Laube, J. C., Mohd Hanif, N., Martinerie, P., Gallacher, E., Fraser, P. J., Langenfelds, R., Brenninkmeijer, C. A., Schwander, J., Witrant, E., Wang, J.-L., et al.: Tropospheric observations of CFC-114 and CFC-114a with a focus on long-term trends and emissions, *Atmospheric Chemistry and Physics*, 16, 15 347–15 358, <https://doi.org/10.5194/acp-16-15347-2016>, 2016.
- 15 Oram, D., Mani, F. S., Laube, J., Newland, M., Reeves, C., Sturges, W., Penkett, S., Brenninkmeijer, C., Röckmann, T., and Fraser, P.: Long-term tropospheric trend of octafluorocyclobutane (c-C₄F₈ or PFC-318), *Atmospheric Chemistry and Physics*, 12, 261–269, <https://doi.org/10.5194/acp-12-261-2012>, 2012.
- 20 Riahi, K., Rao, S., Krey, V., Cho, C., Chirkov, V., Fischer, G., Kindermann, G., Nakicenovic, N., and Rafaj, P.: RCP 8.5—A scenario of comparatively high greenhouse gas emissions, *Climatic Change*, 109, 33, <https://doi.org/10.1007/s10584-011-0149-y>, 2011.
- Van Vuuren, D. P., Edmonds, J., Kainuma, M., Riahi, K., Thomson, A., Hibbard, K., Hurtt, G. C., Kram, T., Krey, V., Lamarque, J.-F., et al.: The representative concentration pathways: an overview, *Climatic change*, 109, 5, <https://doi.org/10.1007/s10584-011-0148-z>, 2011.